

EVALUATION OF DIELECTRIC MATERIALS FOR
OZONE GENERATION IN PLASMA REACTORS

By

ARUN KRISHNAMOORTHY

Bachelor of Engineering (Honors)

Birla Institute of Technology & Science

Pilani, INDIA

1993

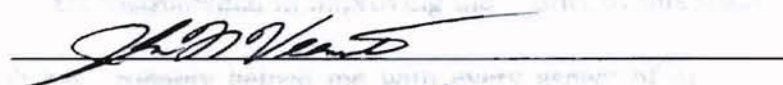
Submitted to the Faculty of the
Graduate College of the
Oklahoma State University
in partial fulfillment of
the requirements for
the Degree of
MASTER OF SCIENCE
December, 1996

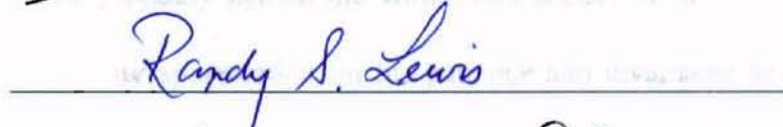
EVALUATION OF DIELECTRIC MATERIALS FOR
OZONE GENERATION IN PLASMA REACTORS

Thesis Approved:



Thesis Adviser







Dean of the Graduate College

ACKNOWLEDGEMENTS

I wish to thank all who have helped me, both directly and indirectly, successfully complete this MS program. I am indebted to Dr. Arland H. Johannes, my adviser, for his valuable guidance, constant encouragement, technical assistance and a friendly attitude without which this work might not have been possible. Greg Holland deserves special mention for all the help rendered - truly, a great team-mate and friend.

My thanks to all my friends, especially Suresh Parthasarathi, Satish Venkataraman, and Venkataraghavan Raman, for their encouragement and constructive criticism which were instrumental in improving the quality of this study. Mr. Cliff at the Engineering lab has probably helped me with every aspect of my equipment setup - I would like to extend my appreciation for his patience and invaluable help. My greatest appreciation and love to my parents, sister and brother-in-law for all the love and monetary support that they have provided me.

Finally, Dr. Randy Lewis and Dr. Veenstra , my committee members, deserve special mention for their interest in the project.

TABLE OF CONTENTS

Chapter	Page
I. INTRODUCTION	1
II. LITERATURE SURVEY	6
Background	6
Definition of Plasma State	6
Major Factors Affecting Choice of Insulation	7
Electric Field	7
Dielectric Strength	8
Insulation Life	8
Dielectric Loss	10
Dielectric Constant	11
Dielectric Polarization	13
Ozone Generation by Electrical Discharge	15
Mechanism of Ozone Formation in Electrical Discharge	15
III. MATERIAL SELECTION	18
Plastics	19
Thermoplastic Materials	19
Thermosetting Plastics	21
Ceramics	23
IV. EXPERIMENTAL SETUP AND PROCEDURE	25
Equipment Calibration	25
Experimental Apparatus Description	25
Tests for Experimentation	26
Open-circuit Tests	26
Operational Procedures for Open-circuit Tests	28
Usability Tests	28
Operational Procedures for Usability Tests	29
Ozone Generation Tests	31

Chapter	Page
Operational Procedures for Ozone Generation Tests	31
V. RESULTS AND DISCUSSIONS	34
Open-circuit Tests	34
Usability Tests	38
Ozone Generation Tests	72
Varying Surface Area and Annulus Width Test	73
Varying Thickness and Annulus Width Test	78
Varying Thickness and Surface Area Test	81
Heat Generation Tests	84
Reproducibility Tests	92
VI. CONCLUSIONS AND RECOMMENDATIONS	95
Conclusions	95
Recommendations	97
REFERENCES	101
APPENDICES	102
APPENDIX A. Properties of Materials Selected for Experimentation	103
APPENDIX B. Experimental Data for Open-circuit Tests	107
APPENDIX C. Experimental Data for Usability Tests	113
APPENDIX D. Experimental Data for Ozone Generation Tests	130
APPENDIX D1. Varying Surface Area and Annulus Width Tests	131
APPENDIX D2. Varying Wall Thickness and Annulus Width Tests	146
APPENDIX D3. Varying Wall Thickness and Surface Area Tests	153
APPENDIX D4. Heat Generation Tests	162
APPENDIX E. Reproducibility Tests	177

LIST OF TABLES

Table	Page
I. Properties of Dielectric Materials Selected	104
II. Parameters for Plasma Reactor	18
III. Desirable Properties for Plasma Reactors	20
IV. Evaluation of Thermoplastic Materials Selected	21
V. Evaluation of Thermosetting Plastics Selected	22
VI. Evaluation of Ceramic Material Selected	24
VII. Reactor Configuration for Usability Tests	30
VIII. Reactor Configuration for Ozone Generation Tests	32
IX. Open-circuit Tests for Transformer	108
X. Power Loss of Transformer	112
XI. Results of Usability Tests Conducted	40
XII. Variation of Secondary Voltage with Frequency at Constant Primary Voltage (Usability Tests)	114
XIII. Variation of Secondary Current with Frequency at Constant Primary Voltage (Usability Tests)	116
XIV. Variation of Exit Gas Temperature with Frequency at Constant Primary Voltage (Usability Tests)	118

Table	Page
XV. Variation of Exit Gas Temperature with Time at Constant Primary Voltage (Usability Tests)	120
XVI. Variation of Secondary Voltage with Time at Constant Primary Voltage (Usability Tests)	122
XVII. Variation of Secondary current with Time at Constant Primary Voltage (Usability Tests)	124
XVIII. Variation of Secondary Voltage, Secondary Current and Exit Gas Temperature with Frequency for 1/32 inch Wall Acrylic	126
XIX. Variation of Secondary voltage, Secondary Current and Exit Gas Temperature with Time for 1/32 inch Wall Acrylic	128
XX. Burning Properties of Paper- and Glass-filled Resin	50
XXI. Variation of Air Breakdown Voltage with Dielectric Constant (k) at Various Primary Voltages	130
XXII. Capacitance of Air and the Outer Cylinder for Different Configurations	77
XXIII. Experimental Data for 1/16 inch Air-gap Thickness (Varying Surface Area and Annulus Test)	132
XXIV. Experimental Data for 3/16 inch Air-gap Thickness (Varying Surface Area and Annulus Test)	134
XXV. Experimental Data for 1/4 inch Air-gap Thickness (Varying Surface Area and Annulus Test)	136
XXVI. Experimental Data for 5/16 inch Air-gap Thickness (Varying Surface Area and Annulus Test)	138
XXVII. Experimental Data for 7/16 inch Air-gap Thickness (Varying Surface Area and Annulus Test)	140
XXVIII. Experimental Data for 1/2 inch Air-gap Thickness (Varying Surface Area and Annulus Test)	142

Table	Page
XXIX. Experimental Data for 11/16 inch Air-gap Thickness (Varying Surface Area and Annulus Test)	144
XXX. Experimental Data for 1/32 inch Dielectric Wall Thickness (Varying Wall Thickness and Annulus Test)	147
XXXI. Experimental Data for 1/16 inch Dielectric Wall Thickness (Varying Wall Thickness and Annulus Test)	149
XXXII. Experimental Data for 3/16 inch Dielectric Wall Thickness (Varying Wall Thickness and Annulus Test).....	151
XXXIII. Experimental Data for 1/8 inch Dielectric Wall Thickness (Varying Wall Thickness and Surface Area Test)	154
XXXIV. Experimental Data for 1/16 inch Dielectric Wall Thickness (Varying Wall Thickness and Surface Area Test)	156
XXXV. Experimental Data for 1/8 inch Dielectric Wall Thickness (Varying Wall Thickness and Surface Area Test)	158
XXXVI. Experimental Data for 1/4 inch Dielectric Wall Thickness (Varying Wall Thickness and Surface Area Test)	160
XXXVII. Variation of Secondary Voltage with Frequency at Constant Primary Voltage (Heat Generation Test)	163
XXXVIII. Variation of Secondary Current with Frequency at Constant Primary Voltage (Heat Generation Test)	165
XXXIX. Variation of Exit Gas Temperature with Frequency at Constant Primary Voltage (Heat Generation Test)	167
XXXX. Variation of Ozone Concentration with Frequency at Constant Primary Voltage (Heat Generation Test)	169
XXXXI. Variation of Exit Gas Temperature with Time at Constant Primary Voltage (Heat Generation Test)	171
XXXXII. Variation of Ozone Concentration with Time at Constant Primary Voltage (Heat Generation Test)	173

Table	Page
XXXXIII. Variation of Secondary Voltage with Time at Constant Primary Voltage (Heat Generation Test)	174
XXXXIV. Variation of Secondary Current with Time at Constant Primary Voltage (Heat Generation Test)	176
XXXXV. Reproducibility Data for Open-circuit Tests	178
XXXXVI. Reproducibility Data for Variation of Secondary Voltage/Current, Temperature, and Concentration with Frequency	179
XXXXVII. Reproducibility Data for Variation of Secondary Voltage/Current, Temperature, and Concentration with Time	183

LIST OF FIGURES

Figure		Page
1.	Plasma Reactor	2
2.	Schematic of Plasma Reactor System	27
3.	Variation of Secondary Voltage with Frequency at Different Primary Voltages Under Open-circuit Conditions	35
4.	Variation of Secondary Current with Frequency at Different Primary Voltages Under Open-circuit Conditions	36
5.	Variation of Power Factor with Frequency	39
6.	Electrical Breakdown of Phenolic Resin (Paper-filled)	
	(a) Inner Dielectric	42
	(b) Outer Surface of the Outer Dielectric	44
	(c) Inner Surface of the Outer Dielectric	45
7.	Electrical Breakdown of Phenolic resin (Glass-filled)	
	(a) Inner Dielectric	47
	(b) Outer Surface of the Outer Dielectric	48
	(c) Inner Surface of the Outer Dielectric	49
8.	Electrical Breakdown of CAB Resin	
	(a) Rupture of the Inner Dielectric	54
	(b) Dimensional Change of the Inner Dielectric	52
	(c) Rupture of the Outer Dielectric	55
	(d) Dimensional Change of the Outer Dielectric	53
9.	Variation of Secondary Current with Time at Constant Primary Voltage (Usability Tests)	58
10.	Variation of Exit Gas Temperature with Time at Constant Primary Voltage (Usability Tests)	59

Figure

11.	Variation of Secondary Voltage with Time at Constant Primary Voltage (Usability Tests)	60
12.	Variation of Secondary Voltage with Frequency at Constant Primary Voltage (Usability Tests)	62
13.	Variation of Secondary Current with Frequency at Constant Primary Voltage (Usability Tests)	63
14.	Variation of Exit Gas Temperature with Frequency at Constant Primary Voltage (Usability Test)	64
15.	Electrical Breakdown of Pyrex Glass	67
16.	Electrical Breakdown of Quartz Glass	70
17.	Variation of Air Breakdown Voltage with Dielectric Constant (k) at Various Primary Voltages	71
18.	Variation of Air Breakdown Voltage and Strength with Air-gap Thickness (Varying Surface Area and Annulus Width Test)	74
19.	Secondary Voltage Required to Produce an Ozone Concentration of 150 and 200 ppm for Different Air-gap Thickness (Varying Surface Area and Annulus Width Test)	79
20.	Variation of Air Breakdown Strength with Dielectric Wall Thickness (Varying Thickness and Annulus Width Test)	80
21.	Variation of Air Breakdown Strength with Dielectric Wall Thickness (Varying Thickness and Surface Area Test)	82
22.	Secondary Voltage Required to Produce an Ozone Concentration of 150 and 200 ppm for Different Air-gap Thickness (Varying Thickness and Surface Area Test)	83
23.	Variation of Exit Gas Temperature with Frequency at Constant Primary Voltage (Heat Generation Test)	87
24.	Variation of Secondary Current with Frequency at Constant Primary Voltage (Heat Generation Test)	84

Figure		Page
25.	Variation of Secondary Voltage with Frequency at Constant Primary Voltage (Heat Generation Test)	86
26.	Variation of Ozone Concentration with Frequency at Constant Primary Voltage (Heat Generation Test)	87
27.	Variation of Secondary Current with Time at Constant Primary Voltage (Heat Generation Test)	89
28.	Variation of Exit Gas Temperature with Time at Constant Primary Voltage (Heat Generation Test)	93
29.	Variation of Ozone Concentration with Time at Constant Primary Voltage (Heat Generation Test)	90
30.	Variation of Secondary Voltage with Time at Constant Primary Voltage (Heat Generation Test)	91
31.	Liquid Electrode Plasma Reactor - a Pipe-dream?	99

NOMENCLATURE

C_{air}	capacitance of air, μF
C_{inner}	capacitance of the inner cylinder, μF
C_{outer}	capacitance of the outer cylinder, μF
C_{total}	total capacitance of the reactor, μF
L	length of the discharge zone, m
d_1	inner diameter of the inner dielectric, m or inch
d_2	outer diameter of the inner dielectric, m or inch
d_3	inner diameter of the outer dielectric, m or inch
d_4	outer diameter of the outer dielectric, m or inch
k_a	dielectric constant of air, dimensionless
k_g	dielectric constant of dielectric material, dimensionless

CHAPTER I

INTRODUCTION

Numerous studies have been carried out by engineers and scientists on the subject of electrical insulation. An engineer generally has the choice of several insulating materials for any particular engineering application. Selection of the best material demands a thorough knowledge of the electrical and mechanical functions to be performed by the insulation. Also, for proper selection, an engineer must consider the operating requirements, including the effects of moisture and oxidation which promote electrical and chemical degradation of the insulation.

The need for an insulating material in plasma reactors can be realized through an understanding of the breakdown of air between two electrodes. Under normal conditions, air and most other gases are almost complete non-conductors of electricity. But, if the voltage (alternating or direct current) between two electrodes (conductors) is sufficiently increased, the air which serves as a dielectric (insulating medium) suddenly loses part or almost all of its insulating properties. The electric breakthrough in air occurs in the form of a spark or an arc, starting as a glow on the electrodes (violet, feebly glowing light) and with further increase of voltage, changing to a discharge in the form of one or more light brushes. The breakthrough is complete when the air starts to arc between the electrodes (Schwaiger and Sorensen, 1932). In this study the reactor in which ozone is to be generated consists of two concentric cylinders (inner and outer electrodes) with an air gap in the annulus (Figure 1). Application of a high voltage is essential to change oxygen to

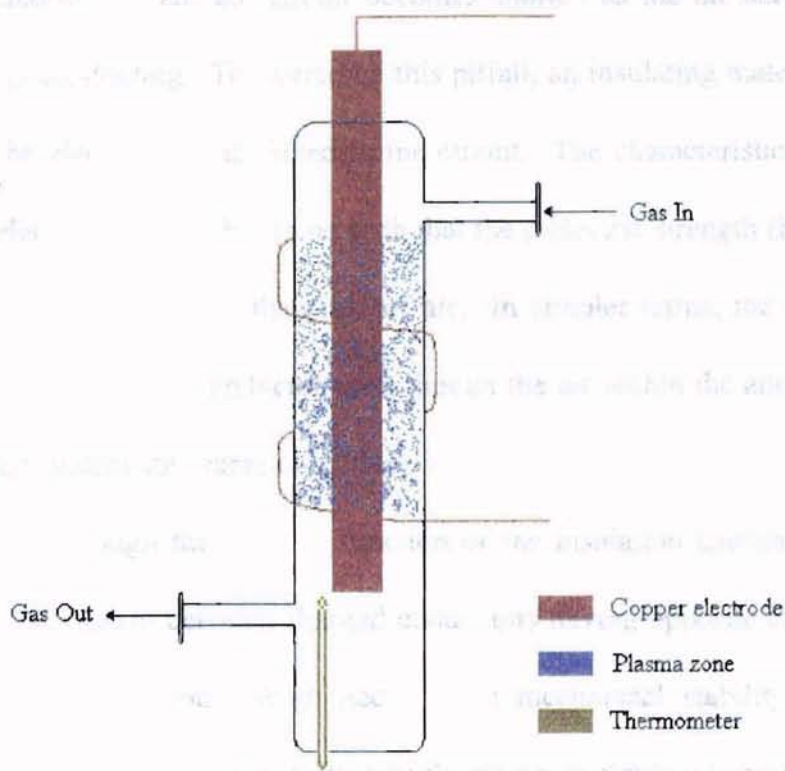


Figure 1. Plasma Reactor

its elemental state for ozone generation. Since this would cause an almost complete breakdown of air, the circuit becomes shorted as the air between the metal electrodes starts conducting. To overcome this pitfall, an insulating material taking the same shape as the electrodes is included in the circuit. The characteristic of the insulating material (dielectric) chosen should be such that the dielectric strength (breakdown strength) of the solid is much higher than that of air. In simpler terms, the insulating material should always be a poor conductor even though the air within the annulus becomes a conductor under electric discharge conditions.

Though the primary function of the insulation chosen is to prevent the flow of electric current between charged conductors having opposite charges, there are two more important functions which need focus: mechanical stability and heat transfer. The mechanical stress which is frequently set up in electrical equipment during long periods of commercial use amplifies the mechanical stability of the material as an important criteria for viability as a dielectric. The importance of the third function, heat transfer, is amplified for a system undergoing highly exothermic reactions. The heat released must be adequately dissipated to prevent excessive heat accumulation which would lead to the decomposition of the material flowing through the annulus or the destruction of the insulating material itself. The effect of increased temperatures on ozone production have been discussed by Horvath et al. (1985): *the gas stream (air or oxygen) entering the region of electrical discharge takes up the temperature of the discharge space, under steady interchange with the temperature of its surroundings (discharge space). If the temperature of the discharge is low, there is practically no ozone decomposition and the ozone concentration in the product increases proportionally to the electrical power*

supplied to the system. If the dielectric material has poor heat transfer characteristics, a substantial increase in gas stream temperature can be expected. This would lower both the energy yield efficiency and ozone concentration at the outlet, which in this study is undesirable. In addition, heat is also generated by the dielectric losses (discussed in Chapter II) in the insulation. For adequate heat dissipation, the dielectric should possess excellent thermal conductivity. The thermal conductivity of an insulation may in some applications have an importance which transcends even the mechanical and dielectric properties of the insulation (Clark, 1962).

My predecessors in plasma research conducted at Oklahoma State University have always used pyrex or quartz glass as the dielectric material because of easy availability and cheaper costs. Pyrex glass usage was often hampered by the cracks that frequently developed in the material during short or long-time exposures to high voltage stress. Quartz glass proved to be a better alternative, but is also susceptible to high voltage stress. The inefficacy of glass as a dielectric stems from the fact that the heat conductivity of glass is low, irrespective of its composition. The low heat conductivity of glass accentuates the problem of glass breakage due to internal mechanical stresses caused by thermal gradients developed during its use in plasma reactors. The tendency of glass to be destroyed is also closely related to its thermal expansion which can be high for particular compositions (Clark, 1962). Quartz glass, which is characterized by the lowest value of thermal expansion, has the greatest resistance to thermal effects. For the current reactor setup, the presence of continuous electrical stress may propagate thermal gradients within the solid dielectric thereby initiating the cracking of glass. Properties of quartz and pyrex glass have been included in Table I (Appendix A).

The specific objectives of this thesis are :

- (1) evaluate the usability of different dielectric materials in plasma reactors,
- (2) determine the influence of surface area and thickness of dielectric material used on ozone generation,
- (3) investigate the effects of sustained periods of reactor operation on ozone generation for different materials and hence determine suitable dielectric materials.

CHAPTER II

LITERATURE SURVEY

Background

The correct choice of insulating material is governed by an in-depth review of the factors (electrical, chemical and mechanical) which are required of the insulation. Insulation breakdown in commercial use is more frequently the result of chemical degradation than inherent dielectric defects in the material (Clark, 1962). To assess the contribution of dielectric breakdown due to chemical means, an understanding of the plasma state and its chemistry is required.

Definition of plasma state

A simple definition of a plasma is: *an ionized gaseous complex which may be composed of electrons, ions of either polarity, gas atoms, and molecules in the ground or any higher state of any form of excitation* (Venugopalan, 1971). A plasma can be generated by the application of high electrical energy between electrodes so that the air or gas molecules in between are ionized and hence, conduct electricity. During the occurrence of any type of discharge, thermal and electron effects are involved which result in the formation of ions initiating the discharge. The formation of a host of chemically active species including free radicals and ions (positive and negative) in the plasma state provides the basis for chemically destroying or generating different chemical

species (Horvath et al., 1985). The chemical species thus generated may have adverse effects on the dielectric properties of the material. For instance, an insulating material like polyethylene which is sensitive to oxidation should not be used in a plasma system. In the manufacture of ozone generating equipment, special materials like PVC are used for parts which are in direct contact with ozone.

Major factors affecting choice of insulation

The discussion in this section is limited to a brief review of those electrical factors which are important in the application of insulation in plasma reactors from a commercial standpoint. Based on this discussion, material selection will be dealt with in the following chapter.

Electric Field

In most commercial applications, the electric field to which the insulation is subjected is rarely uniform. This lack of uniformity may be due to irregularities on the conductor surface. The lack of uniformity in the electric field subjects the insulation to localized field strengths of higher value. The presence of these localized areas of high field strength frequently results in the inefficient use of insulation (Clark, 1962). This may lead to use of a dielectric wall thickness much greater than that required for a uniform electric field; hence, a sizable increase in the manufacturing cost of the equipment. An ideal way to circumvent this problem would be to use liquid electrodes on the inside and outside of the annular gas-gap. However, the associated problems of

choosing appropriate solutions would require extensive research and is beyond the scope of this thesis.

Dielectric Strength

The dielectric strength of insulation (frequently referred to as the electric or insulation breakdown strength) is the minimum voltage which can be applied to a material with the resulting destruction of its insulating properties. Most frequently, the dielectric strength value is indicated by the passage of an arc through the insulation (Clark, 1962). As discussed earlier, care should be taken to ensure the dielectric strength is greater for the insulating material than for the gas-gap. If the dielectric were to break down at a voltage lower than or equal to gas breakdown voltage, current would pass through the insulating material initiating the arc through the material. This arcing may result in a crack through the material at its weakest point, indicating the passage of electric current through it. This would render the reactor inoperable because of the inability of the material to provide a dielectric barrier.

Insulation Life

Insulation life is defined as the period of time during which the insulation can be exposed to conditions which promote degradation without decrease in its properties beyond those values which have been previously established to define its limit of usability (Clark, 1962). The properties primarily under consideration to quantify insulation life are electrical and chemical. This thesis is essentially a step towards establishing a procedure to determine the properties required for an apt choice of dielectric material for use in

plasma reactors. At present no literature exists which provide the property values beyond which dielectric usage in plasma reactors becomes improbable. Since extensive testing of different dielectric materials is labor and cost intensive, no attempts were made to establish the limiting values for properties (for instance, thermal conductivity or coefficient of thermal expansion). Instead, tests for insulation life were considered as that period of time during which voltage can be applied to the insulation under the exaggerated conditions of its use without dielectric breakdown as mentioned by Clark (1962). Based on this definition, insulation life can be quantified directly for those materials which fail during the dielectric usability tests. For other materials, tests for insulation life will be based on the insulating material's ability to

- (1) maintain a sustained plasma free from arcing,
- (2) resist excessive heating due to prolonged external stress (period of 18 hours), and
- (3) withstand electrical fractures (cracks due to arcing).

With regard to insulation life based on chemical degradation, the primary focus is on oxidation degradation properties of the insulating material tested. For the purpose of this thesis, only those materials which are strongly resistant to oxidation over a long period of time have been considered. Physical changes in the material, if any, at the end of the usability tests were used to gauge the utility of the insulating material as a dielectric for our system.

A key point which has relevance to insulation life is the concept of functional testing. The usability tests for the dielectric material were conducted in a flowing air system. Since the overall objective was to use an air system to generate ozone, the usability tests simulate the actual conditions. Hence, the stability of the material under

actual conditions could be estimated based on usability studies. For example, a dielectric material which has resistance to pyrolysis but is extremely susceptible to chemical degradation when air is present may be classed in two ways (Clark, 1962):

- (1) its usability limitations in the presence of air, and
- (2) its usability limitations in the absence of air.

So, an insulating material best suited for this system may not be adequate for a different system due to problems of chemical degradation. However, a material which has an obvious dielectric defect (for instance, excessive affinity for moisture or high coefficient of thermal expansion) may be eliminated from future considerations for material selection.

Dielectric Loss

When an alternating voltage is applied between two electrodes, the dielectric material is subjected to periodic stresses and displacements. If the material were perfectly elastic, no energy would be lost during any cycle, because the energy stored during the periods of increased voltage would be given up to the circuit when the voltage is decreased. However, since the electric elasticity of dielectrics is not perfect, the applied voltage has to overcome molecular friction or viscosity, in addition to the elastic forces. The work done against friction is converted into heat and is lost. This is termed the dielectric loss of the material (Clark, 1962).

It must be understood that only a perfect dielectric passes no conduction current between the charged electrodes. All practical dielectrics conduct electricity to a greater or lesser extent under the influence of an electric field. The presence of this conductivity in

dielectrics frequently determines their commercial usability. The actual dielectric loss of most commercial dielectrics varies as a function of the frequency of the voltage applied. At high frequencies, the molecular constitution of the dielectric material departs further from that of electrical symmetry and hence, dielectric loss becomes more pronounced (Clark, 1962). In this experimental setup, the reactor is operated at higher frequencies to ensure excitation of free electrons and ions within the gas-gap so that they gain enough kinetic energy to generate more free radicals by impact or collision. Since energy expended to the walls as dielectric loss is undesirable, the material chosen should exhibit low dielectric loss characteristics.

The dielectric loss of a material can be quantified in terms of frequency and dielectric loss (or power) factor which is the product of the dielectric constant of an electrical insulating material (to be defined in the subsequent section) and the tangent of the dielectric loss angle. The charging current of a perfect dielectric will lead the applied voltage by 90 degrees. The angle by which the current vector of a commercial (imperfect) dielectric is less than 90 degrees is designated as the dielectric loss angle (Clark, 1962). Experimental values are available for dielectric loss angle at different frequencies which may be used to calculate the dielectric loss of a material at a particular frequency.

Dielectric Constant

The dielectric constant is defined as the ratio of the capacitance of a material measured with a given electrode configuration to the capacitance of the same electrode configuration and spacing with air (or vacuum) as a dielectric (Clark, 1962). The value obtained is usually qualified with reference to the conditions of its measurement (voltage,

frequency, and temperature). Capacitance is a measure of the energy storable in a material in the presence of an electric field. It reflects the ability of a conductor-dielectric system to contain electrostatic charge.

The value of the dielectric constant depends on the number of atoms or molecules per unit volume (molar density) and the ability of each to be polarized (have a net displacement of charge in the direction of the applied voltage stress). Values of dielectric constant range from unity for vacuum to slightly greater than 10,000 for titanate ceramics (Fink and Beaty, 1978). The choice of a material for this system based on dielectric constants requires a knowledge of the effect of AC voltage stress distribution across a composite insulation. It was assumed that the gas-gap and the dielectric material together can be considered as two dielectrics in series based on the system configuration. Clark (1962) has determined the ratio of voltage stress distribution across a dielectric assembly for materials of equal thickness to be inversely proportional to the dielectric constants of the materials present. The objective was to create a plasma state with minimum supply of energy for an electrode configuration. To achieve this, energy utilization has to be a maximum (i.e.) most of the energy supplied to the reactor should be utilized by the gas to reach a higher energy state (plasma). This would favor a higher voltage stress in the gas-gap to ensure quicker breakdown of the gas. Hence, a material of high dielectric constant (much higher than the dielectric constant of the gas) would be most suitable for this system if the thickness of the dielectric and the gas-gap are both the same. But, in the experiments which follow, the gas-gap to dielectric thickness ratio is much higher than one. So, a wide range of materials having different dielectric constants were tested to determine the effect of dielectric constants on ozone generation.

Dielectric Polarization

Polarization is the net displacement of charge in a dielectric material under the influence of an electric field. This phenomenon can be understood better by considering a capacitor having two metal electrodes and air in between. On application of an external voltage (ac or dc), electrostatic charge is set up on the conductors. The charges on the plates cause an electric field in the space between the plates. When a dielectric is introduced into the conductor while the external voltage is kept constant, more charge flows into the capacitor whose storage capacity (capacitance) is increased by the presence of the dielectric. The increased capacitance is due to the polarization of the dielectric in the sense that positive and negative charges within it are displaced slightly from their normal positions. Since matter is built up from charged units, greater or lesser displacements of this kind occur in every material.

The need for understanding polarization can be illustrated by analyzing the current-flow characteristics of dielectrics. Current flow in dielectrics can be divided into two parts (Fink and Beaty, 1978):

(a) the true current, which is constant with time and would flow indefinitely, is associated with a transport of charge from one electrode into the dielectric, through the dielectric, and out into the other electrode. For this system, there are two additional layers to be penetrated also, which are the gas-gap and second wall of dielectric.

(b) the polarization or absorption current, which involves, not charge flow through the interface between the dielectric and the electrode, but rather the displacement of charge within the dielectric.

Polarization current results from any of the various forms of limited charge displacement which can occur in the dielectric. The displacements occurring first (in the order of nanoseconds) are those corresponding to electron displacement with respect to the nuclei (electronic polarization), which is responsible for the very-high frequency polarizability of the material (Hippel, 1995). Electronic polarization responds to changing field instantaneously at all frequencies used for electrical measurements and hence, is not observable. The displacement most commonly observed in the dielectric is due to the very slow rotation of dipolar molecules and groups moving up to internal barriers in the material. This displacement (dipole polarization) can occur only in molecules which have a slight positive or negative charge present due to the stronger attraction of a particular atom for electrons. Hence, polar materials tend to turn in an electric field. This effect does not occur in balanced or symmetrical molecules which do not have a net positive or negative charge. Only electronic polarization can occur for materials made up of symmetrical molecules. Dipole polarization would increase the polarization charge which would cause an increase in the total current flowing through the material. The question as to whether a high current is desirable for formation of plasma state, even though the power supplied increases for a fixed secondary voltage remains to be determined. From the insulation life standpoint, higher current flowing through the material is undesirable because this may cause heating of the dielectric which in turn may result in freeing of electrons so that a higher current flows, initiating a cascade effect.

Ozone generation by electrical discharge

Currently, there are five principal methods by which ozone can be generated for the beneficial use of its powerful biocidal and oxidizing properties. Four of these techniques viz., photochemical, thermal, chemonuclear, and electrolysis, have very limited use in industrial applications. Synthesis of ozone from molecular oxygen by silent electrical discharge is the only method widely used for production on an industrial scale since it is the most economical process. The reaction is carried out in an ozonizer in which the electric discharge takes place between electrodes connected to a high-voltage source (5000 to 30000 volts). The electrodes are separated by a dielectric layer (glass or ceramic) and a gas-gap. Air or oxygen is passed through the gas-gap and reacts to form ozone. Glass was used as the dielectric material in the earliest generators. Ceramic materials are currently more popular, but the high costs associated with manufacture of ceramics in addition to mechanical inadequacies, has paved way for use of polymers as a substitute.

Mechanism of ozone formation in electric discharge

To determine the effect of the major parameters viz., form of applied voltage (ac or dc), magnitude of voltage, distance between electrodes, the gas in the electrode space and state of the gas (pressure, temperature) on the formation ratios and equilibrium constants, a clear idea about the reaction mechanism is required.

The synthesis of ozone from air or oxygen is characterized by numerous contradictions based on thermodynamic considerations. Intuitively, the main reaction for ozone formation has to be endothermic, (i.e.) the reaction can take place only with

consumption of thermal energy to convert the stable oxygen molecule into ozone. Although, according to the equation



the gas-phase reaction for ozone formation takes place endothermally with an energy input of $\Delta H = 143 \text{ KJ/mole}$, the equilibrium constant remains negligible even at

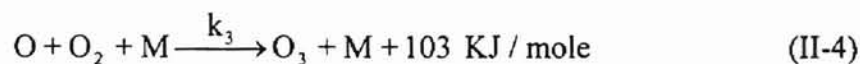
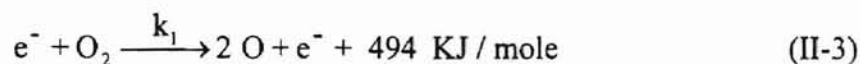
temperatures of several thousand Kelvin (i.e.) $K_c = \frac{k_1}{k_2} = \frac{[\text{O}_3]^2}{[\text{O}_2]^3} \rightarrow 0$. This implies

that the rate of ozone decomposition is greater at high temperatures. Hence, the required energy cannot be made available exclusively by thermal action. Horvath et al. (1985) confirmed that the energy required has to be transmitted by way of electron excitation to ensure that the excited molecules or oxygen atoms generated by collision process react to form considerable amounts of ozone. By supplying energy with electron excitation, if the oxygen molecule has an energy of about 143 KJ / mole in the excited state, the reaction can take place according to the equation

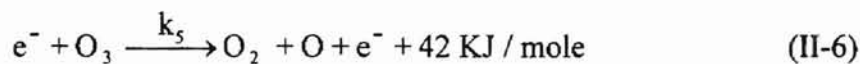
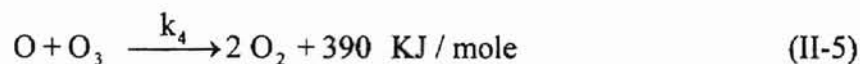


at constant temperatures. Benson and Axworthy (1975) have shown that the equilibrium constant k_3 is too small for rapid formation of ozone in the temperature range between 273 and 373 K. Operation at higher temperatures to achieve higher conversions is impossible due to the increasing decomposition rate of ozone. Hence, generation of ozone according to equation (II-2) is negligible. Pignolet et al. (1990) and Horvath et al. (1985) have proposed a scheme of four governing equations which can be regarded as the most simplified process for formation and decomposition of ozone in a gas discharge.

Formation Mechanism :



Decomposition Mechanism :



For formation of O atoms according to the above equation, the threshold energy required for production of excited electrons is 494 KJ / mole (5.1 eV). Using an analytical method to calculate the ozone production in a single discharge based on the above mechanism, Gutierrez-Tapia et al. (1994) have shown that the most important parameter affecting the efficiency of ozone production is the atomic oxygen concentration. This would mean that oxygen atom generation through equations (II-3) and (II-6) and decomposition through equations (II-4) and (II-5) would control the rate of ozone production. The suggested mechanism is based on the existence of an ideal silent electric discharge. In practice, it is not possible to achieve this condition due to feed gas contamination, non-uniformity of electrodes, and dielectric deformation resulting from thermal effects due to continuous operation (Horvath et al., 1985).

CHAPTER III

MATERIAL SELECTION

The first step in the selection of an insulating material for a specific engineering application must include the written enumeration of those conditions to which the material will be subjected while in use. Table II gives a listing of the conditions which the dielectric material may have to withstand for ozone generation using electrical discharge reactors developed at Oklahoma State University.

TABLE II
Parameters for plasma reactor.

Parameters	Condition
System	Air and ozone
Maximum Voltage	15000 volts
Frequency Range	60 to 1000 Hz
Pressure	Atmospheric
Inlet gas (air) temperature	Approximately room temperature
Flow	3.5 liters/min.

The next step is to establish a listing of the properties which must be possessed by the dielectric selected. In compiling such lists, the importance of each property, the interrelation of one property with another, and the requirement, based on its effects on the

proper functioning of the reactor subject to normal and extreme conditions must be evaluated. Table III gives a listing of the properties to be considered for assessing potential insulating materials along with their requirements, effects on reactor functioning and variation with temperature and frequency.

Material selection has been made from two different classifications of modern insulating materials currently popular commercially, viz. : plastics and ceramics.

Plastics

Material selection from plastics has been made from the two main classes available, viz. thermoplastic and thermosetting materials.

Thermoplastic Materials

Thermoplastic materials are compounds which may be deformed under the influence of heat and pressure, retaining their new shape on cooling and releasing the pressure, but which may again be re-softened by heat and re-molded (Fleck, 1949).

These materials consist of long linear molecules which may have some branching but are not interconnected (cross-linked) to other molecules.

TABLE III
Desirable properties for plasma reactors

Properties	Requirement	Effect on reactor	Variation with temperature	Variation with frequency
Electrical:				
Dielectric constant	Not known	Increases capacitance / polarizability	Decreases	Decreases
Power factor	Low value	Increases energy losses	Increases	Usually has a maxima
Dielectric strength	High value	Reduces scope for electrical puncture	Decreases	Usually decreases
Volume resistivity	High value	Lowers electrical conduction	Decreases	*
Surface resistivity	High value	Lowers electrical conduction	Decreases	*
Mechanical :				
Tensile strength	High value	Reduces mechanical rupture	*	*
Compressive strength	High value	Reduces mechanical rupture	*	*
Impact strength	High value	Reduces mechanical rupture	*	*
Thermal :				
Coefficient of thermal expansion	Low value	Reduces tensile stress	*	*
Thermal conductivity	High value	Reduces tensile stress	Increases	*

* - data not available based on literature review made in this study

Typically, thermoplastic materials are characterized by toughness, stiffness, smoothness (low friction properties), resistance to weathering, dimensional stability, and good thermal stability (Fink and Beaty, 1978). The thermoplastic materials listed with their structural advantages or limitations in Table IV (Fink and Beaty, 1978) have been chosen for experimentation. Their properties are listed in Table I (Appendix A).

TABLE IV
Evaluation of thermoplastic materials selected.

Thermoplastic Material	Characteristic	Advantage	Limitations
Acrylics (plexiglas)	Moderately polar	Excellent weathering resistance, good electrical insulation, dimensional stability	Mechanical and electrical properties are strongly dependent on temperature
Cellulose Acetate Butyrate (CAB)	Moderately polar	Non-flammable, high dielectric strength	Weak chemical resistance, susceptible to strain.
Polycarbonate	Slightly polar	Excellent rigidity / toughness (upto 140 °C), self-extinguishing, good insulation.	--
PVC, nonrigid (unfilled, 25 % plasticizer)	Moderately polar	Excellent chemical resistance, good insulation.	Moderate water absorption.
PVC, rigid (5 % plasticizer)	Moderately polar	Excellent chemical resistance, good insulation.	High water absorption.

Thermosetting Plastics

Thermosetting plastics are partly polymerized materials which may be deformed under the influence of heat and pressure, the material being converted into an infusible product not responsive to pressure (Fleck, 1949). Unlike thermoplastic materials,

thermosetting materials cannot be re-softened because a chemical change takes place during initial heating which makes the shape permanent. In general, thermosetting resins are combined with fillers and reinforcements to provide adequate strength to the material. Reinforcements may be fiberglass, synthetic fibers, or cellulose. A Phenolic was the only material chosen for testing amongst the various thermosetting plastics available. Table V (Fink and Beaty, 1978) lists the structural limitations of phenolics for paper- and glass-fillers. Electrical, mechanical and thermal properties of phenolics have been listed in Table I (Appendix A).

Electrical tracking is the formation of a permanent conducting path at an interface (usually between an electrode and a insulating medium) in an insulating system caused by localized concentration of surface currents or by an electrical flashover, resulting in the pyrolytic decomposition of the surface layer of the insulation in the area affected (Clark, 1962). The voltage favoring the occurrence of tracking in a phenolic resin is usually very high (about 30,000 volts), leaving enough scope for its usage in the plasma system.

Table V
Evaluation of thermosetting plastics selected.

Thermosetting Material	Characteristic	Advantage	Limitations
Phenolic - glass filled	Highly polar	Good thermal and water resistance	Tracks under arcs
Phenolic - paper-filled	Highly polar	Good chemical and thermal resistance	Susceptible to water absorption, tracks under arcs

Ceramics

Ceramic materials are characterized by excellent chemical and dielectric stability over a wide range of operating temperatures. In comparison with plastics, the mechanical properties (especially, impact strength) of ceramics are inadequate. However, ceramic materials are widely used in a multitude of dielectric applications. The electrical and physical properties of ceramics are greatly influenced by the relative portions of the crystalline and amorphous phases which are present. The firing operation plays a significant role in determining the crystalline structure and the relative amounts of the crystalline and amorphous phases of the ceramic (Clark, 1962).

The classification of ceramics for dielectric use may be described broadly as clay containing porcelains, alumina ceramics, talc containing steatites and the titanates. The composition of each type varies widely, depending on the specific engineering requirement. Chemically, a ceramic insulation is usually made from a combination of silicon dioxide, aluminium oxide, magnesium oxide, zirconium oxide, or titanium oxide. Each of these oxides contributes a special quality to the fired commercial ceramic. This special quality may concern any of the following properties : electrical resistance, power factor, dielectric constant, dielectric strength, coefficient of linear expansion, heat conductivity, and impact or compression strength (Clark, 1962).

The ability of a ceramic body to withstand a heat shock depends upon thermal conductivity and coefficient of linear expansion. The basic factor causing dielectric breakdown is the establishment of a high thermal gradient within the ceramic body. Although silent discharge reactors operate essentially under isothermal conditions, heat accumulation within the dielectric will occur due to increased dielectric losses over long-

time exposure to electrical stress. Destruction of the dielectric inevitably follows the establishment of a high thermal gradient within the ceramic body because of the severe tensile stresses which are formed as the result of localized thermal expansion. Those ceramic structures which possess the highest thermal conductivity and the lowest thermal expansion characteristics possess the greatest resistance to thermal shock (Clark, 1962).

Ceramic materials carry exorbitant costs - the purchased alumina tubes (one foot in length) cost \$30 apiece, the least expensive variety available commercially. Other high-glazed ceramics which possess excellent thermal and electrical properties range between \$300 and \$1000 (one foot length) in cost. The dimensions of the inner and outer tubes have been mentioned in Table VII (Chapter IV). Since the focus of this study was on viable cheaper materials, only alumina (99.5 % pure) was tested. Table VI (Fink and Beaty, 1978) shows the structural advantages or limitations of alumina ceramics. Properties for alumina ceramics have been included in Table I (Appendix A).

Table VI
Evaluation of ceramic material selected

Ceramic Material	Characteristic	Advantage	Limitations
Alumina (99.5 % pure)	Highly polar	Extreme hardness, permanent dimensional stability, chemically inert, superior resistance to wear and abrasion, excellent electrical properties	Low compressive strength; exorbitant cost.

CHAPTER IV

EXPERIMENTAL SETUP AND PROCEDURE

Experimentation involved two phases. The first phase of the experimental effort was oriented towards material testing for usability in plasma reactors. The second phase of the experiments viz., ozone-generation, was done only for those materials which proved adequate for dielectric use based on the usability tests. Though the feed stock (air) was not hazardous, the product generated, ozone, may pose an environmental hazard at higher concentrations. Hence, the reactor system was housed under a well-ventilated hood.

Equipment calibration

The flow meter was calibrated for air under ambient conditions using a bubble flow meter. The time taken for the bubble to flow the length of a 100 ml burette was clocked, thus giving the actual flow corresponding to the rotameter scale.

The auxiliary electrical instruments used (ammeter, voltmeter, and Cathode Ray Oscilloscope (CRO)) were calibrated at the Electrical Engineering Lab at OSU using previously calibrated instruments.

Experimental apparatus description

The discharge reactor was constructed using two concentric cylinders with an annulus in between the inner and outer cylinders. Ports for gas inlet and outlet were

made by drilling holes through the outer cylinder wall, with tygon tubing of appropriate size inserted to enable gas in- and out-flow through the reactor. To prevent gas leakage around the tubing, a sealant was used to block the area not covered by the tygon tubing. Gas (compressed air (zero grade)) inlet and outlet ports were at the top and bottom of the reactor respectively. A copper electrode rod was positioned inside the inner cylinder such that no air-gap existed between the electrode and the dielectric wall. This electrode was connected to one end of the secondary side of a center-tapped iron-core transformer. The secondary voltage of the transformer was varied using an oscillator. The oscillator produces a nearly perfect sine wave with less than 1% distortion from 20 to 200 Hz. The output range of the oscillator was from 40 to 5000 Hz. The outer tube was wrapped with a copper mesh and connected to the other end of the secondary side of the transformer. A high voltage probe (Tektronix, Model P6015A) was used to measure the secondary transformer voltage. The output from the high-voltage probe was fed to a Cathode Ray Oscilloscope (CRO) to monitor the wave-form changes at higher frequencies and also to a digital multi-meter to measure the secondary voltage. An ammeter (0-100 mA) was connected across the secondary of the transformer to measure the secondary current. Pictorial representation of the setup has been made in figure 2.

Tests for experimentation

Open-circuit tests

Prior to material evaluation, the influence of frequency on the power (core) loss, voltage and current of the transformer was evaluated. This test was conducted to verify if

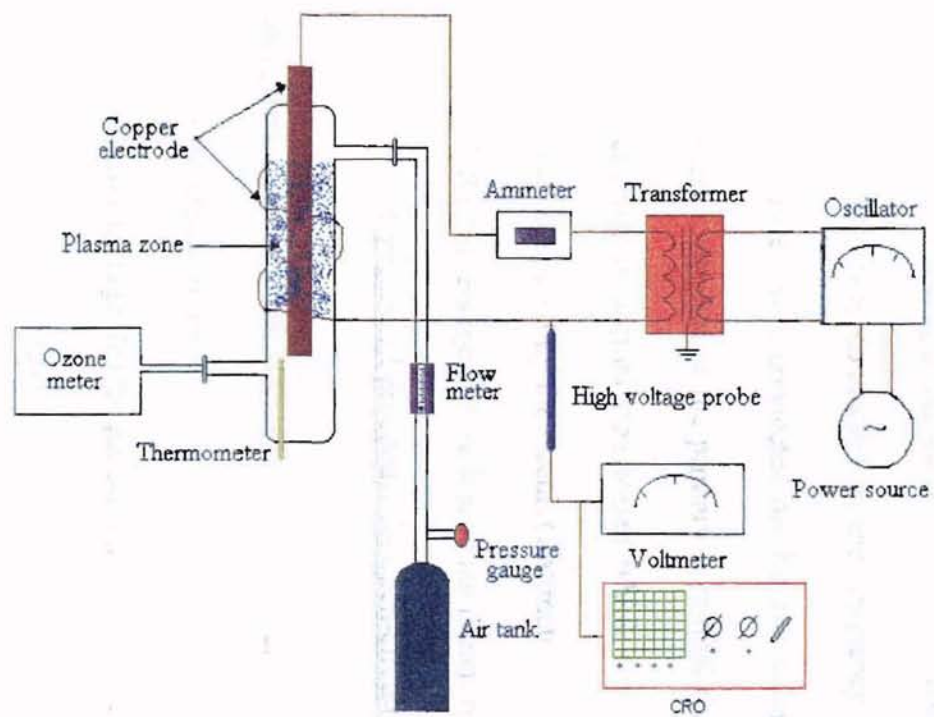


Figure 2. Schematic of Plasma Reactor System

there are any undesired effects on transformer characteristics due to its operation at a frequency greater than 60 Hz.. Operation of the system within the limits defined by this test, called the Open-Circuit Test, would ensure optimum usage of the transformer with the possibility of a transformer burn-out reduced to a minimum.

The high voltage winding of the transformer was left open (no-load condition) and the low voltage winding was connected to the frequency oscillator. A wattmeter , voltmeter and an ammeter were connected on the low-voltage (primary) winding side. For a particular voltage supplied to the primary, a normal flux was set up in the core of the transformer resulting in normal iron losses which was recorded by the wattmeter. Since the total power consumed by the circuit (wattmeter connected to the power source) was also measured, the percentage of core loss in the transformer was evaluated.

Operational procedure for open-circuit tests

- (1) The secondary side of the transformer was disconnected. This was a no-load condition for the transformer.
- (2) For a fixed primary voltage, the frequency was varied from 60 Hz until the rated voltage of the transformer (15,000 V) was reached.
- (3) The second step was repeated for different primary voltages.

Usability tests

For the chosen range (frequency and primary voltage) of operation, the dielectric usability tests were conducted. For a fixed primary voltage, the effect of extended periods of electrical stress on the dielectric material was determined by allowing the

plasma reactor to run continuously for a period of 18 hours at the maximum voltage which could be attained for a particular reactor configuration, within the maximum allowable voltage for the transformer (15,000 volts). This procedure of testing material durability was done for each material. The usability tests were conducted with air flowing through the annulus at a flow rate of 3.5 litres/minute.. Only those materials which did not fracture were considered for ozone generation. Table VII gives a listing of the materials along with the configuration used for dielectric usability tests.

Operational procedure for usability tests

- (1) The power switch of the frequency generator was turned on and the primary voltage was set. The frequency generator was allowed to run for a period of time until the wave form is perfectly sinusoidal, as confirmed by the image on the Cathode Ray Oscilloscope (CRO) screen.
- (2) Compressed air was allowed to flow through the annulus for a few minutes at a fixed flow rate to purge the gas in the annulus.
- (3) The frequency was increased until a plasma state is formed in the air flowing through the annulus and was tuned until the plasma in the annulus became uniform - an indicator of silent discharge conditions.
- (4) The system was allowed to run continuously for a period of 18 hours. The voltage and current across the secondary side of the transformer were monitored every hour.
- (5) The above steps were repeated for different materials.

Table VII
Reactor configuration for usability tests

Material	Reactor configuration			
	Inner tube		Outer tube	
	Outer diameter (inches)	Wall thickness (inches)	Outer diameter (inches)	Wall thickness (inches)
Phenolic - paper-filled	1/4	1/32	1	1/32
Phenolic - glass filled	1	1/8	2	1/16
Cellulose Acetate Butyrate	1/4	1/32	1	1/32
Acrylic	1	1/8	2	1/8
Polycarbonate	1	1/8	2	1/8
Polyvinyl chloride, rigid	1	1/8	2	1/8
Polyvinyl chloride, nonrigid (unfilled)	1	1/8	2	1/8
Alumina	1	1/8	2	1/8
Polyvinylidene fluoride	3/4	1/8	2	1/8
Quartz glass	3/4	1/32	1 1/2	1/32
Pyrex glass	1/2	1/32	1 1/8	1/32

Ozone generation tests

Ozone was generated by creating a plasma within a flowing air stream at a fixed flow rate and primary voltage. The frequency, hence the secondary voltage, was varied to determine its effects on ozone generation. The annulus width, dielectric wall thickness, and surface area of the plasma reactor with acrylic as a dielectric were varied. Finally, the impact of heat generation due to extended periods of reactor operation on ozone concentration was evaluated by adopting the same procedure as the usability tests with the ozone concentration being measured at one-hour intervals. Only those materials which pass the dielectric usability test were considered for heat generation tests. Table VIII gives a listing of the materials along with their configuration used for ozone generation tests.

Operational procedure for ozone generation tests

- (1) In addition to steps 1 to 3 in the usability tests, the concentration of ozone was measured using a Dragermeter (± 10 % accuracy) at selected frequencies for the varying surface area, annulus width, and thickness tests.
- (2) For the effect of extended periods of reactor operation on ozone generation, the reactor was operated at the frequency corresponding to the maximum ozone concentration possible for each material, within the maximum operable voltage for the transformer (15000 volts). The maximum ozone concentration was determined by making measurements at the reactor outlet for the operating frequency range at a constant primary voltage.

Table VIII
Reactor configuration for ozone generation tests

Test	Material	Reactor configuration			
		Inner tube		Outer tube	
		Outer diameter (inches)	Wall thickness (inches)	Outer diameter (inches)	Wall thickness (inches)
(I) Thickness, annulus and surface area test					
Varying surface area and annulus width test					
	Acrylic	3/8	1/16	3/4	1/8
		3/8	1/16	1	1/8
		3/8	1/16	1 1/8	1/8
		3/8	1/16	1 1/4	1/8
		3/8	1/16	1 1/2	1/8
		3/8	1/16	1 5/8	1/8
		3/8	1/16	2	1/8
Varying wall thickness annulus width test					
	Acrylic	3/8	1/16	1	1/32
		3/8	1/16	1	1/16
		3/8	1/16	1	3/16
		3/8	1/16	1	1/8
Varying wall thickness and surface area test					
	Acrylic	3/8	1/16	1	1/16
		3/8	1/16	1 1/8	1/8
		3/8	1/16	1 1/4	1/4
(II) Heat generation tests					
	Acrylic	1	1/8	2	1/8
	Poly carbonate	1	1/8	2	1/8
	PVC, rigid	1	1/8	2	1/8
	PVC, nonrigid	1	1/8	2	1/8
	Alumina	1	1/8	2	1/8
	Polyvinylidene fluoride	1	1/8	2	1/8

- (3) Ozone concentration was measured at one hour intervals to evaluate heat generation effects on functioning of reactor.
- (4) Ozone concentration measurements were made at a point just beyond the plasma so that the reduction in ozone concentration due to recombination of ozone to oxygen was avoided.
- (5) The above procedure was repeated for different materials.

CHAPTER V

RESULTS AND DISCUSSION

Open-circuit tests

The variations of secondary voltage and primary current as a function of frequency under open-circuit conditions have been illustrated in Figures 3 and 4 respectively. The trends observed were in good agreement with those of Tsai (1991) within the frequency range (60 - 950 Hz.) considered in that work. The primary current was found to reach a minimum due to increasing inductance in the primary coil and then increase with increasing frequency while the secondary voltage increased as frequency increases. Tsai (1991) has generalized this trend for all frequencies. However, tests conducted under open-circuit conditions in this study reveal that both secondary voltage and primary current go through a maxima at a higher frequency. The eventual decrease of both the primary current and secondary voltage indicated the presence of increased losses (iron losses in particular) beyond the frequency corresponding to the maxima of both. The data obtained has been tabulated in Table IX (Appendix B).

The primary input current under no-load conditions had to supply

- (1) iron losses in the core i.e. hysteresis and eddy current loss, and
- (2) a minimal amount of copper loss in the primary winding (there being no copper loss in the secondary winding as it was open).

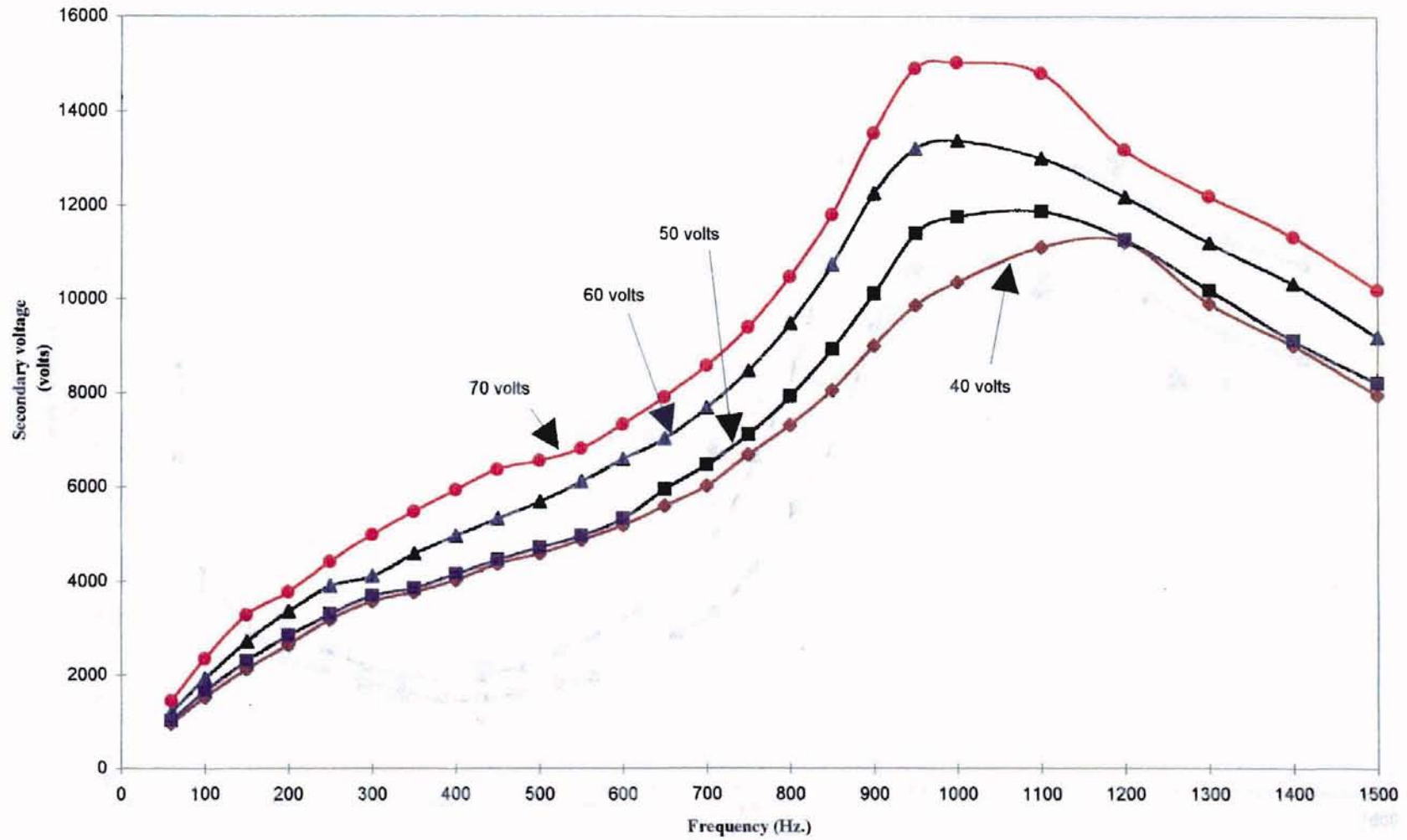


Figure 3. Variation of secondary voltage with frequency at different primary voltages under open-circuit conditions.

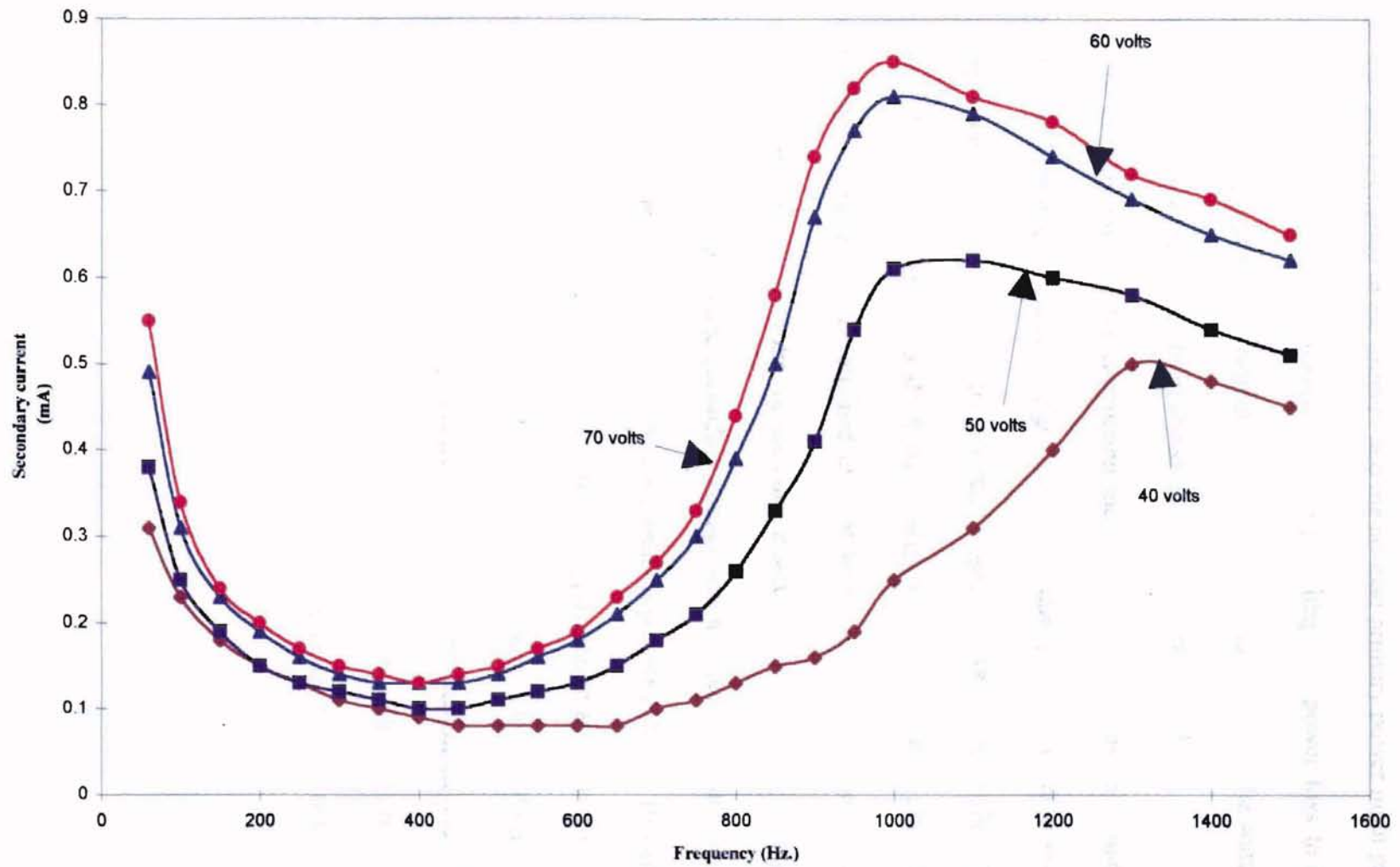


Figure 4. Variation of secondary current with frequency for different primary voltages under open-circuit

However, as the primary no-load current measured by the ammeter was very small, copper loss was negligible in the primary and the no-load primary power input practically equal to the iron-loss in the transformer. The percentage of power loss to the core, calculated as the ratio of no-load primary power input (as measured by the wattmeter) to the total system power input, has been shown in Table X (Appendix B).

The primary purpose for conducting the open-circuit tests in this study was to determine the operable frequency range for a particular primary voltage so that the maximum voltage at which the transformer can be operated was not exceeded. From the data obtained (Table IX, Appendix B), it was evident that the maximum rated secondary voltage (15000 volts) cannot be attained even at frequencies as high as 1500 Hz. for primary voltages less than 60 volts for the current setup. For a primary voltage greater than 60 volts, the maximum rated secondary voltage was attained at frequencies less than 800 Hz. Since the deterioration of dielectric materials is greater at higher frequencies due to the proportionality of dielectric loss with frequency, operation at higher frequencies to attain the same secondary voltage was desirable for this study. This would narrow down the choice of the primary operating voltage to 60 volts. The maximum rated secondary voltage was attained at a frequency of 1000 Hz. for a primary voltage of 60 volts under open-circuit conditions. Hence, the operating frequency range for the transformer was fixed between 60 and 1000 Hz.

Usability tests

The results of the dielectric usability test for the chosen range (frequency and primary voltage) of operation have been tabulated in Table XI. Though the exact cause for the failure of the tested dielectric materials could not be determined due to the functional dependence of important dielectric properties like breakdown strength, dielectric constant, and dielectric loss on temperature (little or no data is available to quantify this functional dependence), plausible reasons have been cited based on the observations made during the experimental runs. Another aspect of utmost importance was the properties of the tested materials tabulated in Table I. The values shown represent only the general class of the materials tested. Also, a range of possible values was tabulated for most of the properties. Hence, these data could never be used to make any confirmed conclusions on the exact cause(s) for the success or failure of a dielectric.

The variation of the power factor, which can be used to quantify dielectric loss as mentioned in Chapter II of this study, with frequency for a phenolic resin has been shown in Figure 5 (Clark, 1962). Though the values shown may not be the same as those for the dielectric material used in this study, it reflects the general trend followed by phenolic resins within the frequency range of interest. The high dielectric loss of the paper- and glass-filled phenolic resins may have initiated the flow of a high electric current through the material due to an increase in their temperature. The flow of a high electric current may have dislodged electrons from the material's stable molecular structure thereby increasing the current drawn even more, which is in agreement with the measured values of current as shown in Table XVII (Appendix C). This would be accompanied by

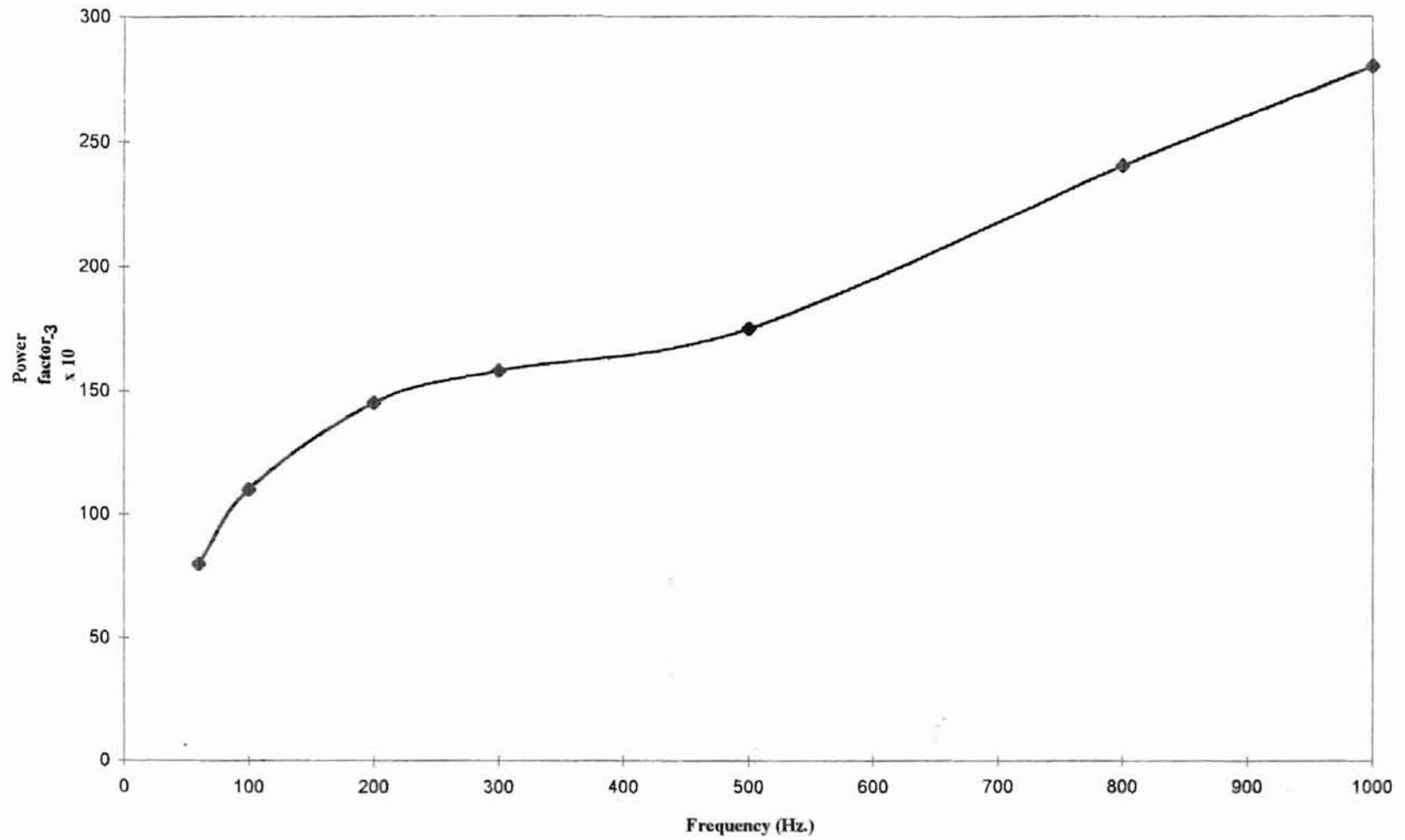


Figure 5. Variation of power factor with frequency (adopted from Clark (1962)).

Table XI
Results of usability tests conducted

Material	Test status	Failure time (hours)	Observation	Reason for failure
Phenolic (paper-filled)	Failed	0	Flow of high electric current and dielectric loss caused instantaneous heating of the material	Heating due to high current flow and dielectric loss
Phenolic (glass-filled)	Failed	11	Increasing current flow through the material with time	Heating due to high current flow and dielectric loss
Cellulose Acetate Butyrate	Failed	3	Deformation in structure of both inner and outer dielectrics	Localized field strengths of high value, exceeding breakdown strength of material
Acrylic (plexiglas)	Passed	Not applicable	Heating of air in the annulus	Not applicable
Polycarbonate	Passed	Not applicable	Negligible heating of air in the annulus	Not applicable
PVC, rigid (5 % plasticizer)	Passed	Not applicable	Heating of air in the annulus	Not applicable
PVC, nonrigid (25 % plasticizer) (unfilled)	Passed	Not applicable	High electric current did not cause material breakdown; excessive heating of air in the annulus	Not applicable
Alumina (ceramic)	Passed	Not applicable	Heating of air in the annulus	Not applicable
Polyvinylidene fluoride	Passed	Not applicable	Heating of air in the annulus	Not applicable
Pyrex glass (# 7070)	Failed	7	High current drawn caused material heating	Low thermal endurance due to low thermal conductivity and high coefficient of thermal expansion

Table XI (CONTD.)

Material	Test status	Failure time (hours)	Observation	Reason for failure
Quartz glass	Failed	12	High current drawn caused material heating	Lowering of volume resistivity

additional heating of the phenolic resin which would increase the current drawn further. Though the phenolic resin has a higher thermal conductivity than most other plastics, the requirement for spontaneous heat dissipation is never met, thereby causing severe thermal gradients within the phenolic resin. This argument has been confirmed by Whitehead (1951) for phenolic resins based on experimental values for wall temperatures. The increase in the dielectric material's temperature may have lowered its dielectric strength also, although no data seems to be available to support this viewpoint. The outcome of this cascade effect was the passage of an arc through the weakest point in the phenolic resin (see Figures 6 and 7) which caused a burn through the material in the path of the arc, as evident from the charring of both paper- and glass-filled phenolic resins.

A closer look at the charred phenolic resin suggested that surface breakdown may also have played a role in its destruction in addition to the reason cited above. The outcome of using a low surface resistivity dielectric can be summarized based on Figures 6 and 7. The tangential field i.e. the field parallel to the surface may have been strong enough to cause a conducting track because of excessive field concentration at one point due to surface irregularities and contamination. The tracking of the inner paper-filled dielectric (Figure 6(a)) may have started at one point and progressed in the direction

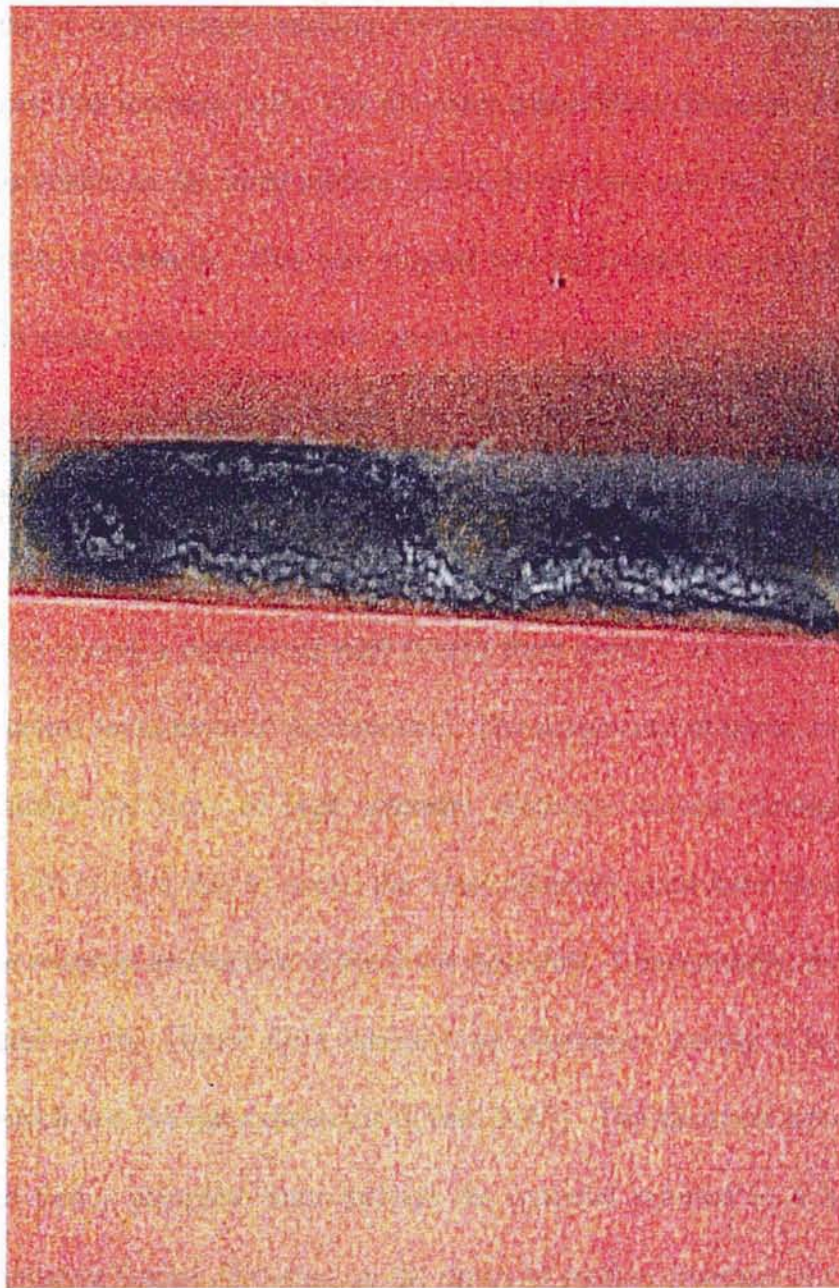


Figure 6a. Electrical breakdown of paper-filled phenolic resin - inner dielectric.

of the field until the surface resistivity at some other point was in excess of the propagated surface field strength, thereby terminating the track beyond that point in the same direction. The bifurcation of tracking observed in Figure 6(a) is a common incorporation of high-voltage tracking (Whitehead, 1951), indicating the presence of more than one low resistant path. For the outer paper-filled dielectric (Figure 6(b)), no tracking was visible on the outer surface except for the two carbonized (black) patches - one with a hole in between. This may suggest that the breakdown probably occurred at two different spots with the field concentration at one spot being more intense than the other, although the discussion to follow proved it otherwise. No visible evidence was available on the outer surface of the outer cylinder to support the occurrence of surface breakdown (tracking is evidence of surface breakdown). However, a picture of the inner surface clearly shows a carbonized path (track) from point 1 in Figure 6 (c) to point 2 indicating surface breakdown of the dielectric. The occurrence of tracks only on the inner surface indicates the flow of high intensity discharge current through the gas-gap (Whitehead, 1951). For this to occur, the inner dielectric must have broken down first, initiating the eventual destruction of the outer dielectric. Conceptually, this phenomenon can be related to the higher field intensity on electrodes having a higher radius of curvature, which was the inner dielectric (Clark, 1962). The electrical intensity at point 2 was so high that a complete burn through the material resulted in a hole formation. Another interesting feature, focusing on the rigors of surface creepage of charge, was the location of the hole made on the outer cylinder - about an inch away from the top of the outer electrode. No arcing was observable on the outer surface of the outer phenolic cylinder during the experimental run. This reiterates the point that the breakdown of the

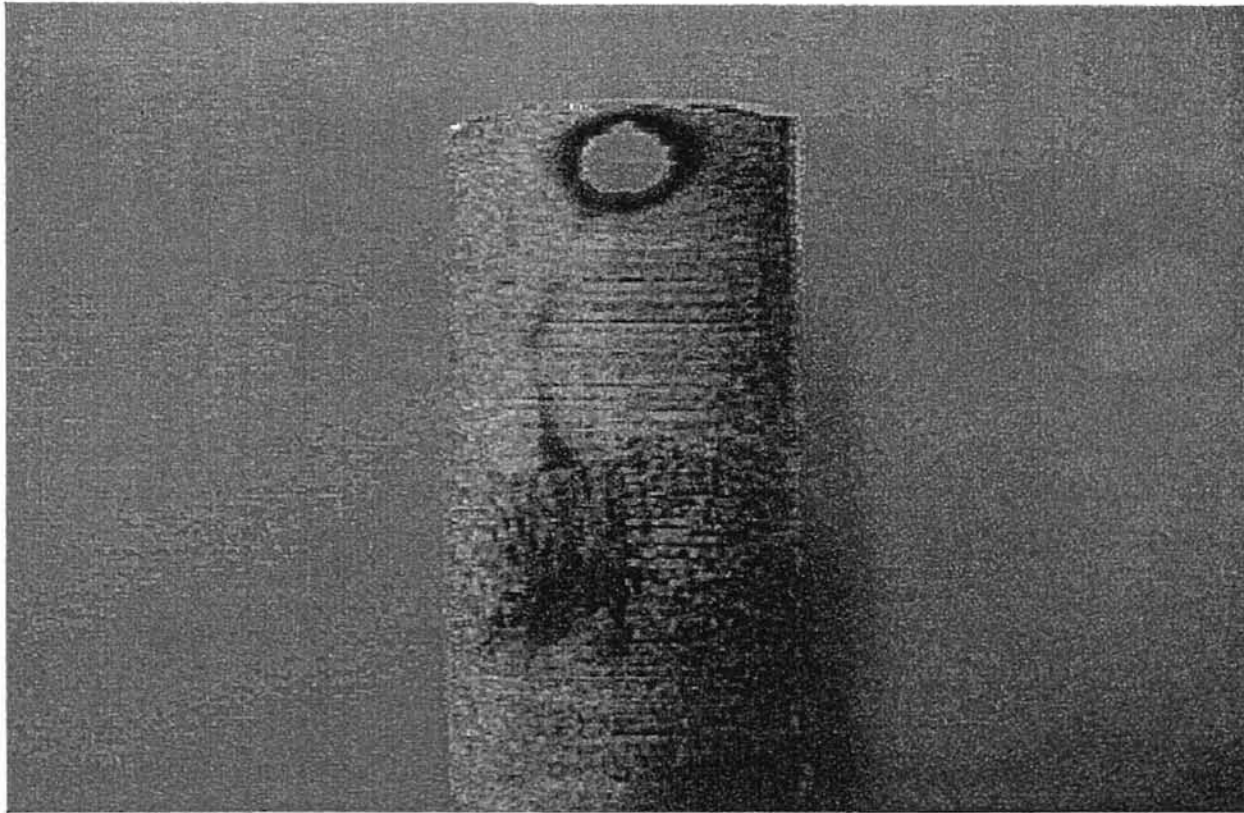


Figure 6b. Electrical breakdown of paper-filled phenolic resin (outer surface of the outer dielectric)

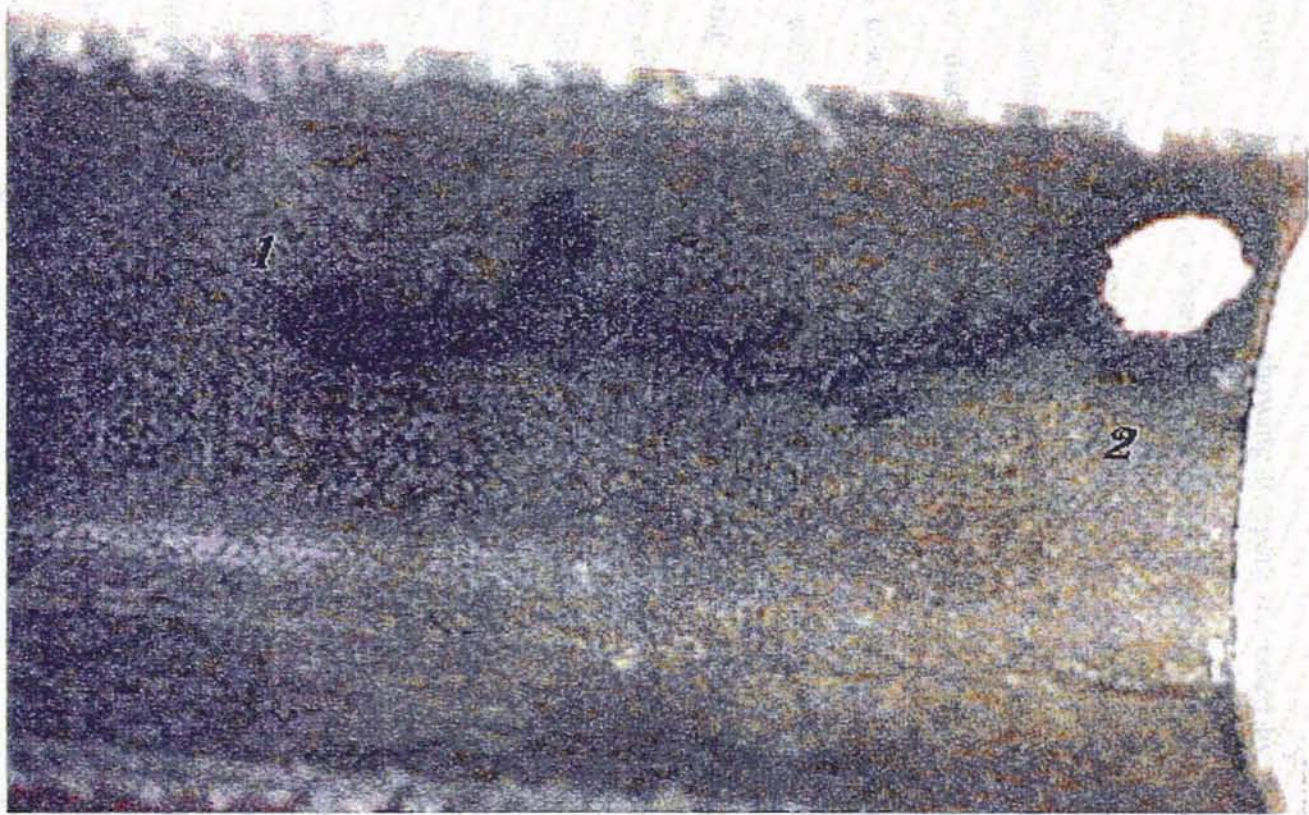


Figure 6c. Electrical breakdown of paper-filled phenolic resin (inner surface of the outer dielectric)

outer dielectric should have started at point 1 in Figure 6 (c) owing to high electrical current flowing through the gas, enhanced by a high voltage and progressed to point 2.

For the glass-filled phenolic resin, severe charring of the inner dielectric in addition to large tree formations (see Figure 7 (a)), showing the path traversed by the track in the direction of the electric field, was observed. The outer dielectric, though showing signs of tracking (Figure 7 (b)), did not have any tree formations on its outer surface, probably indicating a less contaminated surface. Whitehead (1951) designates tree formation in tracking as 'lateral discharges'. Due to intense field concentration at the tip of the track, a glow or corona discharge may occur thereby propagating tracks through multiple paths simultaneously until the total current carried by the main track cannot induce any additional tracking. However, the inner surface of the outer dielectric showed clear signs of tree formation (Figure 7(c)) which could have been due to severe arcing of the gas in the annulus, an indication of the inner dielectric having broken down first.

The phenomenon of surface breakdown favors a contaminated or uneven surface which would enhance field concentration. An obvious solution would be to deliberately reduce the surface resistance by coating the material surface in direct contact with the electrodes with a semi-conducting film to ensure a uniform field distribution which might otherwise be hindered by variations in surface conductivity. Non-uniformities in electrical plasma are bound to exist during any commercial use due to variations in external conditions controlling it. This would mean that arcing at certain points within the gas may exist which could harm the inner surface of the outer dielectric and the outer surface of the inner dielectric. Hence, a semi-conducting film even on the surfaces not in direct contact with the electrodes may enhance longevity of the dielectric material. Also,

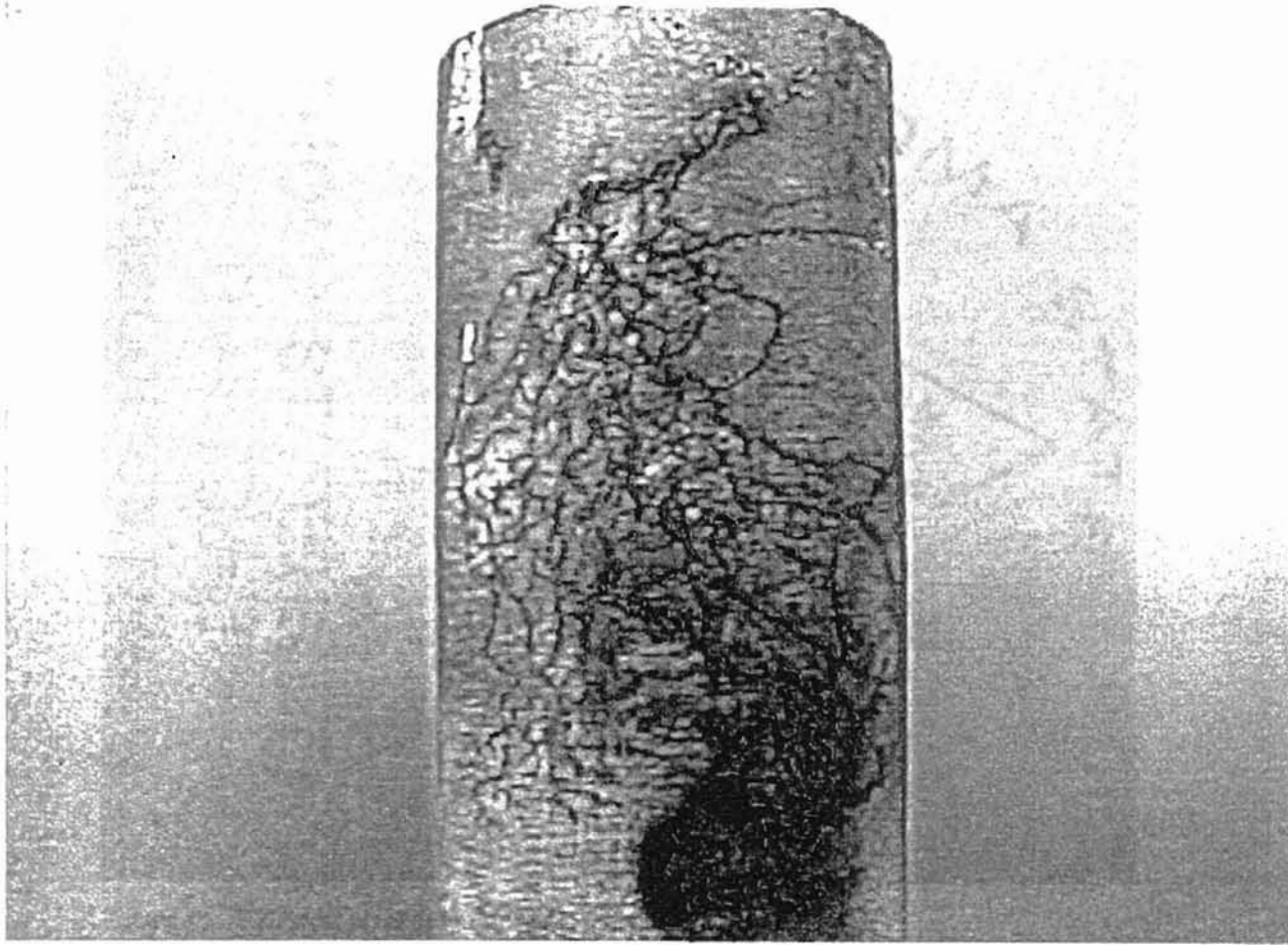


Figure 7a. Electrical breakdown of glass-filled phenolic resin - inner dielectric.



Figure 7b. Electrical breakdown of glass-filled phenolic resin
(outer surface of the outer dielectric)



Figure 7c. Electrical breakdown of glass-filled phenolic resin (inner surface of the outer dielectric)

the presence of water droplets on the dielectric surface may enhance surface conductivity to an alarming degree giving a valid reason for use of only highly hydrophobic materials as dielectrics.

The importance of the filler material used in a phenolic resin is evident from the fact that a glass-filled phenolic resin lasted almost eleven hours longer, under similar severe conditions, despite its higher power factor (hence, dielectric loss) when compared to a paper-filled phenolic resin (see Table I, Appendix A). Though no data was available on the burning period of phenolic resins under high voltage stress, the ignition temperatures of the two resin structures shown in Table XXII (Clark, 1962) gives an insight into the burning properties of glass- and paper-filled phenolic resins.

Table XXII
Burning properties of paper-and glass-filled resins

Resin structure	Ignition temperature (deg. C)	Burning period (seconds)
Phenolic (paper-filled)	340	22
Phenolic (glass-filled)	420 - 425	154 - 161

Since the heat generated due to electrical stress in the phenolic resins is of a much lower magnitude than that due to flame heating, the burning period is much longer for the plasma system. Also, the paper-filled resin burns at a much faster rate due to the high flammability of cellulose. Since the current drawn initially is low, (Table XVII, Appendix C), initial deterioration of the glass-filled resin may have been caused by its high dielectric loss and not by the electric current drawn, although the eventual

destruction of the material was probably due to a combination of both, as explained earlier in this section. The limited availability of data made this line of reasoning speculative.

An interesting feature noticeable with the breakdown of the Cellulose Acetate Butyrate (CAB) material tested was the deformation in its cylindrical structure close to the point of rupture, as shown in Figures 8b and 8d. This brings into focus another important factor never considered earlier, viz. dimensional stability under higher temperatures. Due to its poor dimensional stability, the CAB material underwent changes in its physical structure after the plasma system was allowed to operate for some time : both the inner and outer dielectrics bent away from the electrodes closest to them to reduce the impact of electrical heating. This change was more profound for the inner dielectric due to the higher field strength incident on it, as can be seen from Figures 8(b) and 8(d). This resulted in the approach of both dielectrics toward each other, thereby reducing the air-gap at certain points. An immediate consequence was the effect of localized field strengths. Beyond a certain point of approach, a percentage of applied voltage greater than required for the dielectric breakdown of the material may have been incident on the inner dielectric causing a rupture (Figure 8(a)). This would result in a high current flow through the reactor paving the way for deterioration of the outer dielectric (Figure 8(c)) due to excessive electrical heating. The observations made during the experimental runs confirmed this hypothesis. Though the actual CAB resin was almost colorless (had a slight yellow tinge), the inner dielectric used showed dark yellow patches at the end of the test, indicating chemical deterioration. The patches occurred

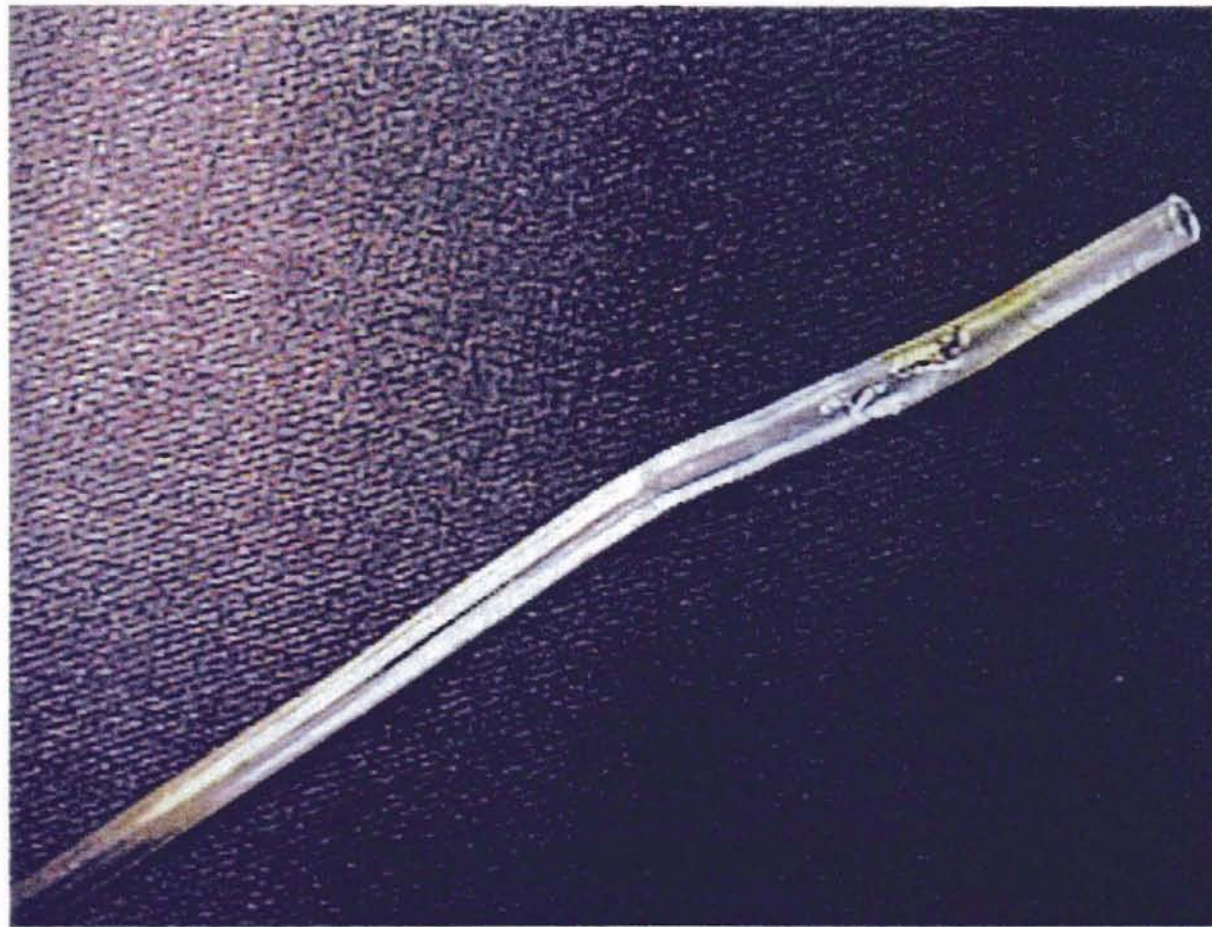


Figure 8b. Electrical breakdown of CAB resin (dimensional change of the inner dielectric)

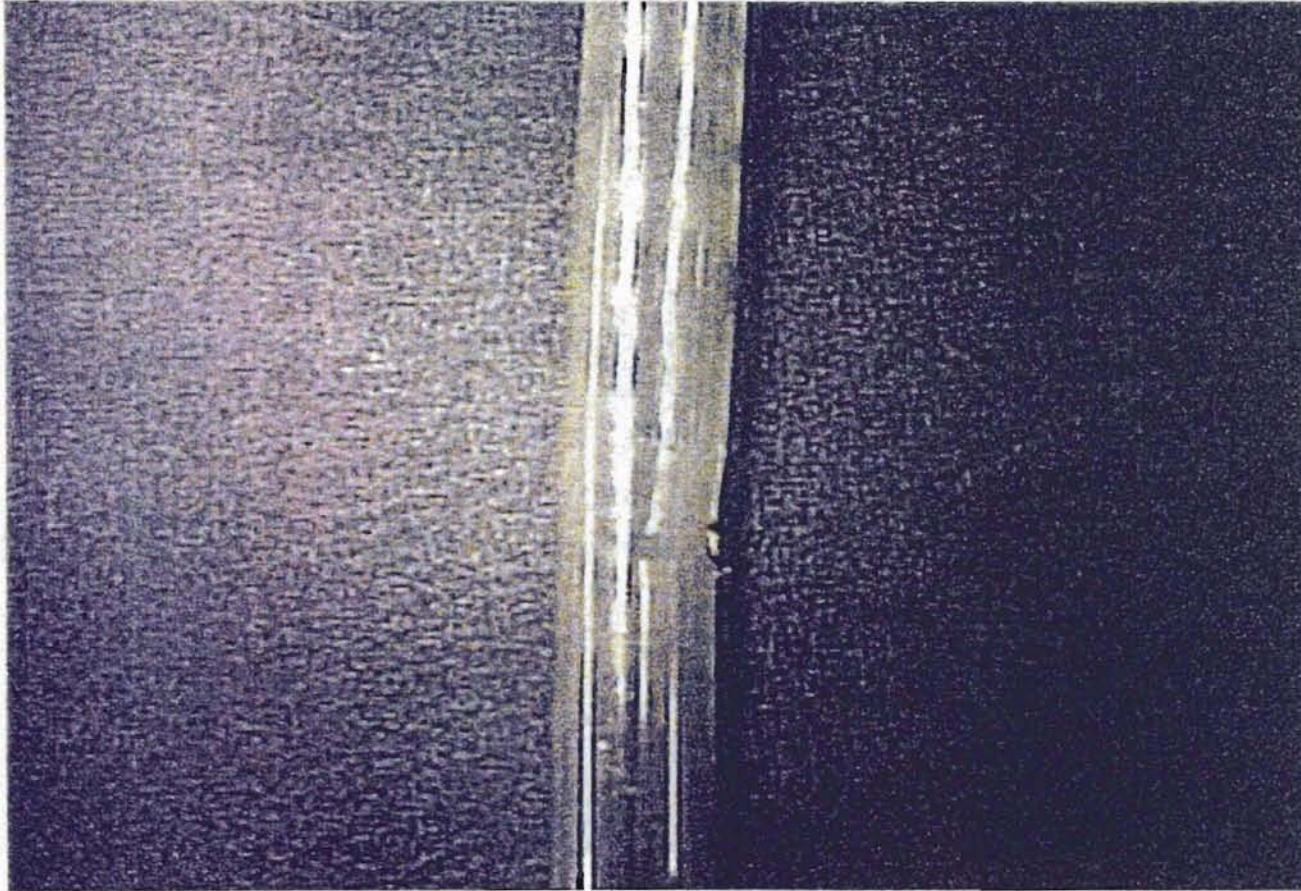


Figure 3d. Electrical breakdown of CAB resin - dimensional change of the outer dielectric.

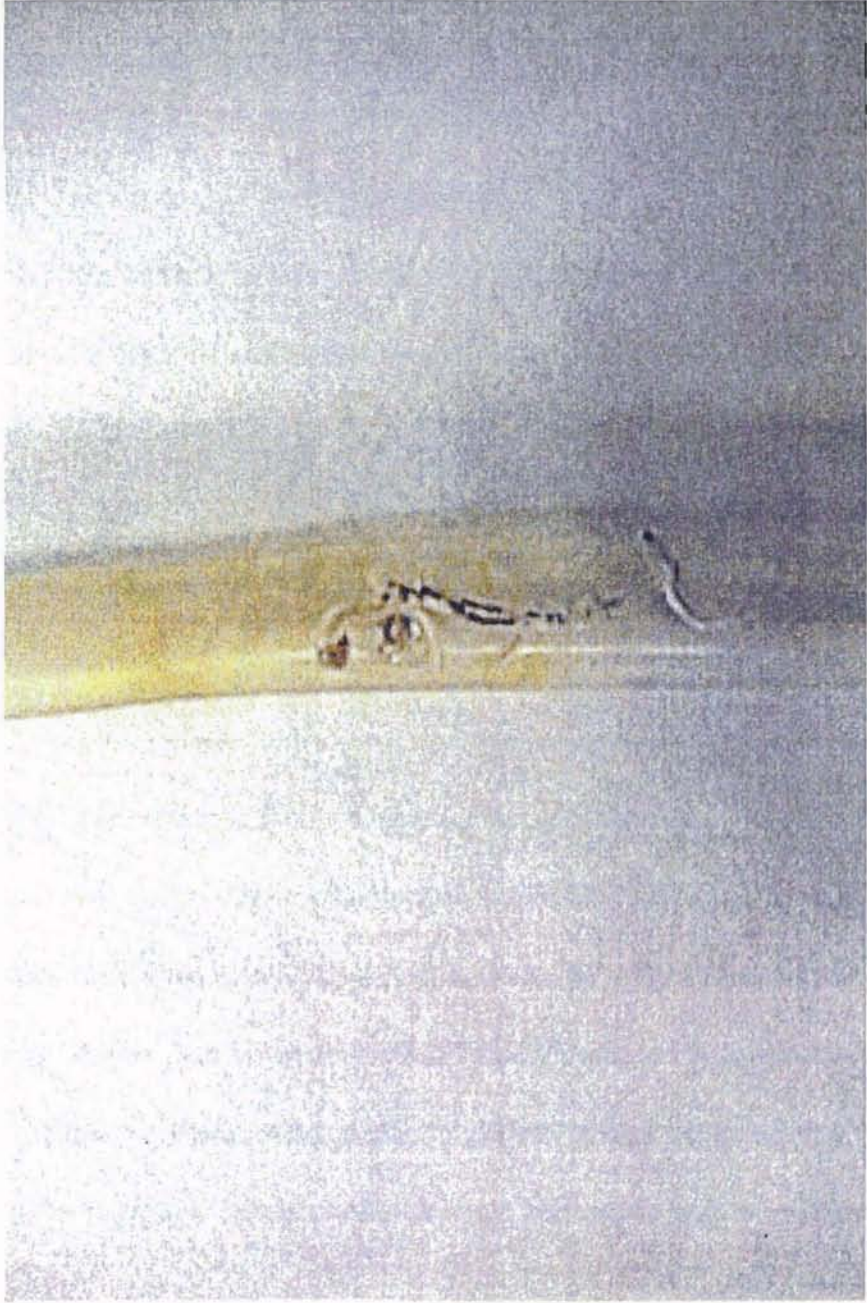


Figure 8a. Electrical breakdown of CAB resin (rupture of the inner dielectric)

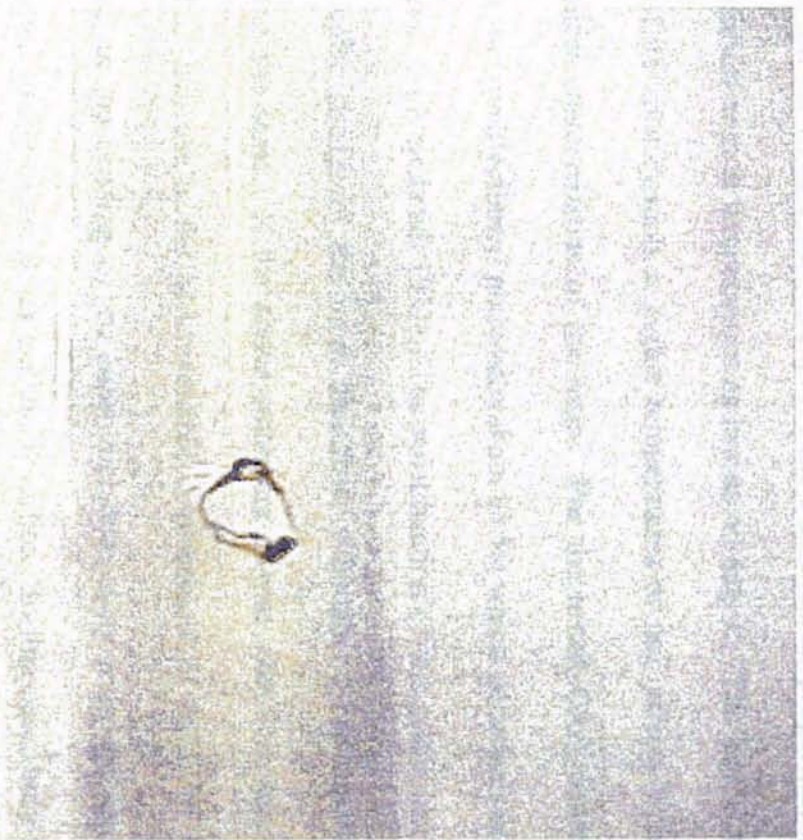


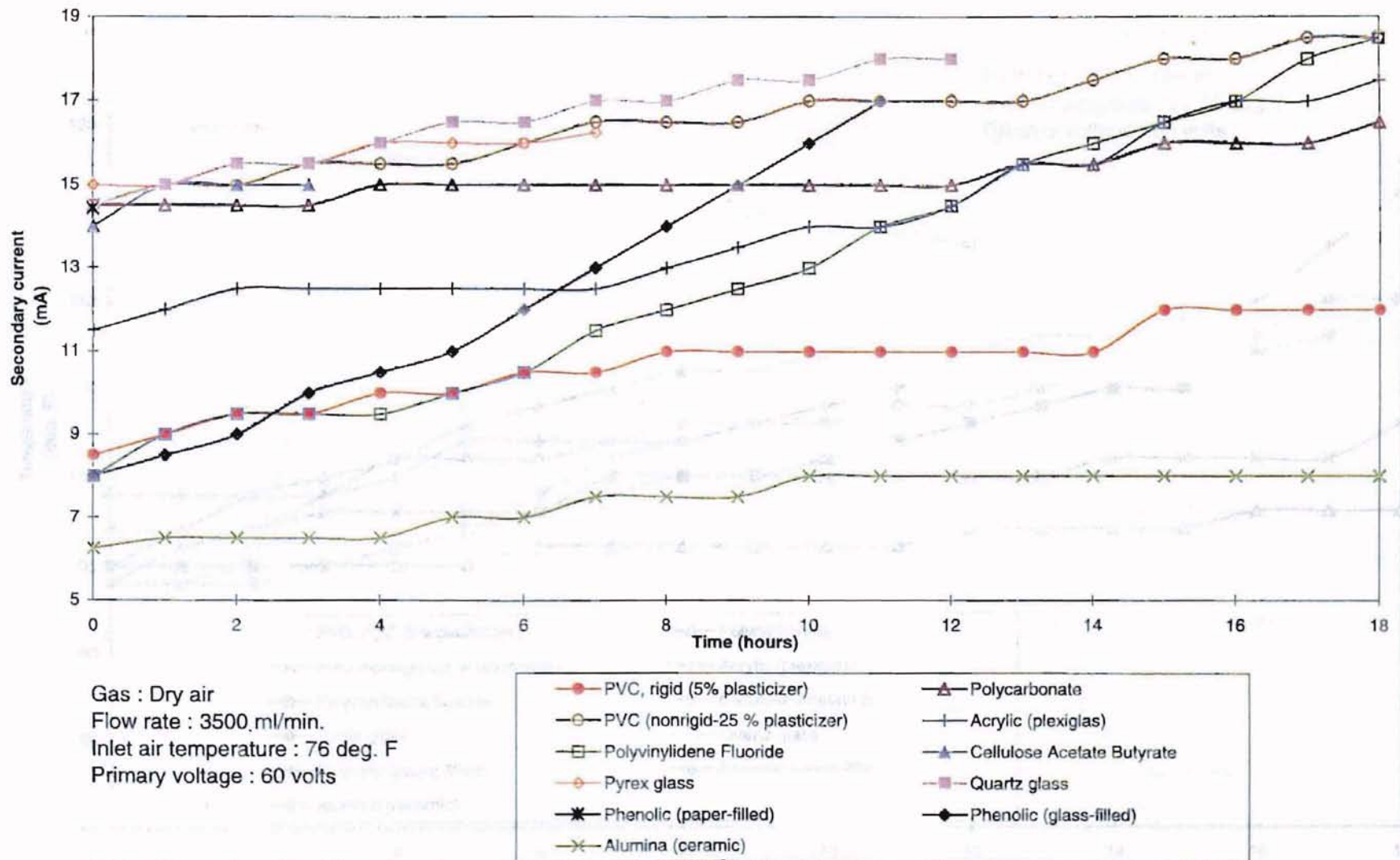
Figure 8c. Electrical breakdown of CAB resin - rupture of the outer dielectric.

around the region of dielectric breakdown only, thereby suggesting the possibility of breakdown due to chemical means. Clark (1962) and Whitehead (1951) have discussed the degradation of the CAB resin due to long-term heating. The plasticizers which are mixed with the CAB resin (to improve their mechanical properties) have a high rate of volatilization even at temperatures as low as 60 deg. C. The loss of the plasticizer, as a result of its volatilization at higher temperatures of use, affects both the electrical and mechanical characteristics of the resin. For the tested CAB material, the plasticizer content was mostly diamyl phthalate (about 85 %) which volatilizes at temperatures close to 90 deg. C (Whitehead, 1951). The volatilization of this plasticizer may have resulted in the color change of the inner dielectric, although no confirmation could be made regarding the same. If the above statement is true, chemical deterioration may have caused an increase in the non-reversible displacement of the CAB resin (Clark, 1962) resulting in the bending of the inner dielectric away from the electrode followed by breakdown of the material, as explained earlier. In this case, only the inner dielectric could have broken down due to chemical deterioration because of the absence of a color change in the outer dielectric. The deformation in the outer dielectric may have resulted from heating effects due to high current flow following the breakdown of the inner dielectric. Since no measurements of the dielectric wall temperatures were made, no evidence to support the deterioration of the CAB resin due to chemical means was available.

Another facet of discussion may be the effect of thickness of dielectric material on durability under high voltage stress. The thickness of the CAB material tested was 1/32 inches, 25 % the thickness of other dielectric materials tested. A potential argument may

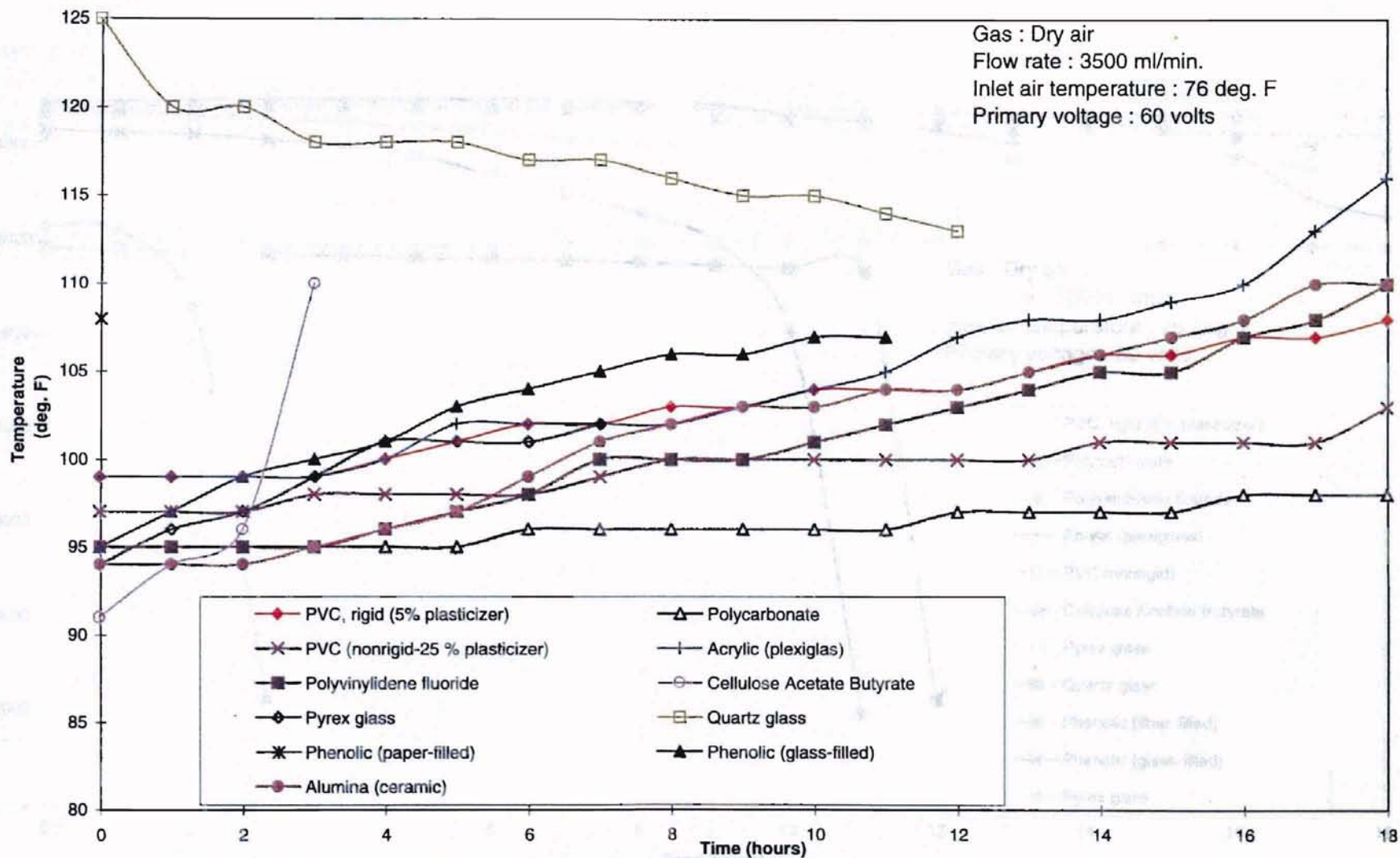
be that under the same conditions, the amount of heat energy per unit volume may be less for a thicker insulation thereby reducing the potential for material breakdown. To test this hypothesis, an acrylic material with exactly the same dimensions as the CAB material was tested. Although heating of the dielectric wall was observed, the acrylic material tested passed the usability test (data shown in Table XVIII, Appendix C). This casts doubt on the argument that the CAB material broke down simply because it was thinner than the other materials tested. However, it should be borne in mind that the amount of heat energy per unit volume of the material may indeed be lower for a thicker insulation. The CAB material may have lasted longer if a thicker insulation had been provided in the plasma system, though the repercussions arising in the form of suspected higher thermal gradients would have to be addressed. This may not adversely affect the functioning of the plastic materials as dielectrics mainly because of their low coefficient of thermal expansion and high tensile strength. However, for commercial glasses and ceramics, this may prove to be a decisive factor for their usability as a dielectric because they lack the same properties.

All the other plastic materials tested, viz. acrylic (plexiglas), polycarbonate, PVC (rigid and nonrigid), and polyvinylidene fluoride passed the usability test (see Table XI). The time variation of the secondary current (Table XVII, Appendix C; Figure 9) flowing through these materials was constantly increasing for the entire test period. The gas temperatures increased continuously with time (Table XV, Appendix C; Figure 10) for all materials except quartz (decreased continuously), which could not be explained in this study. The trend for secondary voltage of all the materials (Table XVI; Figure 11) which passed the usability test was as follows : constantly decreasing after crossing a maxima or



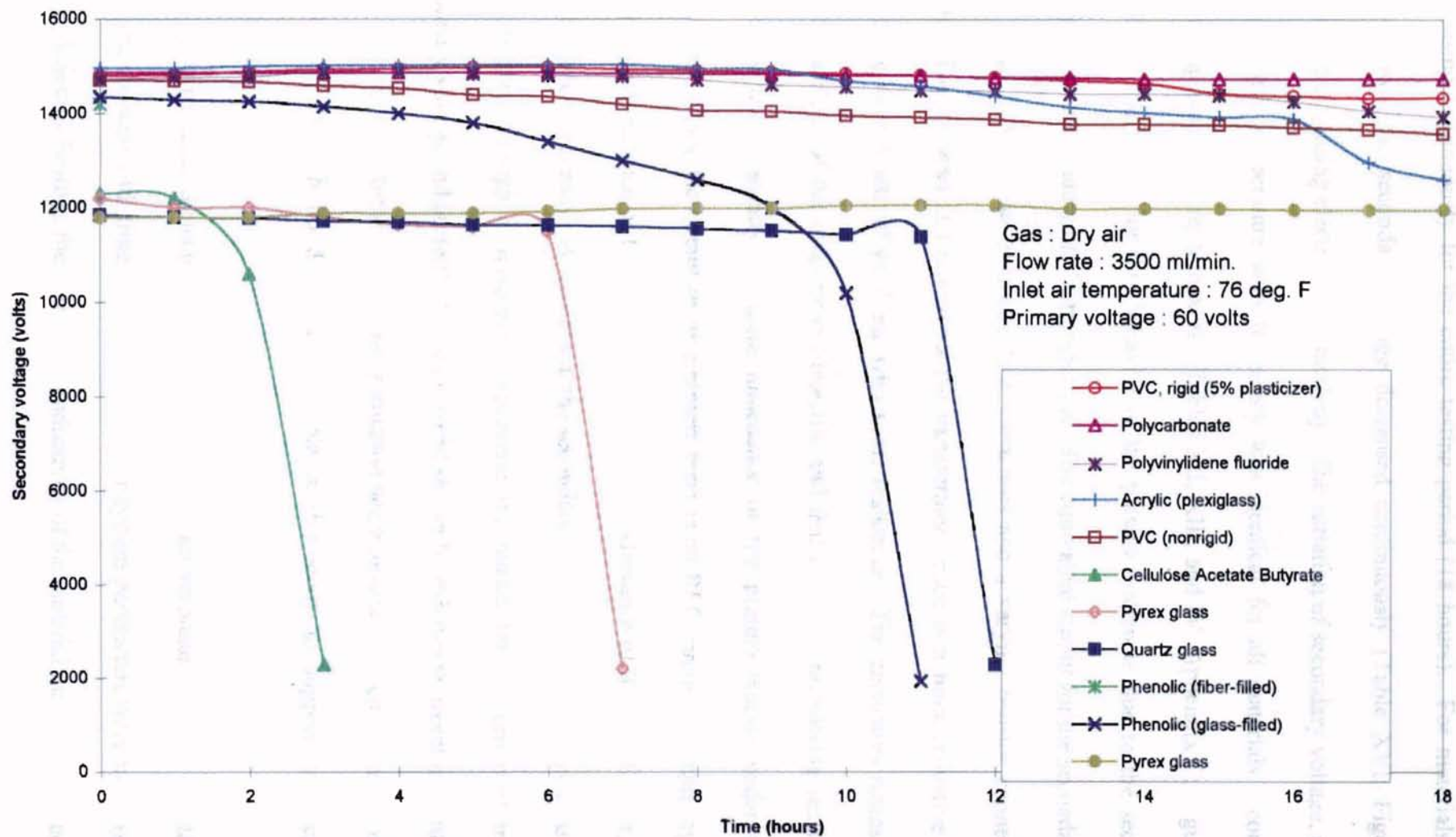
Note : Dimensions for different reactor materials are presented in Table VII.

Figure 9. Variation of secondary current with time at constant primary voltage (usability test).



Note : Dimensions for different reactor materials are presented in Table VII.

Figure 10. Variation of exit gas temperature with time at constant primary voltage (usability test).

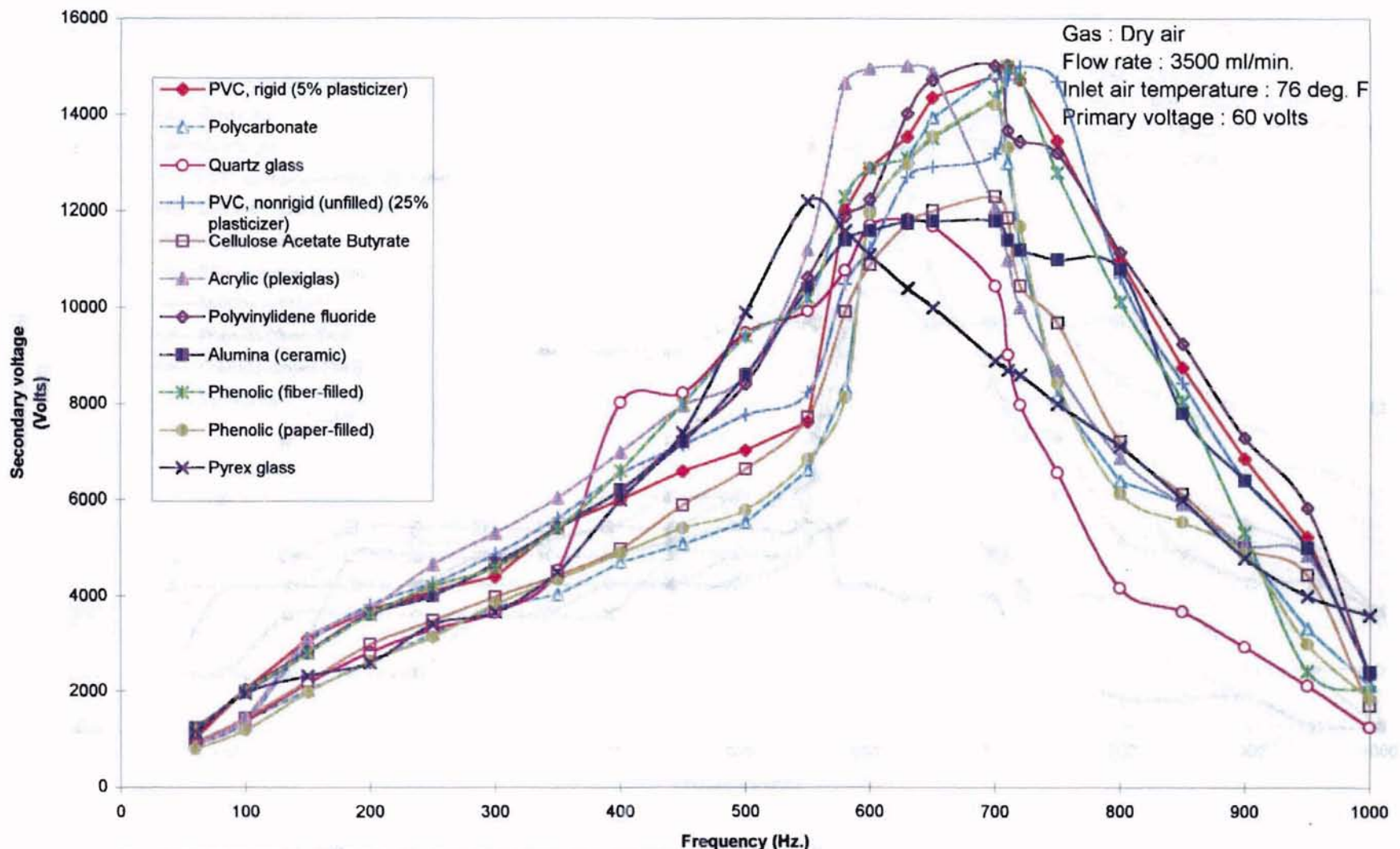


Note : Dimensions for different reactor materials are presented in Table VII.

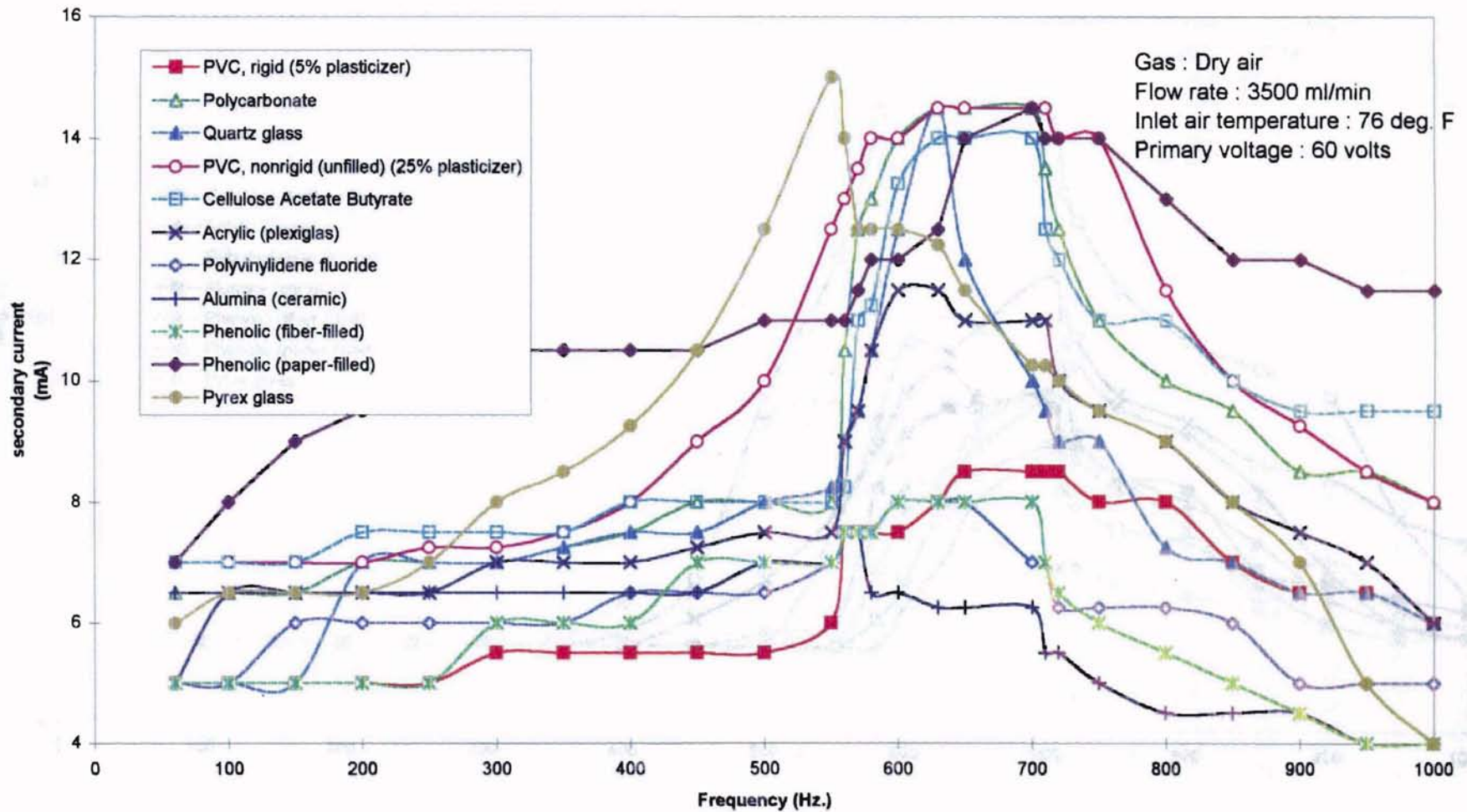
Figure 11. Variation of secondary voltage with time at constant primary voltage (usability)

decreasing continuously for the entire testing period (18 hours). For broke down, the secondary voltage decreased continuously (Table X indicating increasing electrical conductivity. The variation of secondary and exit gas temperature with frequency was identical for all materi decreasing after crossing a maxima (Tables XII, XIII, and IV, Appendi 13, 14). The reason for this behavior of the plasma system is due to electrical circuit loading on the transformer. The equivalent circuit for the may be as follows : an inductor, three capacitors and a varying resist series. The inductor (L) represents the transformer which is a basic i consisting of two sets of windings with some resistance. The capacitance (C) of the outer/inner dielectric and that of air. The vary represents the constantly changing impedance of the plasma reactor conditions. Since the circuit in its simplest form is an RLC circuit, a f where the capacitance of the circuit is equal to the inductance of the tra the resonance frequency. At this point, the secondary voltage (and the po reactor) goes through a maximum, explaining the reason for the obs secondary voltage and current. The same trend shown by exit gas tempera been due to the exothermic ozone formation/decomposition reactions Chapter II, although no data was available in this study to support viewpoint.

For an ideal dielectric (no dielectric loss), the secondary volta remained constant with time, as long as the other system parameters were Due to dielectric heating, the electrical conductivity of the material may be

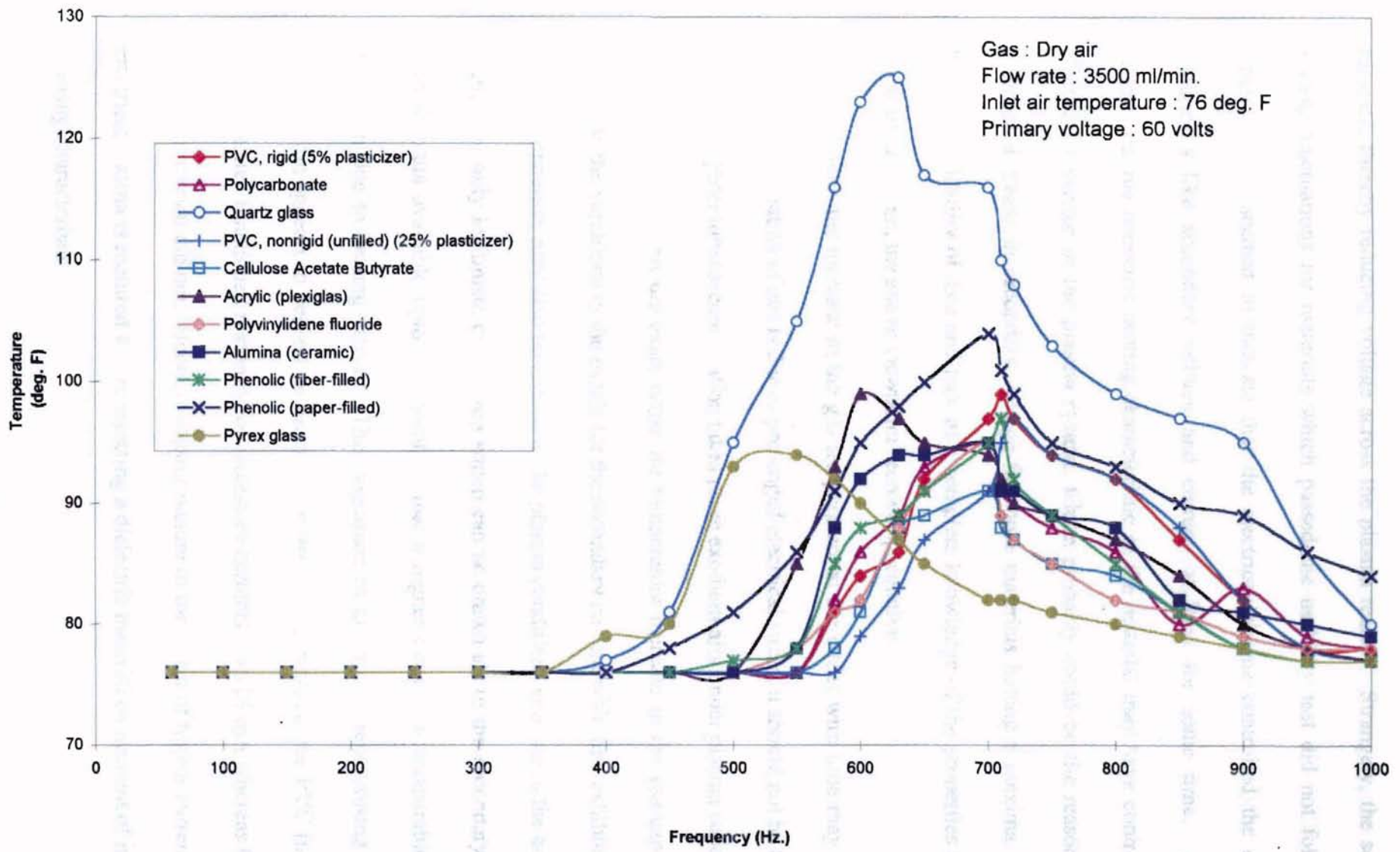


Note: Dimensions for different reactor materials are presented in Table XII.
Figure 12. Variation of secondary voltage with frequency at constant primary voltage (usability test)



Note : Dimensions for different reactor materials are presented in Table VII.

Figure 13. Variation of secondary current with frequency at constant primary voltage (usability test)



Note : Dimensions for different reactor materials are presented in Table VII.
Figure 14. Variation of exit gas temperature with frequency at constant primary voltage (usability test).

increase, thereby reducing voltage across the plasma reactor. Strangely, the secondary voltage fluctuations for materials which passed the usability test did not follow this pattern. This seemed to indicate that the electrical plasma controlled the electrical parameters like secondary voltage and current, at least for some time. As time progressed, the dielectric heating characteristic of the material may have controlled the electrical behavior of the plasma system, which probably could be the reason for the eventual decrease in secondary voltage for those materials having a maxima. Due to limited availability of data and lack of a complete knowledge of the properties affecting the plasma system, the above viewpoint seemed speculative.

Though the increase in the gas temperature at the outlet with time may hint that the electrical heating of gas is due to prolonged electrical stress, it should not be forgotten that ozone generation/decomposition takes place exothermally under plasma conditions in the air-gap. This left the exact cause for temperature increase in the gas-gap unclear. Similarly, the variations in the trends for the secondary current with time exhibited by the different materials may also be related to the plasma conditions existing in the air-gap for each. The only legitimate conclusion which can be drawn about the secondary current, with the data available upto this point, is that a higher current is undesirable for the insulation due to heating effects. The magnitude of electric current causing material deterioration appears to depend on the material itself. For instance, the PVC (non-rigid) material tested functioned normally for secondary currents upto 15 mA whereas CAB and the Phenolic resin did not. Hence, a clearer picture of the effect of higher currents on the electrical plasma is required before rejecting a dielectric material on account of its current drawing characteristic.

Alumina (ceramic) exhibited the same current drawing characteristic as some plastics (Table XVII, Appendix C; Figure 9) - a constantly decreasing secondary current for the entire testing period (18 hours). The maximum voltage which could be applied across the alumina dielectric was much lower than that for plastic materials of the same dimension. A possible explanation could be that the presence of impurities in the ceramic material during the firing operation may have decreased the volume resistivity of the ceramic material, although its value shown (A.S.T.M. standards) in Table I (Appendix A) is comparable with that for the plastics tested. Clark (1962) has confirmed that the mechanical and electrical properties of ceramics are subject to wide variations due to improper firing conditions during their processing even when formed from the same material constituents. This brings into the focus an important point discussed earlier in this chapter - the limitations in using property values applicable for the general class of the tested material. The gas temperature at the exit increased continuously over the entire period of testing (Table XV, Appendix C; Figure 10). The exceptionally high thermal conductivity of alumina (almost 75 -100 times higher than most plastics) may suggest that this may be gas heating due to higher energy supplied and not because of heat accumulation within the annulus, although there was no data to support this argument.

The pyrex (#7070) and quartz glasses tested may have cracked because of heat generated due to a high current flow in the material (Table XVII, Appendix C; Figures 9). However, the cause for eventual deterioration of both the glass-type materials was different. The thermal conductivity of pyrex glass is low and this may have accentuated the establishment of internal mechanical stresses as a result of unequalized temperature gradients within the material. The rigid structure of pyrex glass (Figure 15) combined

In a high voltage field, the surface of the material deteriorate
quickly, events... The main... were
... A

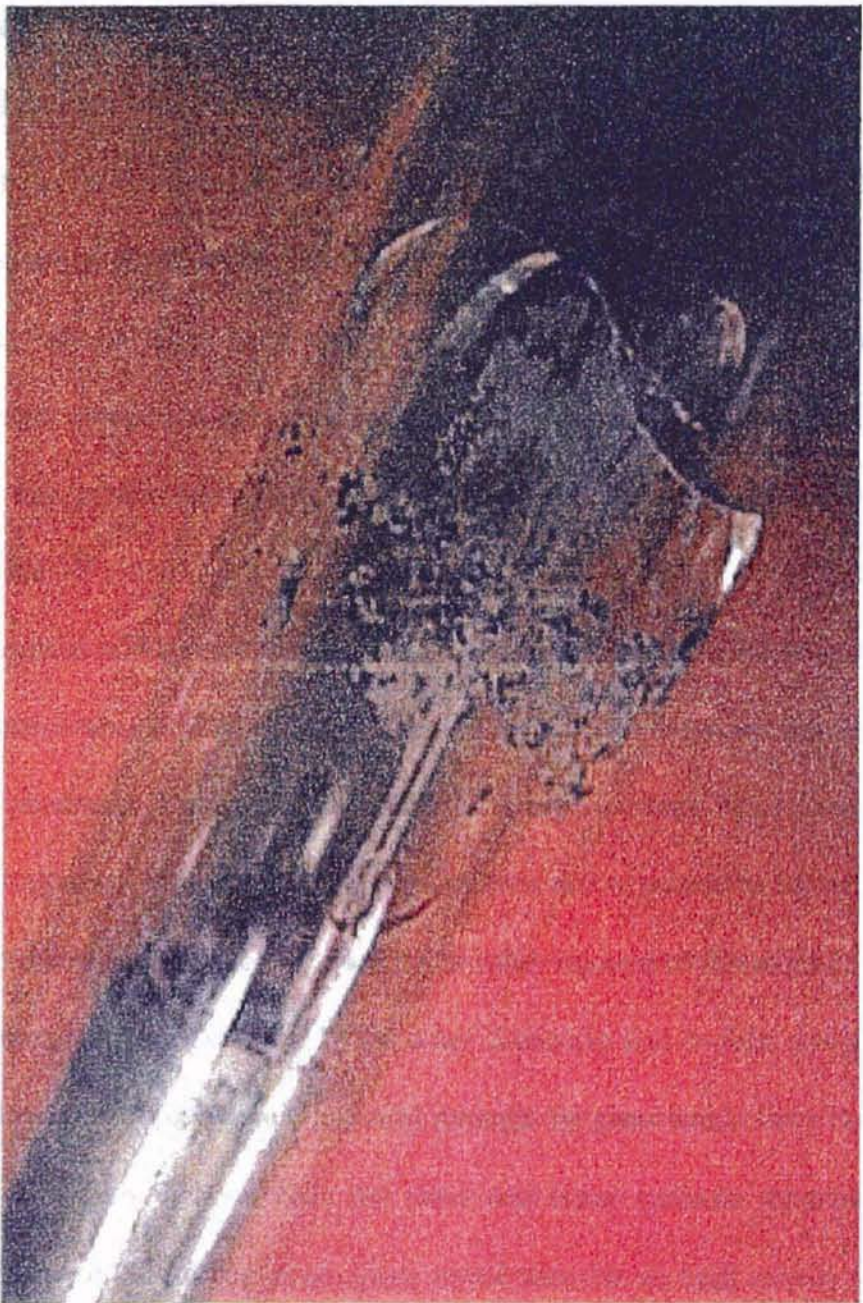


Figure 15. Electrical breakdown of pyrex glass.

with a high coefficient of thermal expansion may have caused the material to deteriorate quickly, eventually cracking the glass. The black spots on the outer surface were remnants of the insulating tape used to hold the outer electrode (copper mesh) in place. A counter argument may be that the copper rod used as the inner electrode expanded due to electrical heating and this volume expansion may have resulted in an increase in the tensile stress on the inner dielectric eventually leading to the cracking of the glass. A close inspection of the outer dielectric indicated cracks in the same region as the inner dielectric with no signs of cracking elsewhere. Since the outer electrode was just a copper mesh wrapped around the outer tube (eliminating the possibility of outer dielectric cracking due to thermal expansion of outer electrode), the only possible reasons for its cracking are

- (1) propagation of the crack on the inner dielectric beyond the point where both the dielectrics were affixed, thereby initiating the crack in the outer dielectric.
- (2) inner dielectric breakdown resulting in a high current flow through the reactor, initiating the breakdown of the outer dielectric due to excessive heating.

Since there was no evidence of cracking at other regions of the reactor, the first reason was automatically eliminated. If the outer dielectric had broken down due to a high current flow, a burn path (black in color) through the glass would have been visible. The absence of a burn path on both the outer and inner surfaces reiterates the fact that electrical breakdown of the pyrex glass tested was due to high tensile stress. No data seems to be available supporting the destruction of pyrex glass due to the lowering of breakdown strength with increasing temperatures under similar conditions. A host of authors, including Clark(1962), have discussed the effect of an increase in frequency on

the degradation in the dielectric strength of pyrex glass. Almost all the published results discuss only the impulse breakdown at 60 Hz. or the long-term effects of high voltage at 60 Hz., and not the long-term effects of high voltage at high frequencies on these glasses, leaving the above argument uncontended. The coefficient of thermal expansion for quartz glass is very low and its tensile strength is much higher than that of pyrex glass. The presence of a burn path through the quartz glass reactor clearly indicated that the breakdown was not due to the same inadequacies as pyrex glass. Clark (1962) has shown the rapid decrease of the volume resistivity of quartz due to dielectric heating (temperature increase). The decrease in the volume resistivity of quartz may have resulted in the cracking of glass at its weakest point, as shown by the black streak on its inner and outer surface indicating the passage of a high electric current (Figure 16). The sizably lower air breakdown voltages observed for both glasses was due to a smaller air-gap thickness.

For the same configurations (Table VII) tested in the usability test, the breakdown voltage of air was determined at various primary voltages for different materials (Table XXIII, Appendix C; Figure 17). The total voltage required for the breakdown of air became progressively higher for increasing primary voltages for all the dielectric materials tested. The frequency at which the breakdown voltages were obtained became lower for increasing primary voltages. The trends observed were in good agreement with those of Tsai (1991). An interesting feature noticed was the relation of a particular property of the dielectric material, viz. dielectric constant, to the air breakdown voltage - for a specified geometry and primary voltage, the air breakdown voltage was higher for a material with smaller value of dielectric constant (average values for the dielectric

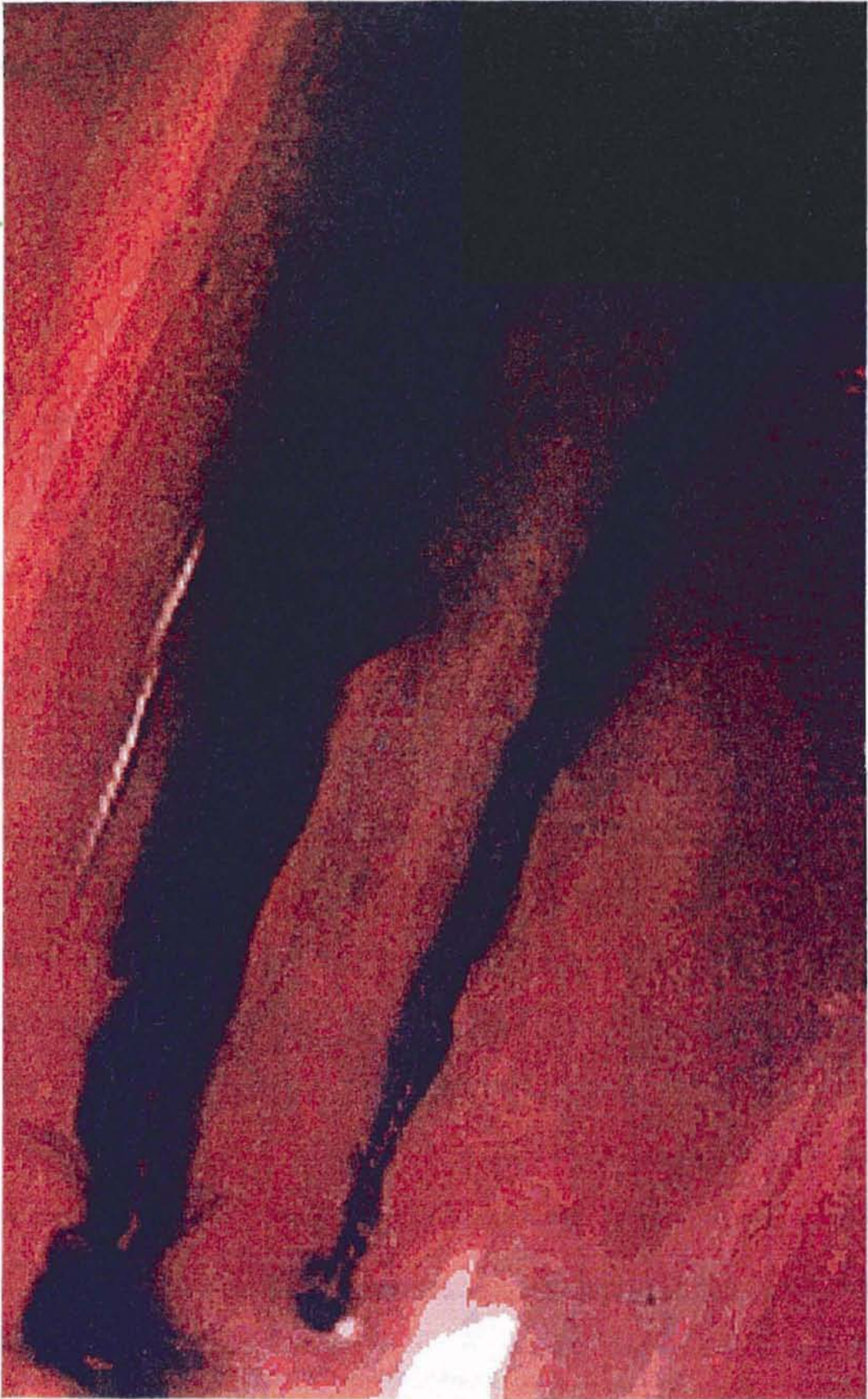
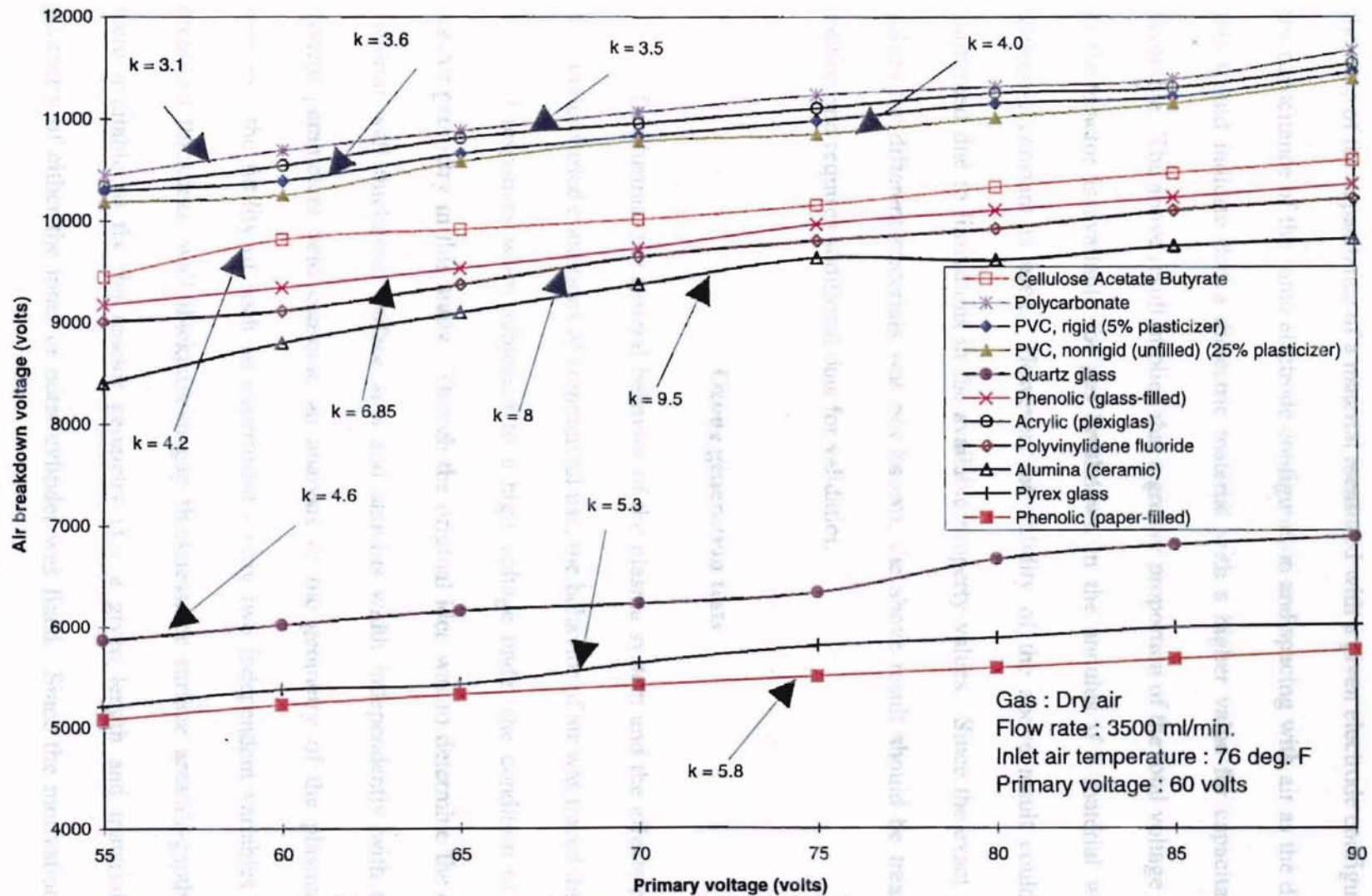


Figure 16. Electrical breakdown of quartz glass.



Note : Dimensions for different reactor materials are presented in Table VII.

Figure 17. Variation of air breakdown voltage with dielectric constant (k) at various primary voltages.

constant, based on values shown in Table I, were used). Since the dielectric constant is the ratio of the capacitance of a material measured with a given electrode configuration to the capacitance of the same electrode configuration and spacing with air as the dielectric, this would indicate that a dielectric material with a higher value for capacitance was favorable. The above result implied that a greater proportion of the total voltage supplied to the reactor is available for gas breakdown in the annulus if a material with high dielectric constant is used. However, the validity of the above result could not be confirmed due to limitations in the available property values. Since the exact property values for different materials was not known, the above result should be treated with caution and requires additional data for validation.

Ozone generation tests

To illustrate the general behavior of the plasma system and the effects produced on it under varied conditions of commercial use, the behavior of air was traced through its manifold responses when subjected to a high voltage under the condition of varying reactor geometry in this study. Though the original idea was to determine the effect of material wall thickness, surface area and annulus width independently with all other system parameters held constant, an analysis of the geometry of the plasma reactor indicated the futility of such an experiment - only two independent variables (surface area/wall thickness, wall thickness/air-gap thickness, or surface area/air-gap thickness) were available to fix the reactor geometry (for a given length and material) if the geometry of either the inner or outer cylinder was fixed. Since the motivation behind conducting these experiments was the practical evaluation of changes in reactor geometry

and not just the conceptual determination of the effect of individual parameters on system functioning, the effect of variations in the outer cylinder geometry (chosen due to the commercial availability of a wider range of geometries for large cylinders), while retaining the same inner cylinder for all cases, on gas breakdown, ozone generation and related parameters like temperature were investigated in this study. Due to the limitations in the cylinder geometries available commercially for most of the plastic materials tested earlier, only acrylic was chosen for experimentation.

Varying surface area and annulus width test

Focusing on the breakdown voltage of air under the condition of varying surface area of outer cylinder (by varying the outer diameter) and annulus width, intuition points towards the direction of increasing voltage requirements as the gap thickness, and hence the mass of air to be broken down, increases. The breakdown voltage values shown for each configuration in Appendix D justify this thought. From a commercial standpoint, the above fact may prove to be a limiting factor for scale-up because of the increasing capital and operating costs for provision of higher voltages to ensure breakdown of greater quantities of air. However, the breakdown strength of air for the tested conditions showed that the rupturing voltage gradient (volts/inch) decreases as the air-gap thickness and the outer surface area of the reactor are increased (Figure 18). The breakdown strength was calculated as the ratio of breakdown voltage (volts) to the air-gap thickness (inch). This result would imply that the voltage required for the breakdown of a given mass of air contained within a thickness of one inch decreases as the air-gap thickness and the outer diameter (hence, surface area) of the reactor are increased.

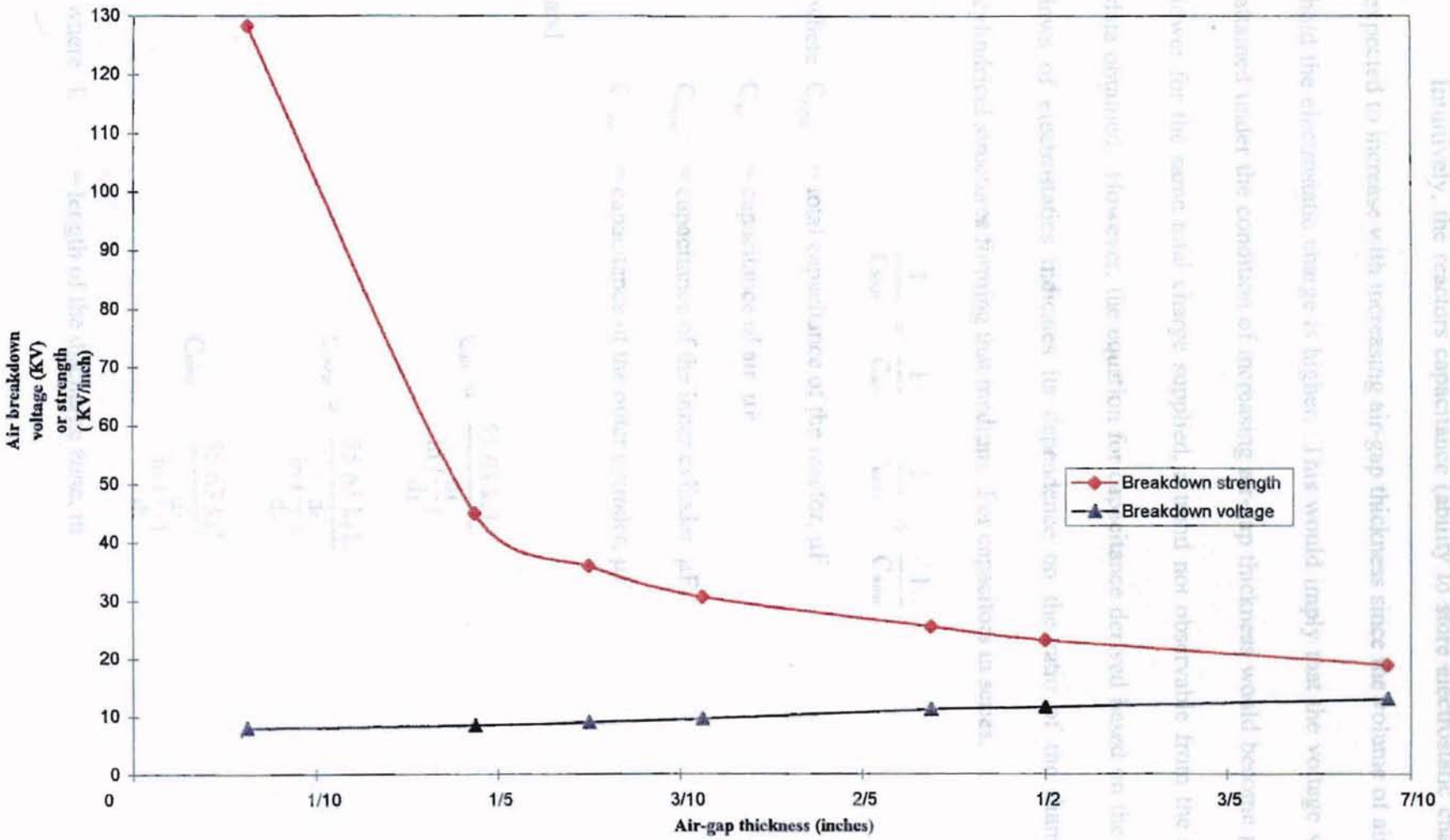


Figure 18. Variation of air breakdown voltage and strength with air-gap thickness (varying surface area and annulus)

Intuitively, the reactors capacitance (ability to store electrostatic charge) may be expected to increase with increasing air-gap thickness since the volume of air available to hold the electrostatic charge is higher. This would imply that the voltage which can be attained under the condition of increasing air-gap thickness would become progressively lower for the same total charge supplied, a trend not observable from the experimental data obtained. However, the equation for capacitance derived based on the fundamental laws of electrostatics indicates its dependence on the ratio of the diameters of the cylindrical structures forming that medium. For capacitors in series,

$$\frac{1}{C_{\text{total}}} = \frac{1}{C_{\text{air}}} + \frac{1}{C_{\text{inner}}} + \frac{1}{C_{\text{outer}}} \quad (\text{V-1})$$

where C_{total} = total capacitance of the reactor, μF

C_{air} = capacitance of air, μF

C_{inner} = capacitance of the inner cylinder, μF

C_{outer} = capacitance of the outer cylinder, μF

and

$$C_{\text{air}} = \frac{55.63 \text{ k}_a L}{\ln\left(\frac{d_3}{d_2}\right)} \quad (\text{V-2})$$

$$C_{\text{outer}} = \frac{55.63 \text{ k}_g L}{\ln\left(\frac{d_4}{d_3}\right)} \quad (\text{V-3})$$

$$C_{\text{inner}} = \frac{55.63 \text{ k}_g L}{\ln\left(\frac{d_2}{d_1}\right)} \quad (\text{V-4})$$

where L = length of the discharge zone, m

- d_1 = inner diameter of the inner dielectric, m or inch
- d_2 = outer diameter of the inner dielectric, m or inch
- d_3 = inner diameter of the outer dielectric, m or inch
- d_4 = outer diameter of the outer dielectric, m or inch
- k_a = dielectric constant of air, dimensionless
- k_g = dielectric constant of dielectric material, dimensionless

The above equations were extracted from Tsai (1991). If the inner diameter ' d_3 ' of the outer cylinder was increased, the capacitance of air would decrease and that of the outer cylinder would increase for the geometries under consideration (see Table XXIV), based on the above equations. The values for capacitance of air are valid only prior to plasma formation in the annulus. Since the geometry of the inner cylinder was unchanged, the capacitance of the inner cylinder remained the same. From equation (V-1), it was evident that the overall capacitance of the reactor may increase or decrease depending on the magnitude of change of capacitance for both air and the outer cylinder. The capacitance of the outer and inner dielectric will not change sizably for a given configuration unless its dielectric constant is a strong function of frequency for the chosen range of operation. For the materials tested, there is very little variation in the dielectric constant with frequency or temperature. Hence, the capacitance of the inner and outer dielectric are practically constant for our purpose. However, the capacitance of the annulus keeps changing constantly due to ionization of air and generation of ozone and other by-products like NO_x . Though the above equation for overall capacitance may be used to explain the voltage variations with frequency for a given configuration, formation of a plasma state would introduce an unknown variable, viz. capacitance of air. Hence, the

trend for the maximum voltage which can be attained for different reactor configurations could not be predicted based on the above equation. No pattern was observable for the maximum voltages attainable or for their corresponding frequencies based on experimental data tabulated in Appendix D.

Table XXIV
Capacitance of air and the outer cylinder for different configurations

Outer diameter of inner cylinder (d ₂) inch	Inner diameter of outer cylinder (d ₃) inch	Outer diameter of outer cylinder (d ₄) inch	Capacitance of air (μF)	Capacitance of outer cylinder (μF)
3/8	1/2	3/4	193.4	480.2
3/8	3/4	1	80.3	676.8
3/8	7/8	1 1/8	65.7	774.7
3/8	1	1 1/4	56.7	872.6
3/8	1 1/4	1 1/2	46.2	1067.9
3/8	1 3/8	1 5/8	42.8	1165.5
3/8	1 3/4	2	36.1	1458.1

The measured ozone concentration for a particular configuration was proportional to the secondary voltage applied (Tables XXV to XXXI, Appendix D) although published results (Horvath et al., 1985) indicate its proportionality is to the active power (voltage x current x power factor) drawn by the reactor. Since the power factor on the secondary side was unknown, the above fact could not be verified. The primary purpose for measuring the ozone concentration in these tests was to determine if it had a functional dependence on reactor geometry, i.e. to determine if the ozone concentration was higher or lower for the same secondary voltage supplied to reactors of different configurations. Due to wide variations in the total capacitance for different configurations, the secondary voltages obtained were never the same under the same external conditions (same frequency and primary voltage), leaving no scope for comparison. However, the

secondary voltage corresponding to a given ozone concentration became sizably higher for increasing air-gap thickness (see Figure 19), based on data shown in Tables XXV to XXXI, Appendix D. A likely reason for this trend could be the increase in mass of air to be broken down for ozone generation.

The temperature of the gas flowing through the annulus increased with increasing concentration of ozone (Tables XXV to XXXI, Appendix D), although no immediate correlation could be made without prior knowledge of temperature increase due to electrical heating.

Varying thickness and annulus width test

Based on the data shown from Tables XXXII to XXXV (Appendix D), a plot of the breakdown strength of air versus the material wall thickness for the different configurations tested has been shown in Figure 20. Evidently, a material with a thinner dielectric wall enables quicker breakdown of the air in the annulus. Since the capacitance of air increases and that of the outer cylinder decreases, based on equations V-1 and V-2, for increasing thickness of the outer cylinder (constant surface area), a potential argument may be that the voltage maintained across the air-gap would be lower and that across the outer cylinder would be higher for a greater dielectric wall thickness, for the same total charge supplied to the reactor. Another plausible indicator of a greater energy being available within the air-gap for thinner wall dielectrics may be the temperature reached at the gas outlet for different configurations. Even for a lower ozone concentration, the gas temperature is distinctly higher for thinner wall dielectrics indicating more electrical heating of the gas.

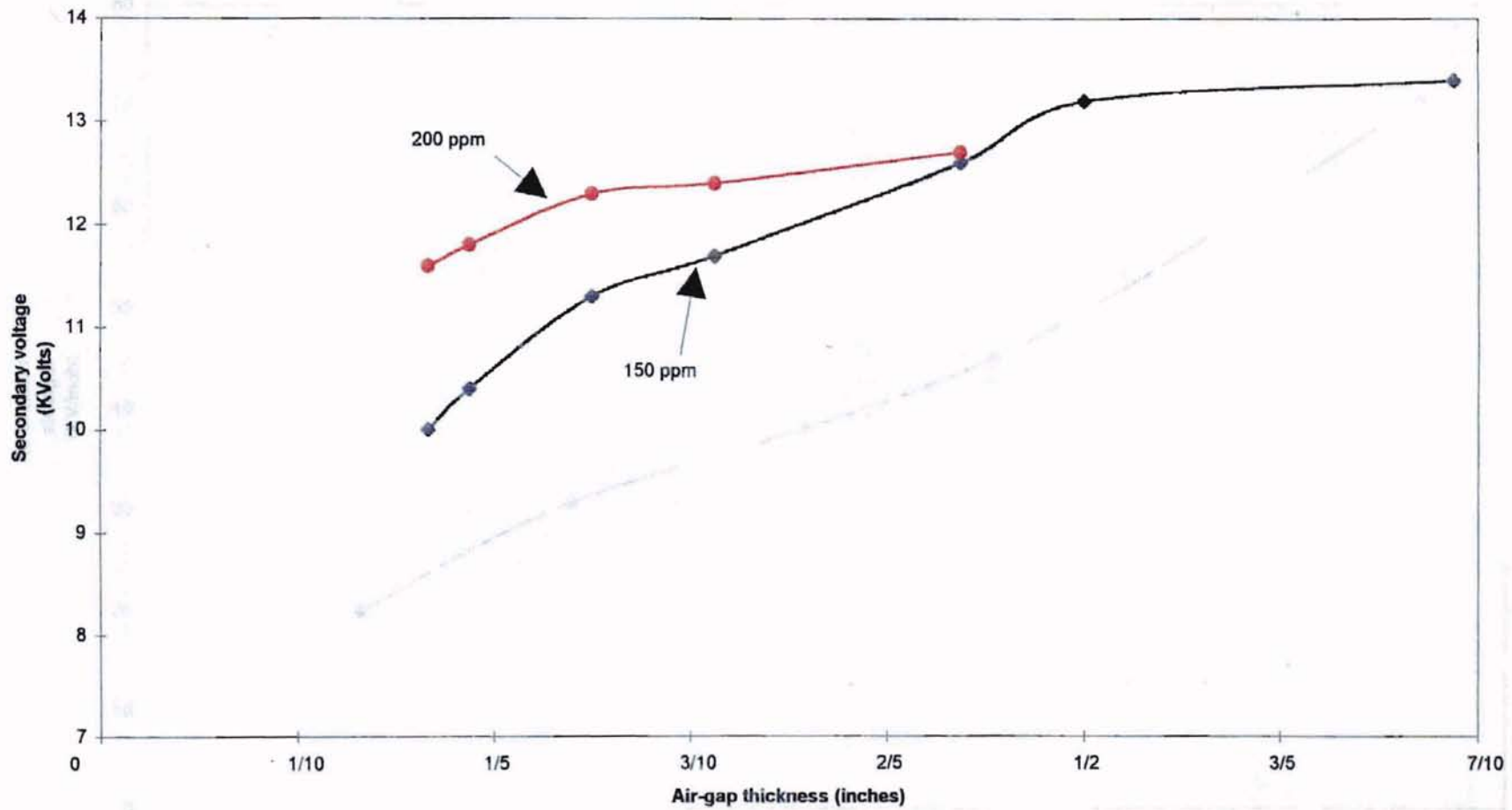


Figure 19. Secondary voltage required to produce an ozone concentration of 150 and 200 ppm for different air-gap thickness (varying surface area and annulus width test)

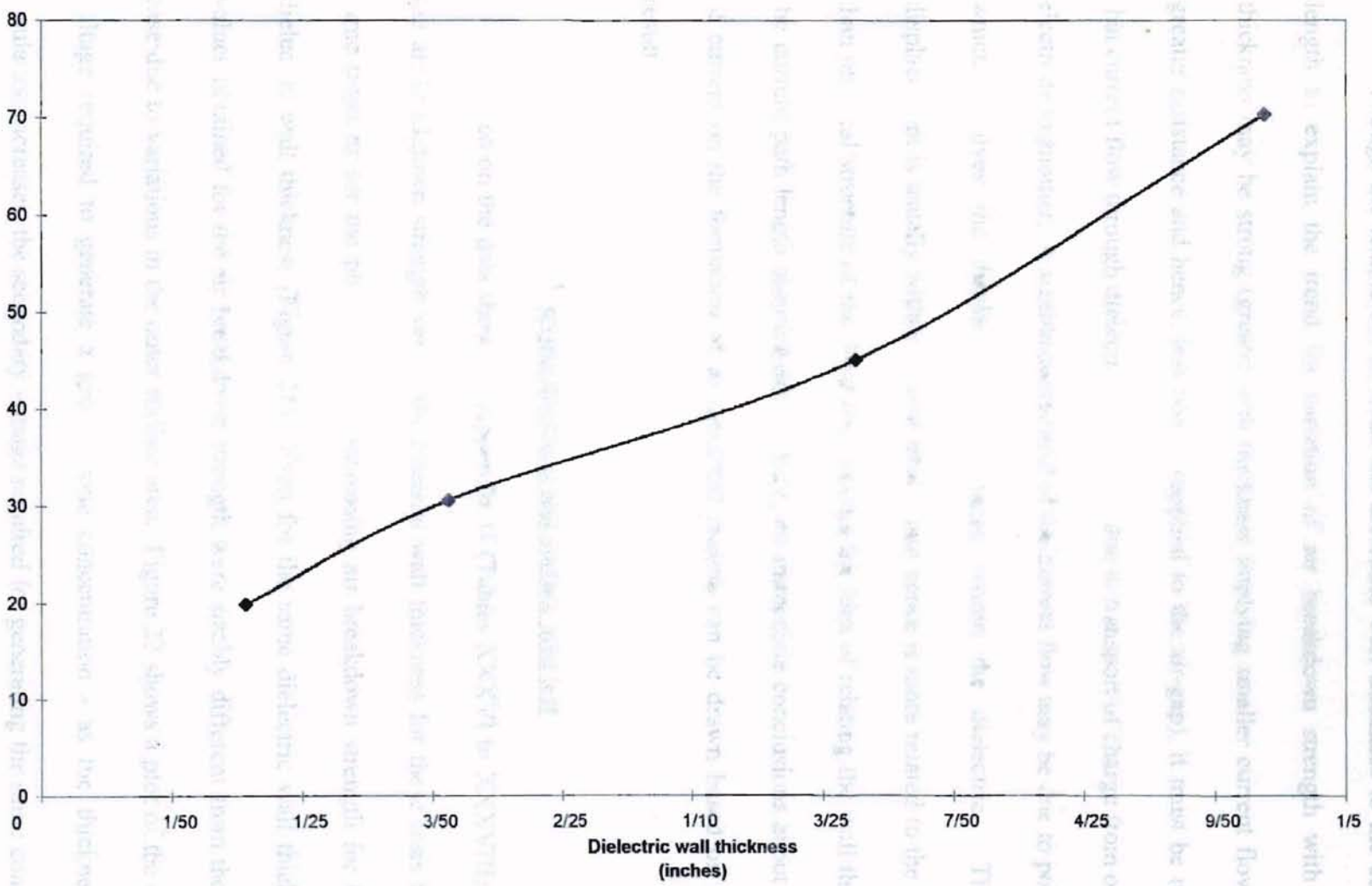


Figure 20. Variation of air breakdown strength with dielectric wall thickness (varying thickness and annulus width test)

Though the temptation to relate the dielectric wall thickness to the current path length to explain the trend for variation of air breakdown strength with dielectric thickness may be strong (greater wall thickness implying smaller current flow due to a greater resistance and hence, less power supplied to the air-gap), it must be understood that current flow through dielectrics is not just due to transport of charge from one electrode to another. A sizable component of the current flow may be due to polarization, which involves the displacement of charge within the dielectric. The charge displacement is usually within a small lattice, and hence is more related to the molecular than physical structure of the dielectric, leaving the idea of relating the wall thickness to the current path length questionable. Hence, no immediate conclusions about the effect of current on the formation of an electrical plasma can be drawn based on the above result.

Varying thickness and surface area test

Based on the data shown in Appendix D (Tables XXXVI to XXXVIII), a plot of the air breakdown strength versus the material wall thickness for these tests follow the same trend as for the previous test - increasing air breakdown strength for increasing dielectric wall thickness (Figure 21). Even for the same dielectric wall thickness, the values obtained for the air breakdown strength were sizably different from the previous case due to variations in the outer surface area. Figure 22 shows a plot of the secondary voltage required to generate a given ozone concentration - as the thickness of the insulation increases, the secondary voltage required for generating the same concentration of ozone also increases. This would mean that the proportion of voltage available for

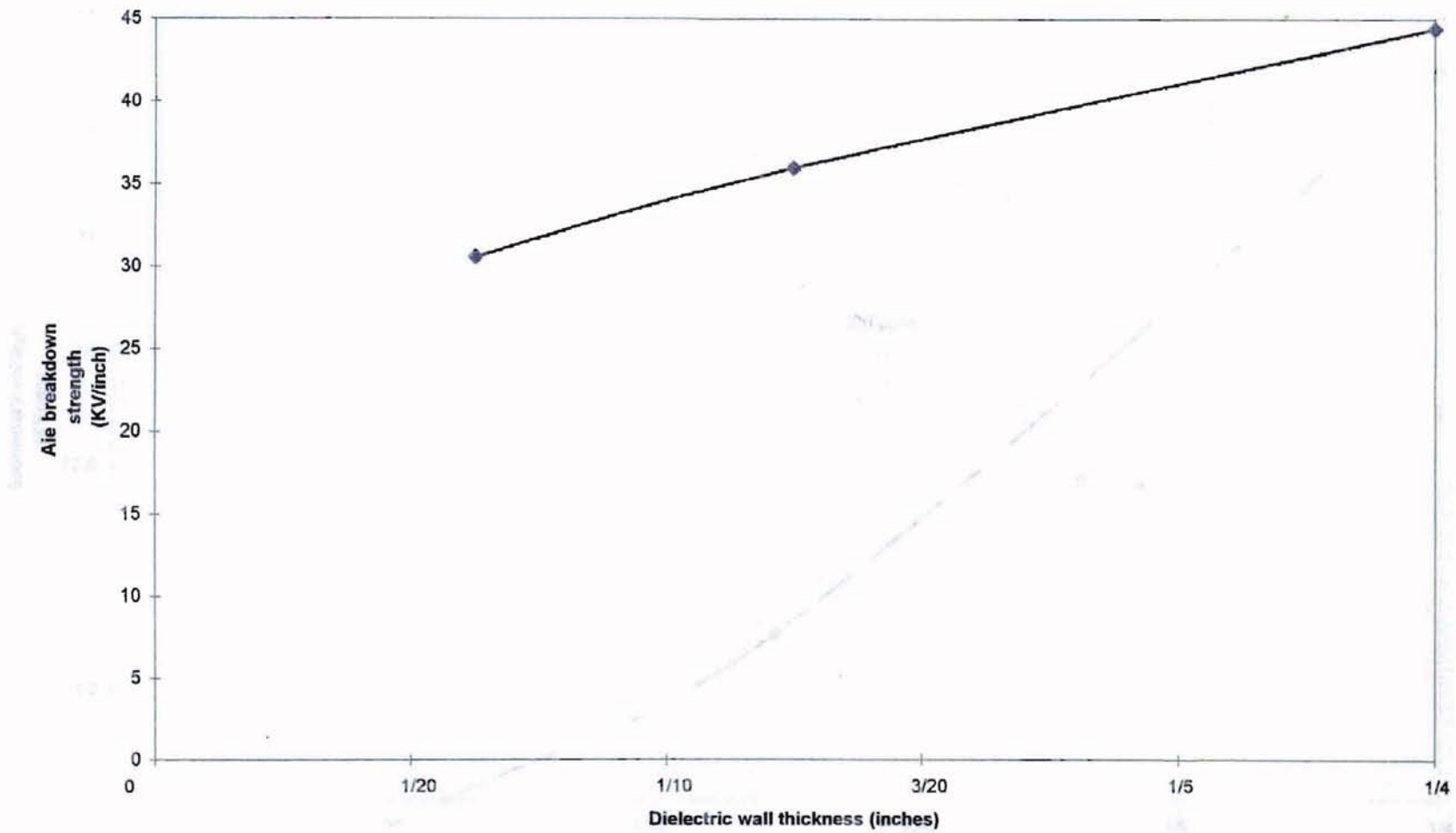


Figure 21. Variation of air breakdown strength with dielectric wall thickness (varying thickness and surface area test)

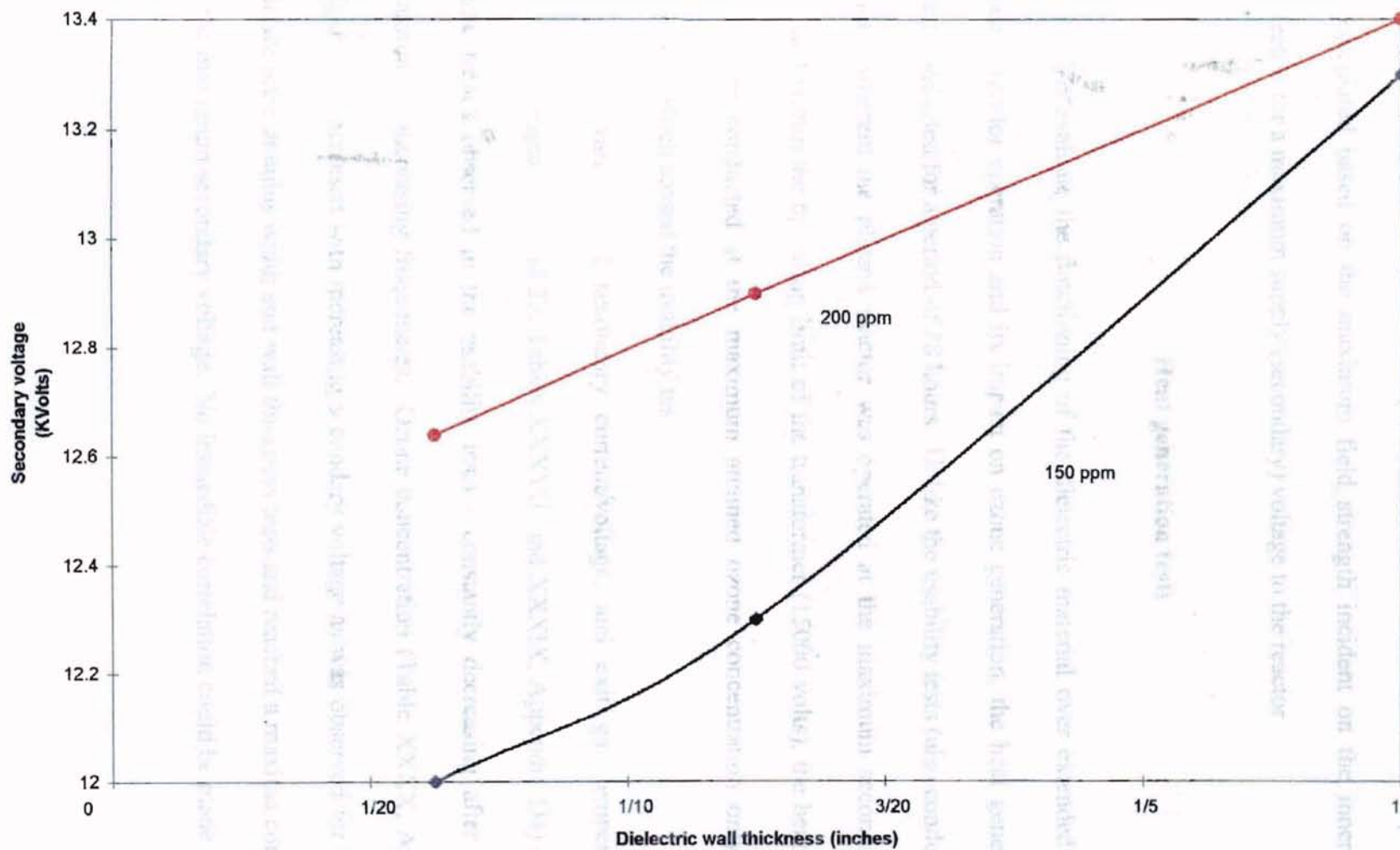


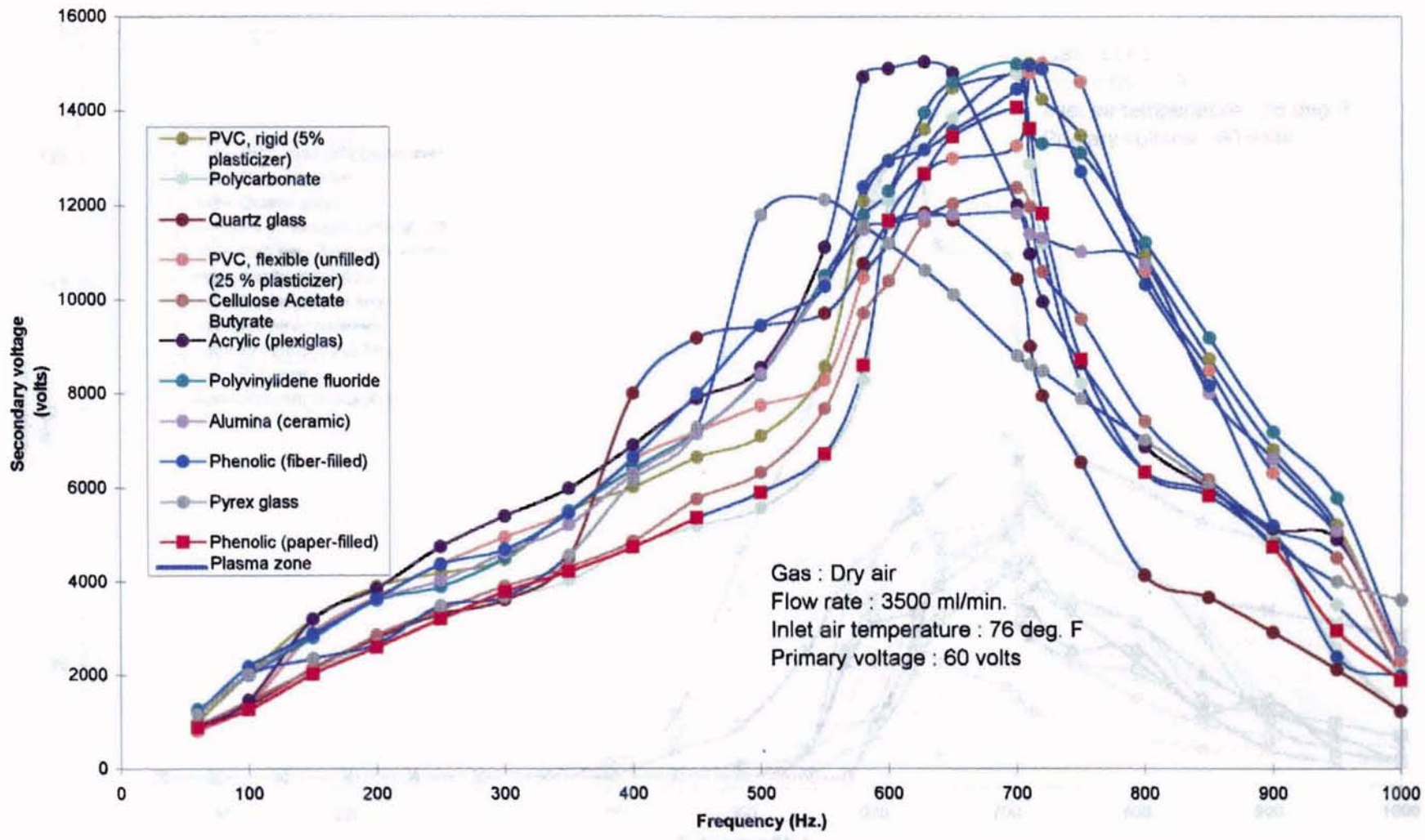
Figure 22. Secondary voltage required to produce an ozone concentration of 150 and 200 ppm for different material thickness (varying thickness and surface area test)

ozone generation is lower for a thicker dielectric wall, thereby agreeing well with the result previously obtained. The least possible dielectric thickness which may be used can be calculated based on the maximum field strength incident on the inner and outer dielectric for a maximum supply (secondary) voltage to the reactor.

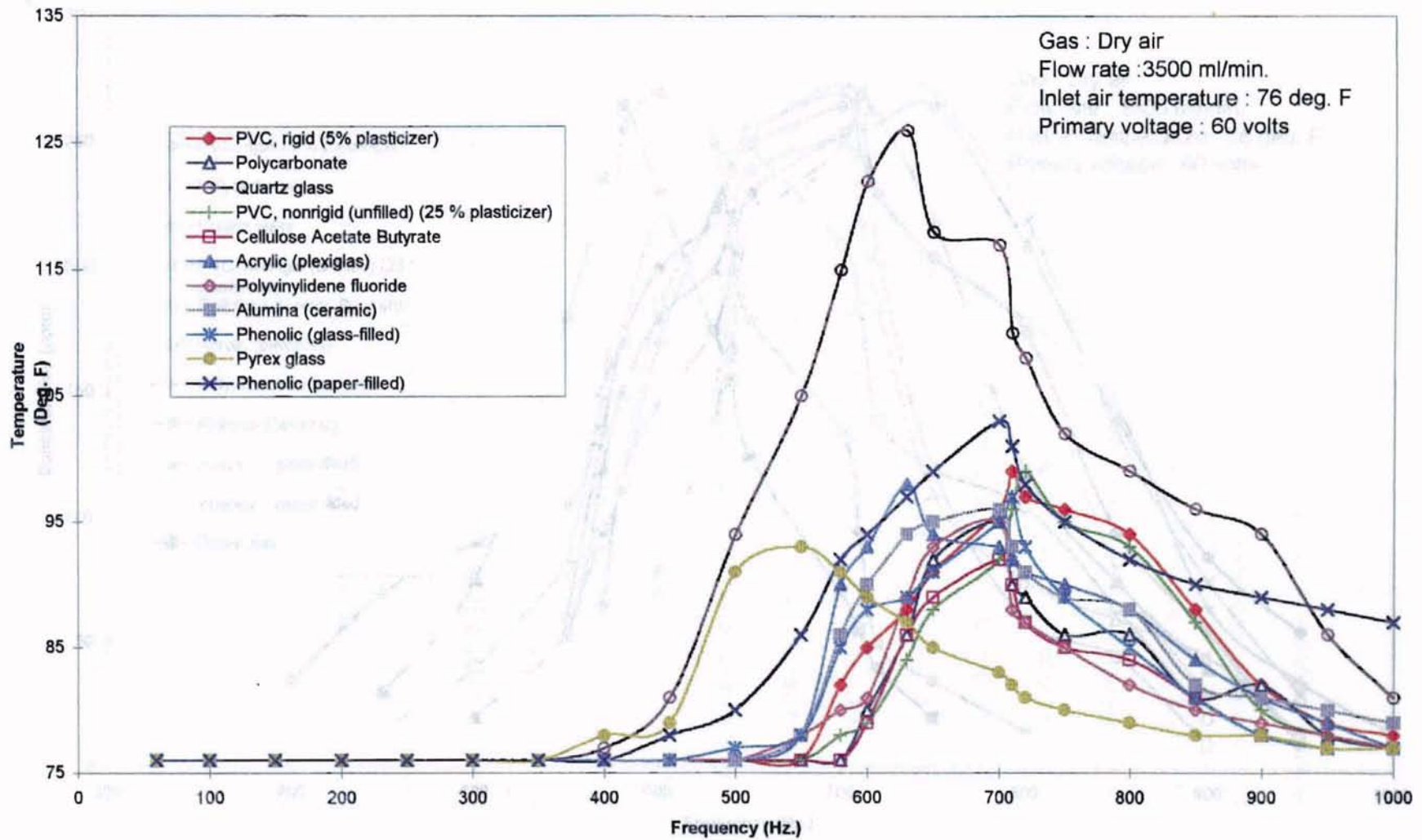
Heat generation tests

To evaluate the functioning of the dielectric material over extended periods of plasma reactor operation and its impact on ozone generation, the heat generation tests were conducted for a period of 18 hours. Unlike the usability tests (also conducted for 18 hours) wherein the plasma reactor was operated at the maximum secondary voltage attained within the operating limit of the transformer (15000 volts), the heat generation tests were conducted at the maximum attained ozone concentration only for those materials which passed the usability test.

The variation of secondary current/voltage, and exit gas temperature with frequency (Figures 25 and 23, Tables XXXVII, and XXXIX, Appendix D4) showed the same trends observed in the usability tests - constantly decreasing after reaching a maxima for increasing frequencies. Ozone concentration (Table XXXX, Appendix D; Figure 26) increased with increasing secondary voltage as was observed for the varying surface area, annulus width and wall thickness tests and reached a maxima corresponding to the maximum secondary voltage. No immediate correlation could be made between

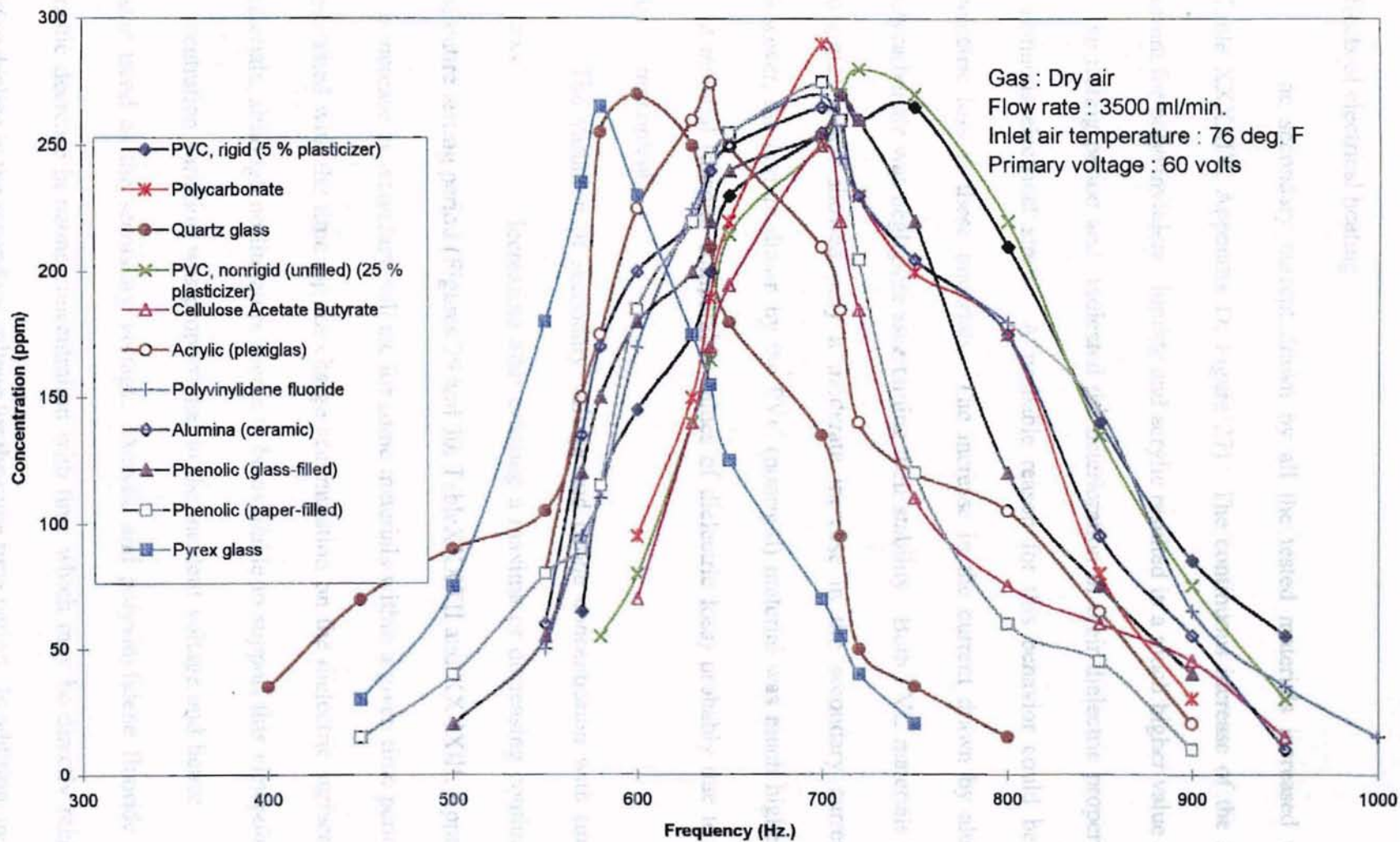


Note : Dimensions for different reactor materials are presented in Table VII.
 Figure 25. Effect of frequency on secondary voltage at constant primary voltage



Note : Dimensions for different reactor materials are presented in Table VIII.

Figure 23. Variation of exit gas temperature with frequency at constant primary voltage (heat generation test).

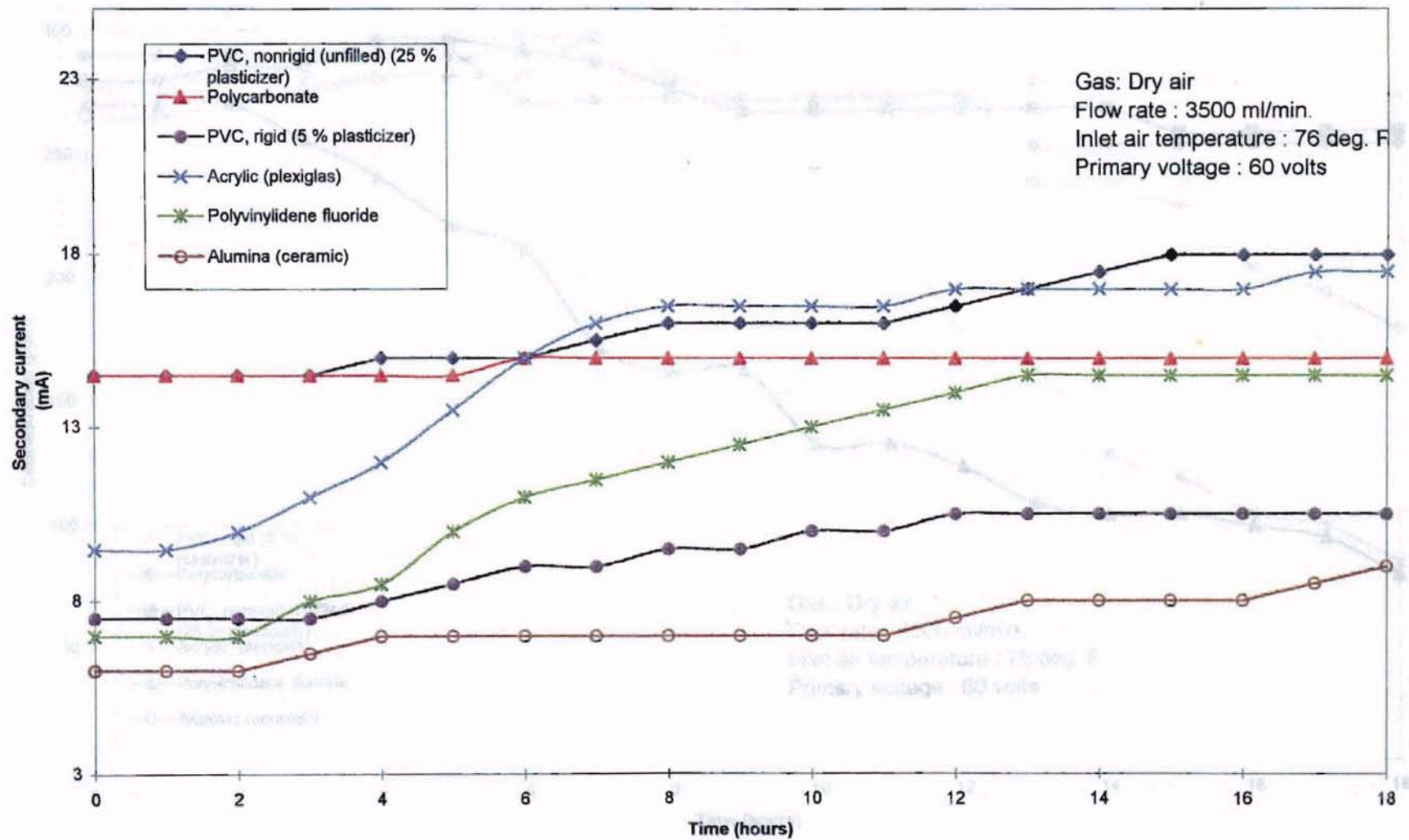


Note : Dimensions for different reactor materials are presented in Table VIII.
Figure 26. Variation of concentration with frequency (heat generation test).

the rise in exit gas temperature and ozone concentration without prior knowledge of the effects of electrical heating.

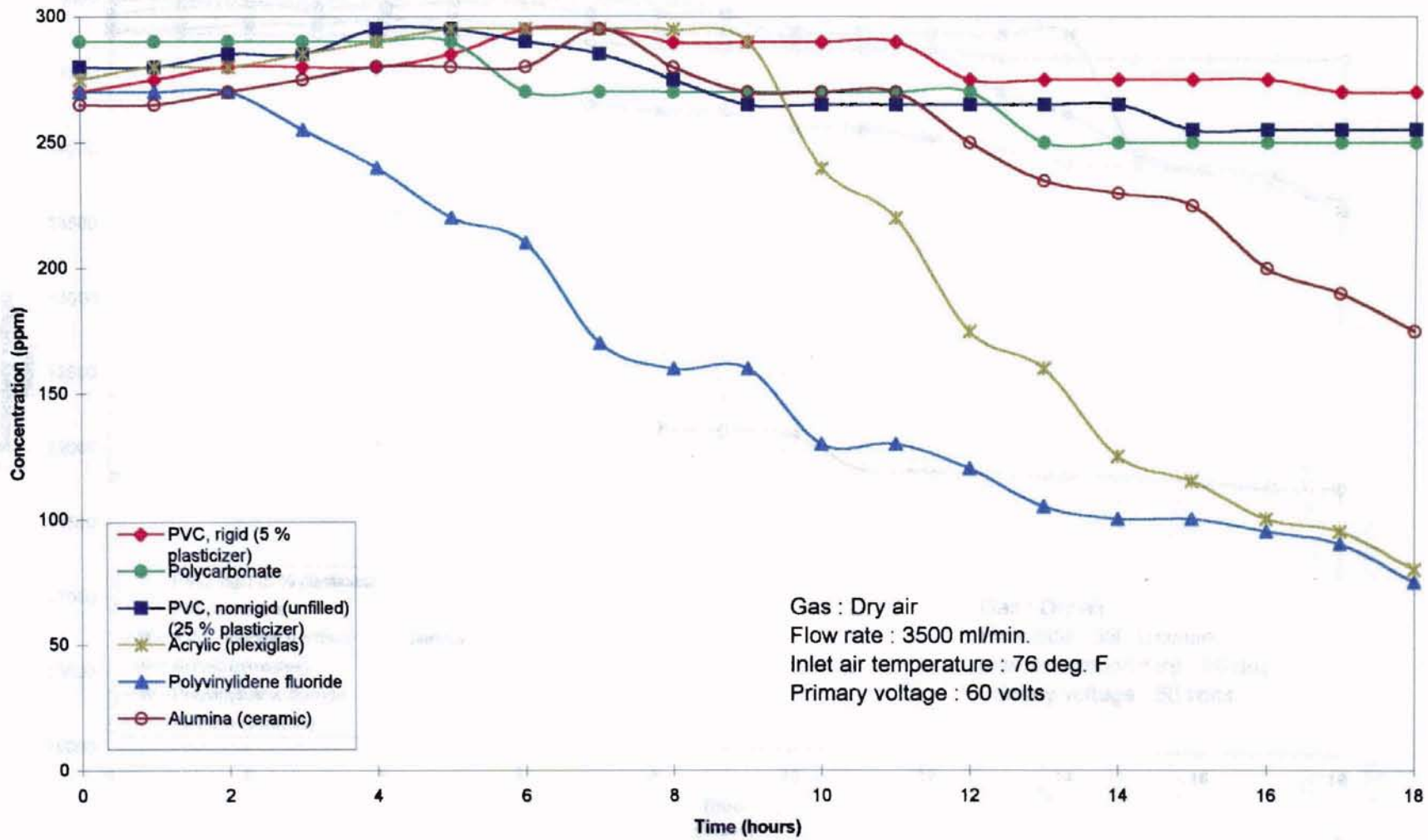
The secondary current drawn by all the tested materials increased with time (Table XXXXIV, Appendix D; Figure 27). The continuous increase of the secondary current for polyvinylidene fluoride and acrylic resulted in a much higher value at the end of the testing period and indicated the deterioration of their dielectric properties under continuous electrical stress. A probable reason for this behavior could be the high dielectric loss of these materials. The increase in the current drawn by alumina and polycarbonate was negligible ascertaining their stability. Both PVC materials (rigid and nonrigid) tested showed only a moderate increase in the secondary current drawn. However, the current drawn by the PVC (nonrigid) material was much higher than the rigid material (despite comparable values of dielectric loss) probably due to its higher plasticizer content.

The variation of secondary voltage and ozone concentration with time was as follows - constantly decreasing after crossing a maxima or decreasing continuously for the entire testing period (Figures 29 and 30; Table XXXXII and XXXXIII, Appendix D4). The increase in secondary voltage for some materials within a given time period may be associated with the time lag for charge accumulation on the dielectric surface for these materials, although no literature seems to be available to support this viewpoint. Ozone concentration variation was proportional to the incident voltage and hence followed the same trend as the secondary voltage. Acrylic and polyvinylidene fluoride showed a drastic decrease in ozone concentration with time which may be directly related to the sharp decline in the secondary voltage for the same time period. In addition, the steep

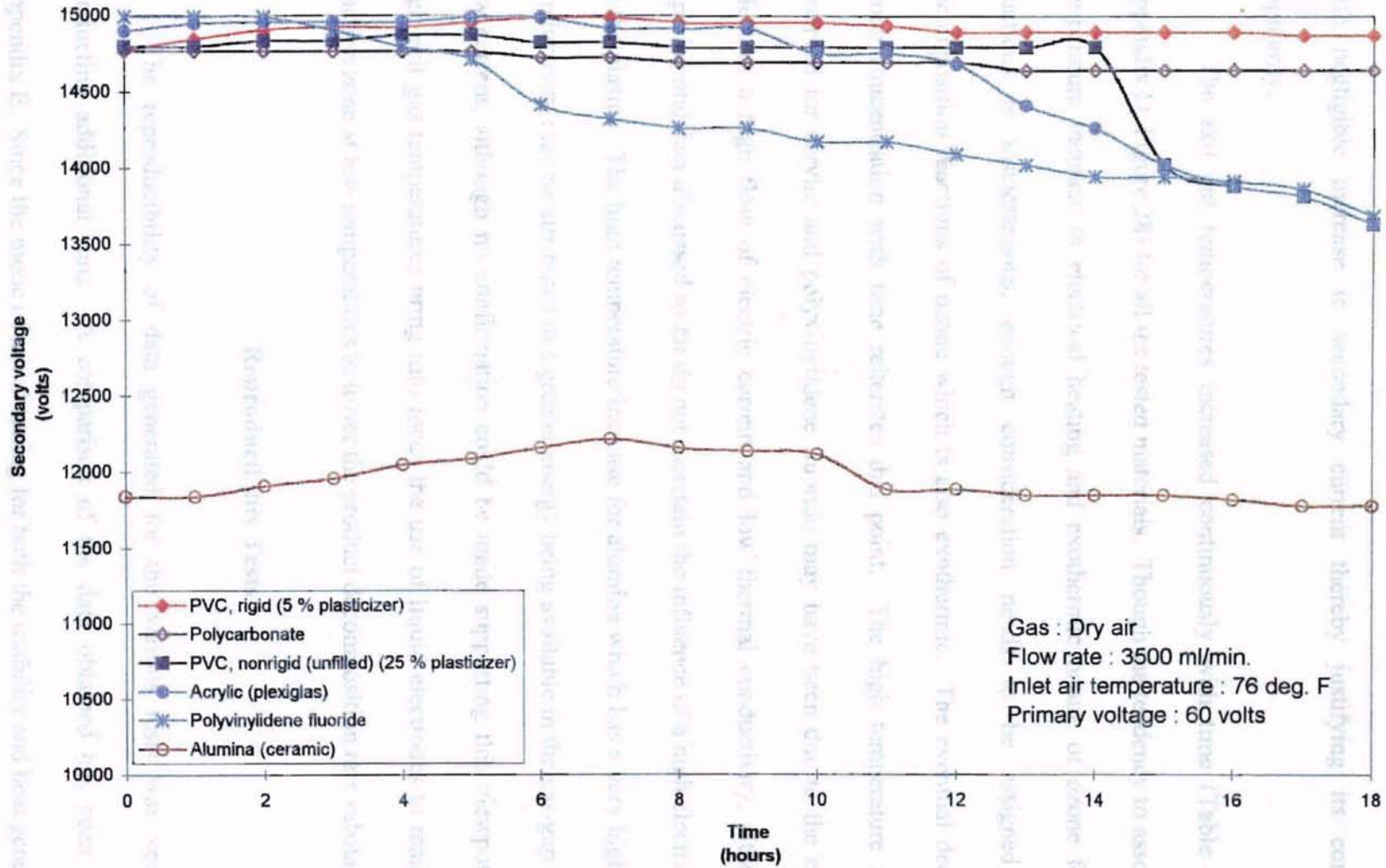


Note : Dimensions for different reactor materials are presented in Table VIII.

Figure 27. Variation of secondary current with time (heat generation test).



Note : Dimensions for different reactor materials are presented in Table VIII.
Figure 29. Variation of concentration with time at constant primary voltage (heat generation test).



Note : Dimensions for different reactor materials are presented in Table VIII.

Figure 30. Variation of secondary voltage with time at constant primary voltage (heat generation test).

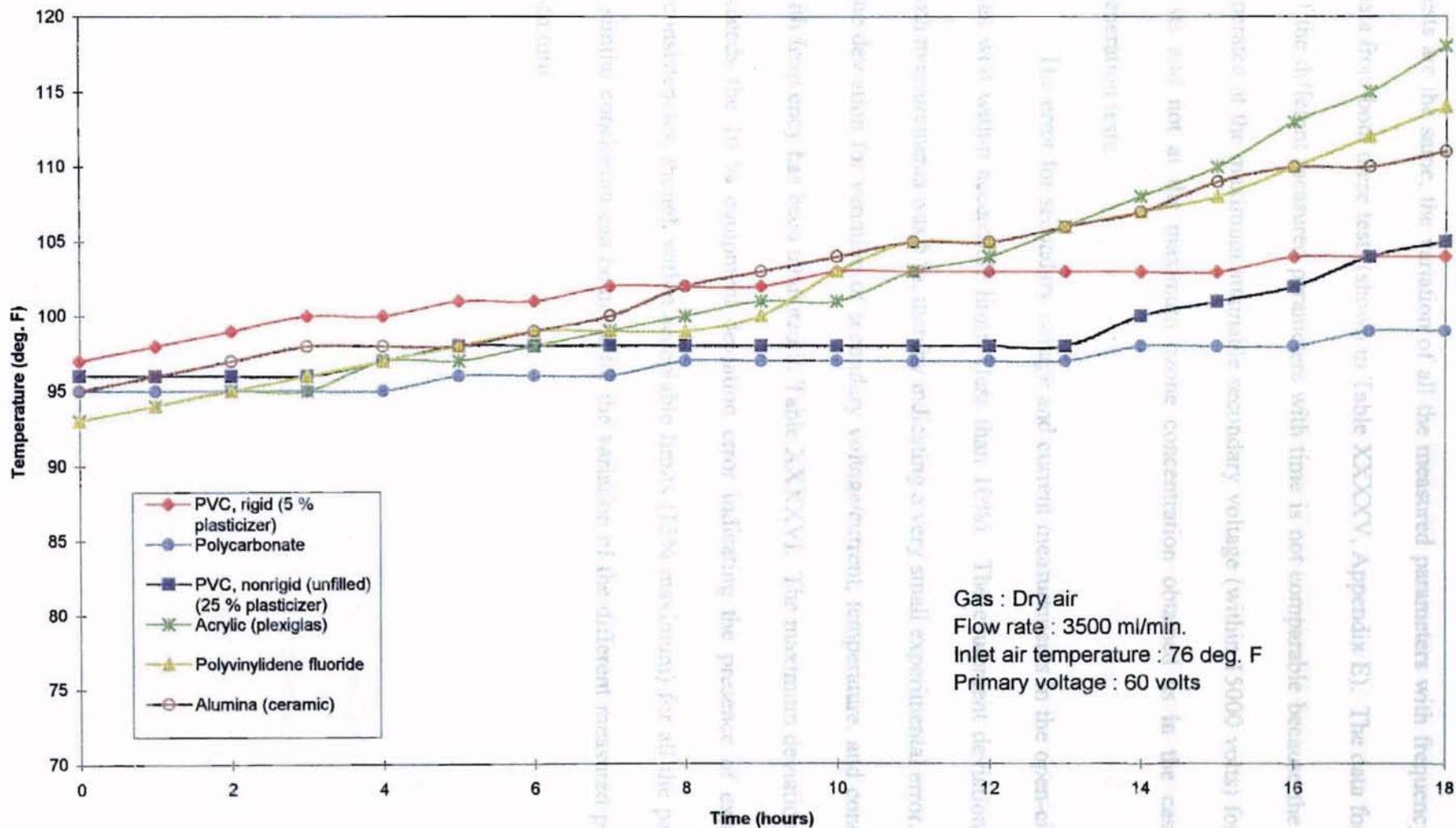
rise in the secondary current drawn by these two materials depict their unsuitability for use in plasma reactors. Alumina showed only a small decrease in ozone concentration with negligible increase in secondary current thereby justifying its commercial popularity.

The exit gas temperatures increased continuously with time (Table XXXXI, Appendix D; Figure 28) for all the tested materials. Though the tendency to associate the temperature increase to electrical heating and exothermic nature of ozone formation reactions is instantaneous, enough consideration needs to be assigned to the decomposition reactions of ozone which is also exothermic. The eventual decrease in ozone concentration with time reiterates this point. The high temperature increases observed for acrylic and polyvinylidene fluoride may have been due to the combined effect of a high flow of electric current and low thermal conductivity, although the *experimental data discussed so far do not ascertain the influence of a high electric current on the plasma*. The high temperature increase for alumina which has a very high thermal conductivity may be attributed to a greater energy being available in the gas-gap despite a low current, although no confirmation could be made supporting this viewpoint. The high exit gas temperatures bring into focus the use of liquid electrodes to maintain the reaction zone at low temperatures to lower the product decomposition rate substantially.

Reproducibility Tests

The reproducibility of data generated for the various tests was verified by conducting additional runs. A comparison of the data obtained has been made in Appendix E. Since the mode of initial testing for both the usability and heat generation

UNIVERSITY



Note : Dimensions for different reactor materials are presented in Table VIII.

Figure 28. Variation of exit gas temperature with time at constant primary voltage (heat generation test)

tests are the same, the variation of all the measured parameters with frequency contains data from both these tests (shown in Table XXXXV, Appendix E). The data for variation of the different measured parameters with time is not comparable because the reactor is operated at the maximum attainable secondary voltage (within 15000 volts) for usability tests and not at the maximum ozone concentration obtained as in the case of heat generation tests.

The error for secondary voltage and current measurements in the open-circuit tests was well within acceptable limits (less than 10%). The equipment deviation error for both measurements was 5 %, thereby indicating a very small experimental error.

The deviation for variation of secondary voltage/current, temperature, and concentration with frequency has been tabulated in Table XXXXVI. The maximum deviation obtained exceeds the 10 % equipment deviation error indicating the presence of experimental inconsistencies, though within acceptable limits (15% maximum) for all the parameters. A similar conclusion can be made for the variation of the different measured parameters with time.

CONCLUSIONS AND RECOMMENDATIONS

Plastics seem to have a good potential as alternative materials for use as dielectrics in plasma reactors. The low cost of the tested plastics justify their use in applications wherein a high thermal conductivity of the dielectric material is not a prerequisite. The highly hydrophobic nature of the tested plastics guarantee their usability in reactors with liquid electrodes. Their high impact and tensile strength would ease the rigors of mechanical wear or accidental breakage, a case more common with the currently used dielectrics, viz. ceramics and glass.

Conclusions

The following conclusions were drawn based on the results obtained in this study :

- (1) Plastics may prove to be a competent alternative in place of the more expensive ceramics and highly fragile glass for use as dielectrics in plasma reactors. Of the eight plastic materials tested, five passed the dielectric usability criteria defined by this study. The failure of three plastic materials viz., phenolic (paper- and glass-filled) and Cellulose Acetate Butyrate (CAB) brought into focus the rigors of dielectric heating, an appendage of all commercial dielectrics, in addition to the importance of dimensional stability under electrical heating. A material with excellent electrical properties may succumb to the impact of electrical heating if it

lacks dimensional stability under such conditions, as in the case of CAB. Based on the data obtained from the usability and heat generation tests, polycarbonate and both PVC types (rigid and nonrigid) functioned well for the entire testing period. Although both acrylic and polyvinylidene fluoride materials tested also passed the usability tests defined by this study, heating of the materials was observed at the end of the experimental runs which may hint unsuitability for extended periods of reactor operation.

- (2) The importance of filler materials used in plastics was brought about by the sizable difference in breakdown time of paper- and glass-filled phenolic resins tested. The filler material used should possess excellent burning characteristics. However, the use of a filler material with excellent burning characteristics may not guarantee its usability in this setup due to the limitations posed by electrical tracking, a characteristic of phenolic resin.
- (3) Only plastic materials with a high tracking resistance should be used as a dielectric for this application. Both the phenolic resins tested proved suspect to a high accumulation of charge at specific points on the surface.
- (4) Based on the trends obtained with the limited data available, the voltage required for the breakdown of a given mass of air contained within a specified air-gap thickness decreased as the air-gap thickness and the outer diameter of the outer cylinder were increased. In other words, the voltage gradient (volts/inch) required for the breakdown of air decreased as the air-gap thickness and the outer cylinder surface area were increased (for a fixed geometry of the inner cylinder). This result requires

UNIVERSITY

further validation.

- (5) For optimum power transfer to the reactor, a dielectric material with a high dielectric constant may be more suitable - a greater proportion of the total voltage applied may be available for gas breakdown in the gas-gap. However, this result was obtained based on the average values for the dielectric constant available for the general class of the plastics tested (A.S.T.M. standards) and requires further validation.
- (6) Based on the trends obtained with the limited data available, a thin dielectric wall seemed to be more suitable for quicker gas breakdown. Though the secondary voltage required for generating the same ozone concentration became higher for increasing dielectric wall thickness, no confirmed conclusions could be made due to the complications arising through ozone destruction at higher temperatures in the gas-gap (Horvath et al., 1985).

Recommendations

Based on the observations made throughout this study and the conclusions reached upon, the following recommendations were made to further plasma research being conducted at Oklahoma State University :

- (1) The low thermal conductivity of the plastic materials tested necessitates the control of the plasma zone temperature by means of external cooling to ensure optimum ozone generation. Since the liquid electrode should possess excellent ionic conductivity to prevent energy dissipation due to self-heating, proper choice of a liquid electrode is

essential. Care should be taken to ensure that the plastic material (used as a dielectric) is highly resistant to the liquid electrode chosen.

- (2) The ozone concentration measurements made in this study with the aid of Drager tubes were not online. Though extreme care was taken to make the concentration measurements just beyond the plasma zone, experimental inaccuracies could not be avoided as evident from the error analysis made. This strongly hinted the need for ozone concentration measuring equipment which are online to obtain reliable data that can be used for future scale-up of the ozone generating equipment.
- (3) Though the primary focus of this study was on dielectric materials and not on varied external conditions like feed temperature/flow rate, adequate knowledge is required about the effect of residence times, pre-cooled feed (air or oxygen), temperature of the plasma zone (maintained by liquid electrodes) and the pressure inside the reactor before any positive step towards commercialization can be made.
- (4) Quantification of the energy required for product formation, an absolute requirement, has not been made in this study due to the unknown value of the power factor on the secondary side. Using correlations for energy losses in the dielectric and gas (due to electrical heating and visible light emission) and knowing the values for the power factor under varying frequencies, attempts should be made to model the current setup to predict ozone formation for a given supply of energy to the reactor.
- (5) Figure 31 shows a liquid cooled plasma reactor recently built at Oklahoma State University. The dimensions of the reactor is as follows :

Inner tube		Outer tube		Air gap thickness (inch)
Outer diameter (inch)	Wall thickness (inch)	Outer diameter (inch)	Wall thickness (inch)	
3/8	3/16	3	3/16	1/2



Figure 31. Liquid electrode plasma reactor - a pipe-dream?

Inner tube		Outer tube		Air gap thickness (inch)
Outer diameter (inch)	Wall thickness (inch)	Outer diameter (inch)	Wall thickness (inch)	
1 5/8	3/16	3	3/16	1/2

Three different liquid solutions viz. copper sulfate, hydrochloric acid (10-30 %), and sulfuric acid (10-30 %) were experimented with to gauge their ability to function as an electrode. With the current setup, a plasma zone could not be generated. Though the large air-gap thickness may be the root cause of this problem, other probable causes like dielectric wall thickness and more importantly, the surface area of the inner cylinder need to be investigated.

REFERENCES

- Benson, S.W., and Axworthy, A.E.**, "Ozone Chemistry and Technology", Proceedings on International Ozone Conference, **21** (1959).
- Brydson, J.A.**, Plastics Materials, John Wiley and Sons, London (1975).
- Clark, F.M.**, Insulating Materials for Design and Engineering Practice, John Wiley and Sons, New York (1962).
- Fink, D.G., and Beaty, H.W.**, Standard Handbook for Electrical Engineers, McGraw Hill, New York (1978).
- Gutierrez - Tapia, C., Camps, E., Olea - Cardoso, O.**, "Perturbative Method for Ozone Synthesis from Oxygen in a Single Discharge Reactor", IEEE Transactions on Plasma Science, **22** (5) (1994).
- Hippel, A.V.**, Dielectric Materials and Applications, Artech House, London (1995).
- Horvath, M., Bilitzky, L., and Huttner, J.**, Ozone, Elsevier, Budapest (1985).
- Pignolet, P., Hadj-Ziane, S., Held, B., Benas, J., and Coste, C.**, "Ozone Generation by Point to Plane Corona Discharge", *J. Phys. D : Appl. Phys.*, **23**, 1069 - 1072 (1990).
- Schwaiger, A., and Sorensen, R.W.**, Theory of Dielectrics, John Wiley and Sons, London (1932).
- Venugopalan, M.**, Reactions under Plasma Conditions, John Wiley and Sons, New York (1971).
- Whitehead, S.**, Dielectric breakdown of solids, Oxford University Press, London (1951).

APPENDICES

Appendix A

Properties of Materials Selected for Experimentation

TABLE I
Properties of materials selected for experimentation.

Properties\Material	Acrylic	Cellulose Acetate Butyrate	Poly carbonate	PVC, rigid
Electrical :				
Dielectric constant				
60 Hz.	3.6	3.5 - 5	2.97 - 3.17	3.2 - 4.0
100 Hz.	3.5	3.6 - 5	3.1	3.4 - 3.9
1000 Hz. (A.S.T.M. D150)	3.3	3.4 - 5	3.0	3.0 - 3.8
Power Factor				
60 Hz.	0.06	0.01-0.04	0.0009	0.007 - 0.01
100 Hz.	0.06	0.01-0.04	0.0014	0.008- 0.01
1000 Hz.	0.04	0.01-0.04	0.0021	.009 - 0.012
Dielectric Strength (Volts/mil.) (A.S.T.M. D149)	450 - 550	225 - 320	400	400 - 500
Volume Resistivity (ohm-cm)	$> 10^{15}$	$10^{11} - 10^{15}$	$> 10^{16}$	$> 10^{16}$
Mechanical :				
Tensile strength (psi x 10^{-4}) A.S.T.M. D638, D651	0.7 - 1.1	0.19 - 0.85	0.85 - 0.95	0.75 - 0.85
Compressive strength (psi x 10^{-4})	1.2 - 2.0	0.21 - 4.0	1.1 - 1.2	0.75 - 0.85
Impact strength (ft b./in.)	0.3 - 0.45	0.5 - 0.6	12 - 16	1 - 3
Thermal :				
Thermal Conductivity (Cal/cm/sq.cm/°C/sec) $\times 10^{-4}$ A.S.T.M. C177	4.5 - 5.5	4 - 8	4.5 - 6.0	3.4 - 3.6
Coefficient of thermal expansion $\left(\frac{\text{in}}{\text{in } ^\circ\text{C}} \right) \times 10^{-5}$ A.S.T.M. D696	9.0	18.0	6.6	10.0
Physical :				
Water Absorption % in 24 hrs., 1/8 thick.	0.25	6.5	0.18	0.4

TABLE I
Properties of materials selected for experimentation.

Properties\Material	Phenolic (glass)	Phenolic (cloth)	Alumina	Pyrex	Quartz
Electrical :					
Dielectric constant					
60 Hz.	7.0	5.9	8 - 9.5	5.3	3.8
100 Hz.	7.0	5.9	8 - 9.5	5.3	3.8
1000 Hz. (A.S.T.M. D150)	6.5	5.5	8 - 9.5	5.3	3.8
Power Factor					
60 Hz.	0.12	0.1	0.0002	0.0055	0.0002
100 Hz.	0.12	0.1	0.0005	0.0051	0.0002
1000 Hz.	0.08	0.05	0.0007 - 0.001	0.0035	0.0001
Dielectric Strength (Volts/mil.) (A.S.T.M. D149)	140 - 400	200 - 370	-	-	-
Volume Resistivity (ohm-cm)	$10^{13} - 10^{15}$	$10^{10} - 10^{13}$	$10^{14} - 10^{16}$	10^{12}	10^{13}
Mechanical :					
Tensile strength (psi x 10^{-4}) A.S.T.M. D638, D651	0.7 - 1.8	0.6 - 0.8	8 - 50	0.2	0.7
Compressive strength (psi x 10^{-4})	1.6 - 7	2 - 2.8	8 - 42	-	1.6
Impact strength (ft lb./in.)	0.5 - 18	0.8 - 3.5	-	-	-
Thermal :					
Thermal Conductivity (Cal/cm/sq.cm/°C/sec) $\times 10^{-4}$ A.S.T.M. C177	8 - 14	9 - 12	690	26	28
Coefficient of thermal expansion $\left(\frac{\text{in}}{\text{in } ^\circ\text{C}} \right) \times 10^{-5}$ A.S.T.M. D696	-	-	0.43	0.32	0.055
Physical :					
Water Absorption % in 24 hrs., 1/8 thick.	0.03 - 1.2	0.6 - 1.8	-	-	-

TABLE I
Properties of materials selected for experimentation.

Properties\Material	PVC, flexible (unfilled)	Polyvinylidene fluoride
Electrical :		
Dielectric constant 60 Hz.	5-6	8.0-8.5
100 Hz.	5-6	8.0-8.5
1000 Hz. (A.S.T.M. D150)	5-6	7.8-8.3
Power Factor 60 Hz.	0.005-0.01	0.039-0.049
100 Hz.	0.009-0.02	0.039-0.049
1000 Hz.	0.009-0.02	0.045-0.049
Dielectric Strength (Volts/mil.) (A.S.T.M. D149)	325-600	260 - 400
Volume Resistivity (ohm-cm)	$10^{13} - 10^{15}$	$> 10^{16}$
Mechanical :		
Tensile strength (psi x 10^{-4}) A.S.T.M. D638, D651	0.6 - 0.8	0.7
Compressive strength (psi x 10^{-4})	0.6 - 0.8	1.0
Impact strength (ft lb./in.)	0.2-1.0	3.0-3.2
Thermal :		
Thermal Conductivity (Cal/cm/sq.cm/°C/sec) $\times 10^{-4}$ A.S.T.M. C177	3.2-3.8	3.8-4.2
Coefficient of thermal expansion $\left(\frac{\text{in}}{\text{in } ^\circ\text{C}} \right) \times 10^{-5}$ A.S.T.M. D696	8.0-9.0	7.0
Physical :		
Water Absorption % in 24 hrs., 1/8 thick.	0.5	0.04

Appendix B

Experimental Data for Open-circuit Tests

TABLE IX
Open-circuit test for transformer
RUN 1

Primary voltage (volts)	Frequency (Hz.)	Secondary voltage (volts)	Primary current (mA)	Primary power (watts)	Total input power (watts)
40					
	60	960	0.31	8.5	90
	100	1520	0.23	6.7	82
	150	2130	0.18	6	77
	200	2640	0.15	5.6	70
	250	3180	0.13	5.3	67
	300	3570	0.11	5	63
	350	3760	0.1	4	61
	400	4010	0.09	2.6	59
	450	4360	0.08	2.4	57
	500	4580	0.08	2.2	55
	550	4870	0.08	2.1	52
	600	5180	0.08	2	50
	650	5590	0.08	1.8	48
	700	6020	0.1	2.4	49
	750	6680	0.11	3.2	51
	800	7310	0.13	3.9	54
	850	8060	0.15	4.8	56
	900	9010	0.16	6.1	58
	950	9870	0.19	7.3	61
	1000	10360	0.25	8.9	64
	1100	11110	0.31	10.1	67
	1200	11230	0.4	12.3	70
	1300	9910	0.5	11.9	68
	1400	9010	0.48	11.4	66
	1500	7960	0.45	9.9	64

TABLE IX (CONTD.)

Primary voltage (volts)	Frequency (Hz.)	Secondary voltage (volts)	Primary current (mA)	Primary power (watts)	Total input power (watts)
50					
	60	1020	0.38	9.6	100
	100	1640	0.25	7.9	96
	150	2300	0.19	6.5	92
	200	2840	0.15	5.9	80
	250	3300	0.13	4.6	72
	300	3680	0.12	3.2	62
	350	3840	0.11	2.6	57
	400	4140	0.1	2.2	53
	450	4440	0.1	2.1	52
	500	4700	0.11	2.2	54
	550	4960	0.12	2.5	60
	600	5320	0.13	2.8	68
	650	5940	0.15	3.5	75
	700	6460	0.18	4.8	79
	750	7120	0.21	5.9	82
	800	7920	0.26	7	86
	850	8940	0.33	7.9	90
	900	10120	0.41	8.9	94
	950	11400	0.54	10.1	97
	1000	11760	0.61	12.3	102
	1100	11880	0.62	14.2	109
	1200	11280	0.61	13.2	105
	1300	10200	0.58	12.4	99
	1400	9120	0.54	11	95
	1500	8210	0.51	10	90

TABLE IX (CONTD.)

Primary voltage (volts)	Frequency (Hz.)	Secondary voltage (volts)	Primary current (mA)	Primary power (watts)	Total input power (watts)
60					
	60	1200	0.49	10.3	106
	100	1925	0.31	9	101
	150	2710	0.23	7.9	95
	200	3350	0.19	6.5	87
	250	3890	0.16	5.3	79
	300	4100	0.14	4.2	71
	350	4580	0.13	3.8	67
	400	4960	0.13	3.7	63
	450	5320	0.13	3.6	59
	500	5680	0.14	4.1	61
	550	6100	0.16	4.6	65
	600	6580	0.18	5.1	68
	650	7020	0.21	5.9	72
	700	7680	0.25	6.7	76
	750	8480	0.3	7.2	79
	800	9480	0.39	7.8	82
	850	10740	0.5	10	89
	900	12260	0.67	11.1	95
	950	13800	0.77	12.5	100
	1000	15010	0.81	14.1	105
	1100	13000	0.8	13.6	99
	1200	12180	0.74	12	96
	1300	11200	0.69	11.3	90
	1400	10320	0.65	10.8	86
	1500	9200	0.62	10.6	82

TABLE IX (CONTD.)

Primary voltage (volts)	Frequency (Hz.)	Secondary voltage (volts)	Primary current (mA)	Primary power (watts)	Total input power (watts)
70					
	60	1440	0.55	10.7	110
	100	2340	0.34	9.4	106
	150	3280	0.24	8.2	100
	200	3760	0.2	7	94
	250	4400	0.17	5.9	88
	300	4980	0.15	4.8	80
	350	5460	0.14	4	75
	400	5920	0.13	3.8	69
	450	6360	0.14	4	71
	500	6800	0.15	4.3	74
	550	7320	0.17	5	79
	600	9400	0.19	5.9	83
	650	11800	0.23	6.8	88
	700	13540	0.27	7.7	91
	750	14900	0.33	8.9	97
	800	15030	0.44	9.4	101
	850	14800	0.58	10.2	105
	900	13180	0.74	12.5	107
	950	12200	0.82	14.7	111
	1000	11320	0.85	14.9	114
	1100	10200	0.81	14.5	110
	1200	10020	0.78	13.9	105
	1300	9930	0.72	13	99
	1400	9870	0.69	11.6	93
	1500	9800	0.65	11.2	87

Table X
Power loss of transformer

Frequency (Hz.)	Primary voltage			
	40 volts	50 volts	60 volts	70 volts
	% power loss of transformer			
60	9.4	9.6	9.7	9.7
100	8.2	8.2	8.9	8.9
150	7.8	7.1	8.3	8.2
200	8.0	7.4	7.5	7.4
250	7.9	6.4	6.7	6.7
300	7.9	5.2	5.9	6.0
350	6.6	4.6	5.7	5.3
400	4.4	4.2	5.9	5.5
450	4.2	4.0	6.1	5.6
500	4.0	4.1	6.7	5.8
550	4.0	4.2	7.1	6.3
600	4.0	4.1	7.5	7.1
650	3.8	4.7	8.2	7.7
700	4.9	6.1	8.8	8.5
750	6.3	7.2	9.1	9.2
800	7.2	8.1	9.5	9.3
850	8.6	8.8	11.2	9.7
900	10.5	9.5	11.7	11.7
950	12.0	10.4	12.5	13.2
1000	13.9	12.1	13.4	13.1
1100	15.1	13.0	13.7	13.2
1200	17.6	12.6	12.5	13.2
1300	17.5	12.5	12.6	13.1
1400	17.3	11.6	12.6	12.5
1500	15.5	11.1	12.9	12.9

Appendix C

Experimental data for usability tests

TABLE XII
 Variation of secondary voltage with frequency at constant primary voltage (usability test)
 EXPERIMENTAL DATA CORRESPONDING TO FIGURE 12
RUN 2

System Conditions :

Gas : Air

Inlet temperature : 76 deg. F

Flow rate : 3500 ml/min.

Reactor dimensions : as presented in Table VII

Reactor length : 6 inches

Primary voltage : 60 volts

Material											
	PVC, rigid	Poly carbonate	Quartz glass	PVC, nonrigid	Cellulose Acetate Butyrate	Acrylic (plexiglas)	Poly vinylidene fluoride	Alumina	Phenolic (glass- filled)	Phenolic (paper- filled)	Pyrex glass
Frequency (Hz.)	Secondary Voltage (volts)										
60	1020	930	860	880	930	890	1120	1240	1200	800	1160
100	2040	1400	1380	1380	1440	1460	2030	1980	2000	1200	1960
150	3100	2020	2170	2990	2210	3100	2840	2800	2800	1980	2320
200	3700	2600	2820	3800	2980	3730	3630	3600	3600	2630	2600
250	4100	3200	3300	4260	3480	4650	4040	4000	4200	3140	3400
300	4400	3760	3640	4870	3970	5300	4620	4680	4600	3820	3650
350	5440	4020	4530	5620	4420	6040	5440	5400	5400	4340	4500
400	6000	4700	6020	6530	4980	6980	6190	6200	6600	4890	6000
450	6590	5080	8220	7130	5890	7960	7280	7200	8000	5410	7400
500	7030	5530	9470	7770	6640	8590	8410	8600	9400	5790	9900

TABLE XII (CONTD.)

Material											
	PVC, rigid	Poly carbonate	Quartz glass	PVC, nonrigid	Cellulose Acetate Butyrate	Acrylic (plexiglas)	Poly vinylidene fluoride	Alumina	Phenolic (glass- filled)	Phenolic (paper- filled)	Pyrex glass
Frequency (Hz.)	Secondary Voltage (volts)										
550	8620	6620	9930	8230	7720	11200	10630	10400	10200	6840	12200
580	12020	9320	10780	10890	8920	14660	11900	11400	12300	8130	11600
600	12900	12110	11720	11230	10200	14960	12250	11600	12890	11970	11100
630	13540	13120	11840	12700	11760	15010	14020	11800	13100	12980	10400
650	14360	13930	11700	12920	12010	14880	14720	11800	13520	13550	10000
700	14810	14870	10450	13200	12300	12060	15020	11800	14360	14210	8900
710	15040	12990	9030	14730	11870	10990	13680	11400	15010	13330	8700
720	14730	11230	7980	15000	10450	10000	13440	11200	14780	11690	8600
750	13460	8140	6560	14690	9680	8690	13210	11000	12800	8430	8000
800	10990	6380	4160	10620	7210	6860	11150	10800	10120	6130	7100
850	8760	5940	3670	8430	6120	5910	9260	7800	8050	5540	6000
900	6850	4970	2940	6410	5010	5080	7290	6400	5320	4890	4800
950	5230	3320	2130	5030	4440	4850	5840	5000	2430	3000	4000
1000	2370	2140	1260	2380	1710	2380	2360	2410	2000	1870	3600

TABLE XIII
 Variation of secondary current with frequency at constant primary voltage (usability test)
 EXPERIMENTAL DATA CORRESPONDING TO FIGURE 13
RUN 2

System Conditions :

Gas : Air

Inlet temperature : 76 deg. F

Flow rate : 3500 ml/min.

Reactor dimensions : as presented in Table VII

Reactor length : 6 inches

Primary voltage : 60 volts

Material											
	PVC, rigid	Poly carbonate	Quartz glass	PVC, nonrigid	Cellulose Acetate Butyrate	Acrylic (plexiglas)	Poly vinylidene fluoride	Alumina	Phenolic (glass- filled)	Phenolic (paper- filled)	Pyrex glass
Frequency (Hz.)	Secondary Current (mA)										
60	5	6.5	5	7	7	5	5	6.5	5	7	6
100	5	6.5	5	7	7	6.5	5	6.5	5	8	6.5
150	5	6.5	5	7	7	6.5	6	6.5	5	9	6.5
200	5	7	7	7	7.5	6.5	6	6.5	5	9.5	6.5
250	5	7	7	7.25	7.5	6.5	6	6.5	5	10	7
300	5.5	7	7	7.25	7.5	7	6	6.5	6	10.5	8
350	5.5	7.25	7.25	7.5	7.5	7	6	6.5	6	10.5	8.5
400	5.5	7.5	7.5	8	8	7	6.5	6.5	6	10.5	9.25
450	5.5	8	7.5	9	8	7.25	6.5	6.5	7	10.5	10.5
500	5.5	8	8	10	8	7.5	6.5	7	7	11	12.5

TABLE XIII (CONTD.)

Material											
	PVC, rigid	Poly carbonate	Quartz glass	PVC, nonrigid	Cellulose Acetate Butyrate	Acrylic (plexiglas)	Poly vinylidene fluoride	Alumina	Phenolic (glass- filled)	Phenolic (paper- filled)	Pyrex glass
Frequency (Hz.)	Secondary Current (mA)										
550	6	8	8.25	12.5	8	7.5	7	7	7	11	15
560	7.5	10.5	9	13	8.25	9	7.5	7.5	7.5	11	14
570	7.5	12.5	9.5	13.5	11	9.5	7.5	7.5	7.5	11.5	12.5
580	7.5	13	10.5	14	11.25	10.5	7.5	6.5	7.5	12	12.5
600	7.5	14	12.5	14.5	13.25	11.5	8	6.5	8	12	12.5
630	8	14.5	14.5	14.5	14	11.5	8	6.25	8	12.5	12.25
650	8.5	14.5	12	14.5	14	11	8	6.25	8	14	11.5
700	8.5	14.5	10	14.5	14	11	7	6.25	8	14.5	10.25
710	8.5	13.5	9.5	14.5	12.5	11	7	5.5	7	14	10.25
720	8.5	12.5	9	14	12	10	6.25	5.5	6.5	14	10
750	8	11	9	14	11	9.5	6.25	5	6	14	9.5
800	8	10	7.25	11.5	11	9	6.25	4.5	5.5	13	9
850	7	9.5	7	10	10	8	6	4.5	5	12	8
900	6.5	8.5	6.5	9.25	9.5	7.5	5	4.5	4.5	12	7
950	6.5	8.5	6.5	8.5	9.5	7	5	4	4	11.5	5
1000	6	8	6	8	9.5	6	5	4	4	11.5	4

TABLE XIV

Variation of exit gas temperature with frequency at constant primary voltage (usability test)

EXPERIMENTAL DATA CORRESPONDING TO FIGURE 14

RUN 2**System Conditions :****Gas :** Air**Inlet temperature :** 76 deg. F**Flow rate :** 3500 ml/min.**Reactor dimensions :** as presented in Table VII**Reactor length :** 6 inches**Primary voltage :** 60 volts

	PVC, rigid	Poly carbonate	Quartz glass	PVC, nonrigid	Cellulose Acetate Butyrate	Acrylic (plexiglas)	Poly vinylidene fluoride	Alumina	Phenolic (glass- filled)	Phenolic (paper- filled)	Pyrex glass
Frequency (Hz.)	Temperature (deg. F)										
60	76	76	76	76	76	76	76	76	76	76	76
100	76	76	76	76	76	76	76	76	76	76	76
150	76	76	76	76	76	76	76	76	76	76	76
200	76	76	76	76	76	76	76	76	76	76	76
250	76	76	76	76	76	76	76	76	76	76	76
300	76	76	76	76	76	76	76	76	76	76	76
350	76	76	76	76	76	76	76	76	76	76	76
400	76	76	77	76	76	76	76	76	76	76	78

TABLE XIV (CONTD.)

Material											
	PVC, rigid	Poly carbonate	Quartz glass	PVC, nonrigid	Cellulose Acetate Butyrate	Acrylic (plexiglas)	Poly vinylidene fluoride	Alumina	Phenolic (glass- filled)	Phenolic (paper- filled)	Pyrex glass
Frequency (Hz.)	Temperature (deg. F)										
450	76	76	81	76	76	76	76	76	76	78	79
500	76	76	94	76	76	76	76	76	77	80	91
550	76	76	105	76	76	78	78	78	78	86	93
580	82	76	115	78	76	90	80	86	85	92	91
600	85	80	122	79	79	93	81	90	88	94	89
630	88	86	126	84	86	98	89	94	89	97	87
650	91	92	118	88	89	94	93	95	91	99	85
700	96	95	117	92	92	93	95	96	95	103	83
710	99	90	110	96	90	92	88	82	97	101	82
720	97	89	108	99	87	91	87	91	93	98	81
750	96	86	102	95	85	90	85	89	89	95	80
800	94	86	99	93	84	88	82	88	85	92	79
850	82	82	96	80	78	81	79	81	81	90	78
900	82	82	94	80	78	81	79	81	78	89	78
950	79	78	86	78	77	79	78	80	77	88	77
1000	78	77	81	77	77	77	77	79	77	87	77

TABLE XV
 Variation of exit gas temperature with time at constant primary voltage (usability test)
 EXPERIMENTAL DATA CORRESPONDING TO FIGURE 10
RUN 3

System Conditions :

Gas : Air

Inlet temperature : 76 deg. F

Flow rate : 3500 ml/min.

Reactor dimensions : as presented in Table VII

Reactor length : 6 inches

Primary voltage : 60 volts

120

Materials											
Frequency	PVC, rigid	Poly carbonate	PVC, nonrigid	Acrylic (plexiglas)	Poly vinylidene fluoride	Cellulose Acetate Butyrate	Pyrex glass	Quartz glass	Phenolic (paper- filled)	Phenolic (glass-filled)	Alumina (ceramic)
Time (hours)	(700 Hz.)	(700 Hz.)	(710 Hz.)	(600 Hz.)	(650 Hz.)	(700 Hz.)	(550 Hz.)	(630 Hz.)	(700 Hz.)	(700 Hz.)	(700 Hz.)
	Temperature (deg. F)										
0	99	95	97	99	95	91	94	125	108	95	94
1	99	95	97	99	95	94	96	120	-	97	94
2	99	95	97	99	95	96	97	120	-	99	94
3	99	95	98	99	95	110	99	118	-	100	95
4	100	95	98	100	96	-	101	118	-	101	96

TABLE XV (CONTD.)

Material											
Frequency	PVC, rigid (700 Hz.)	Poly carbonate (700 Hz.)	PVC, nonrigid (710 Hz.)	Acrylic (plexiglas) (600 Hz.)	Poly vinylidene fluoride (650 Hz.)	Cellulose Acetate Butyrate (700 Hz.)	Pyrex glass (550 Hz.)	Quartz glass (630 Hz.)	Phenolic (paper- filled) (700 Hz.)	Phenolic (glass-filled) (700 Hz.)	Alumina (ceramic) (700 Hz.)
Time (hours)	Temperature (deg. F)										
5	101	95	98	102	97	-	101	118	-	103	97
6	102	96	98	102	98	-	101	117	-	104	99
7	102	96	99	102	100	-	102	117	-	105	101
8	103	96	100	102	100	-	-	116	-	106	102
9	103	96	100	103	100	-	-	115	-	106	103
10	104	96	100	104	101	-	-	115	-	107	103
11	104	96	100	105	102	-	-	114	-	107	104
12	104	97	100	107	103	-	-	113	-	-	104
13	105	97	100	108	104	-	-	-	-	-	105
14	106	97	101	108	105	-	-	-	-	-	106
15	106	97	101	109	105	-	-	-	-	-	107
16	107	98	101	110	107	-	-	-	-	-	108
17	107	98	101	113	108	-	-	-	-	-	110
18	108	98	103	116	110	-	-	-	-	-	110

TABLE XVI
 Variation of secondary voltage with time at constant primary voltage (usability test)
 EXPERIMENTAL DATA CORRESPONDING TO FIGURE 11
RUN 3

System Conditions :

Gas : Air

Inlet temperature : 76 deg. F

Flow rate : 3500 ml/min.

Reactor dimensions : as presented in Table VII

Reactor length : 6 inches

Primary voltage : 60 volts

Material											
Frequency	PVC, rigid (700 Hz.)	Poly carbonate (700 Hz.)	PVC, nonrigid (710 Hz.)	Acrylic (plexiglas) (600 Hz.)	Poly vinylidene fluoride (650 Hz.)	Cellulose Acetate Butyrate (700 Hz.)	Pyrex glass (550 Hz.)	Quartz glass (630 Hz.)	Phenolic (paper- filled) (700 Hz.)	Phenolic (glass-filled) (700 Hz.)	Alumina (ceramic) (700 Hz.)
Time (hours)	Secondary voltage (volts)										
0	14810	14870	14730	14960	14720	12300	12200	11840	14210	14360	11800
1	14830	14870	14760	14960	14700	12200	12000	11800	-	14300	11800
2	14880	14870	14780	15000	14680	10600	12000	11780	-	14260	11800
3	14930	14870	14880	15010	14600	2280	11800	11720	-	14150	11880
4	14950	14870	14880	15010	14540	-	11650	11700	-	14000	11880
5	14980	14870	14840	15020	14400	-	11600	11640	-	13800	11880
6	14980	14870	14800	15020	14360	-	11500	11630	-	13400	11920
7	14930	14850	14780	15020	14200	-	2200	11600	-	13000	11970

Table XVI (CONTD.)

Material											
Frequency	PVC, rigid (700 Hz.)	Poly carbonate (700 Hz.)	PVC, nonrigid (710 Hz.)	Acrylic (plexiglas) (600 Hz.)	Poly vinylidene fluoride (650 Hz.)	Cellulose Acetate Butyrate (700 Hz.)	Pyrex glass (550 Hz.)	Quartz glass (630 Hz.)	Phenolic (paper- filled) (700 Hz.)	Phenolic (glass-filled) (700 Hz.)	Alumina (ceramic) (700 Hz.)
Time (hours)	Secondary voltage (volts)										
8	14910	14850	14730	14960	14080	-	-	11570	-	12600	11990
9	14880	14850	14620	14940	14060	-	-	11530	-	12000	11990
10	14850	14810	14580	14700	13960	-	-	11440	-	10200	12050
11	14810	14810	14500	14590	13930	-	-	11400	-	1930	12060
12	14760	14760	14480	14380	13880	-	-	2280	-	-	12060
13	14710	14760	14430	14140	13780	-	-	-	-	-	11980
14	14650	14740	14430	14020	13780	-	-	-	-	-	11980
15	14440	14740	14400	13930	13760	-	-	-	-	-	11980
16	14380	14740	14260	13880	13700	-	-	-	-	-	11960
17	14340	14740	14060	12970	13660	-	-	-	-	-	11960
18	14340	14740	13930	12590	13570	-	-	-	-	-	11960

TABLE XVII
 Variation of secondary current with time at constant primary voltage (usability test)
 EXPERIMENTAL DATA CORRESPONDING TO FIGURE 9
RUN 3

System Conditions :

Gas : Air

Inlet temperature : 76 deg. F

Flow rate : 3500 ml/min.

Reactor dimensions : as presented in Table VII

Reactor length : 6 inches

Primary voltage : 60 volts

Material											
Frequency	PVC, rigid (700 Hz.)	Poly carbonate (700 Hz.)	PVC, nonrigid (710 Hz.)	Acrylic (plexiglas) (600 Hz.)	Poly vinylidene fluoride (650 Hz.)	Cellulose Acetate Butyrate (700 Hz.)	Pyrex glass (550 Hz.)	Quartz glass (630 Hz.)	Phenolic (paper- filled) (700 Hz.)	Phenolic (glass-filled) (700 Hz.)	Alumina (ceramic) (700 Hz.)
Time (hours)	Secondary current (mA)										
0	8.5	14.5	14.5	11.5	8	14	15	14.5	14.5	8	6.25
1	9	14.5	15	12	9	15	15	15	-	8.5	6.5
2	9.5	14.5	15	12.5	9.5	15	15.5	15.5	-	9	6.5
3	9.5	14.5	15.5	12.5	9.5	15	15.5	15.5	-	10	6.5
4	10	15	15.5	12.5	9.5	-	16	16	-	10.5	6.5
5	10	15	15.5	12.5	10	-	16	16.5	-	11	7
6	10.5	15	16	12.5	10.5	-	16	16.5	-	12	7
7	10.5	15	16.5	12.5	11.5	-	16.25	17	-	13	7.5

TABLE XVII (CONTD.)

Material											
Frequency	PVC, rigid (700 Hz.)	Poly carbonate (700 Hz.)	PVC, nonrigid (710 Hz.)	Acrylic (plexiglas) (600 Hz.)	Poly vinylidene fluoride (650 Hz.)	Cellulose Acetate Butyrate (700 Hz.)	Pyrex glass (550 Hz.)	Quartz glass (630 Hz.)	Phenolic (paper- filled) (700 Hz.)	Phenolic (glass-filled) (700 Hz.)	Alumina (ceramic) (700 Hz.)
Time (hours)	Secondary current (mA)										
8	11	15	16.5	13	12	-	-	17	-	14	7.5
9	11	15	16.5	13.5	12.5	-	-	17.5	-	15	7.5
10	11	15	17	14	13	-	-	17.5	-	16	8
11	11	15	17	14	14	-	-	18	-	17	8
12	11	15	17	14.5	14.5	-	-	18	-	-	8
13	11	15.5	17	15.5	15.5	-	-	-	-	-	8
14	11	15.5	17.5	15.5	16	-	-	-	-	-	8
15	12	16	18	16.5	16.5	-	-	-	-	-	8
16	12	16	18	17	17	-	-	-	-	-	8
17	12	16	18.5	17	18	-	-	-	-	-	8
18	12	16.5	18.5	17.5	18.5	-	-	-	-	-	8

TABLE XVIII

Variation of secondary voltage, secondary current and exit gas temperature with frequency for 1/32 inch wall acrylic

RUN 4

System Conditions :

Gas : Air
Inlet temperature : 76 deg. F
Flow rate : 3500 ml/min.
Material : Acrylic (plexiglas)
Reactor dimensions :

Breakdown Characteristics :

Breakdown voltage : 8450 volts
Breakdown frequency : 490 Hz.

Inner tube		Outer tube		Air gap thickness (inch)
Outer diameter (inch)	Wall thickness (inch)	Outer diameter (inch)	Wall thickness (inch)	
1/4	1/32	1	1/32	11/32

Reactor length : 6 inches
Primary voltage : 60 volts

Frequency (Hz.)	Secondary voltage (volts)	Secondary current (mA)	Temperature (deg. F)
60	880	8	76
100	1390	8	76
150	2000	8	76
200	2580	8	76
250	2990	8	76
300	3600	8.5	76
350	4800	9	76
400	6400	9.5	76
450	8800	10	79
500	10200	10	83
550	11900	10.5	90

TABLE XVIII (CONTD.)

Frequency (Hz.)	Secondary voltage (volts)	Secondary current (mA)	Temperature (deg. F)
570	12800	11	94
580	12920	11.5	96
600	12960	12	98
630	12640	12	97
640	12280	11	94
650	11910	10.5	92
700	11450	9.5	89
710	11000	9.5	88
720	10380	9	86
750	9670	9	85
800	8100	9	83
850	6660	8.5	82
900	4670	8.5	81
950	3280	8	80
1000	1980	8	79

TABLE XIX

Variation of secondary voltage, secondary current and exit gas temperature with time for
1/32 inch wall acrylic

RUN 5

System Conditions :

Gas : Air
Inlet temperature : 76 deg. F
Flow rate : 3500 ml/min.
Material : Acrylic (plexiglas)
Reactor dimensions :

Breakdown Characteristics :

Breakdown voltage : 8450 volts
Breakdown frequency : 490 Hz.

Inner tube		Outer tube		Air gap thickness (inch)
Outer diameter (inch)	Wall thickness (inch)	Outer diameter (inch)	Wall thickness (inch)	
1/4	1/32	1	1/32	11/32

Reactor length : 6 inches
Primary voltage : 60 volts

Time (hours)	Secondary voltage (volts)	Secondary current (mA)	Temperature (deg. F)
0	12960	12	98
1	13020	12	99
2	13040	13	100
3	13020	13	102
4	13000	13.5	103
5	12960	13.5	105
6	12920	14	106
7	12900	14	108
8	12890	14	109
9	12890	14	110
10	12830	14.5	112
11	12800	14.5	114
12	12760	15	115
13	12720	15	116
14	12700	15	118
15	12680	15	118
17	12660	15.5	119
18	12650	15.5	120

TABLE XXI
Variation of air breakdown voltage with dielectric constant (k) at various primary
voltages
EXPERIMENTAL DATA CORRESPONDING TO FIGURE 17

RUN 6

System Conditions :

Gas : Air

Inlet temperature : 76 deg. F

Flow rate : 3500 ml/min.

Reactor dimensions : as presented in Table VII

Reactor length : 6 inches

Material / Primary voltage (Frequency)	55 volts (Hz.)	60 volts (Hz.)	65 volts (Hz.)	70 volts (Hz.)	75 volts (Hz.)	80 volts (Hz.)	85 volts (Hz.)	90 volts (Hz.)
Cellulose Acetate Butyrate	9450 (620)	9780 (590)	9880 (570)	10020 (530)	10160 (510)	10340 (490)	10480 (460)	10610 (420)
Polycarbonate	10450 (600)	10700 (590)	10890 (530)	11070 (510)	11240 (500)	11320 (480)	11390 (460)	11670 (440)
PVC, rigid (5 % plasticizer)	10300 (580)	10400 (560)	10670 (540)	10840 (520)	10990 (510)	11160 (500)	11220 (480)	11460 (460)
PVC, nonrigid (25 % plasticizer)	10190 (580)	10260 (560)	10590 (540)	10790 (530)	10860 (490)	11020 (470)	11160 (460)	11400 (420)
Quartz glass	5870 (430)	6020 (400)	6160 (380)	6230 (350)	6340 (320)	6670 (290)	6810 (270)	6890 (260)
Phenolic, glass- filled	9180 (520)	9350 (490)	9540 (480)	9730 (460)	9970 (450)	10110 (440)	10240 (420)	10370 (400)
Acrylic (plexiglas)	10340 (580)	10550 (540)	10820 (520)	10960 (500)	11110 (470)	11260 (450)	11310 (430)	11540 (410)
Polyvinylidene fluoride	9010 (550)	9120 (520)	9380 (500)	9650 (480)	9810 (450)	9930 (440)	10110 (420)	10230 (390)
Alumina (ceramic)	8400 (530)	8800 (510)	9100 (500)	9380 (480)	9640 (460)	9620 (430)	9760 (410)	9830 (380)
Pyrex glass	5210 (400)	5380 (380)	5430 (360)	5640 (330)	5810 (310)	5890 (290)	5990 (270)	6020 (250)
Phenolic (paper- filled)	5080 (470)	5230 (440)	5340 (420)	5420 (400)	5510 (380)	5590 (360)	5680 (340)	5770 (310)

Appendix D

Experimental data for ozone generation tests

on the surface area and width of

the surface of the annulus

Appendix D1

Varying surface area and annulus width tests

TABLE XXIII

Experimental data for 1/16 inch air-gap thickness (varying surface area and annulus test)

RUN 7**System Conditions :****Gas :** Air**Inlet temperature :** 76 deg. F**Flow rate :** 3500 ml/min.**Material :** Acrylic (plexiglas)**Reactor dimensions :****Breakdown Characteristics :****Breakdown voltage :** 8020 volts**Breakdown frequency :** 460 Hz.**Breakdown strength :** 128.3 KV/inch

Inner tube		Outer tube		Air gap thickness
Outer diameter (inch)	Wall thickness (inch)	Outer diameter (inch)	Wall thickness (inch)	
3/8	1/16	3/4	1/8	1/16 inch.

Reactor length : 6 inches**Primary voltage :** 60 volts

Frequency (Hz.)	Secondary voltage (volts)	Concentration (ppm)	Secondary current (mA)	Temperature (deg. F)
60	800	-	6	76
100	2000	-	6	76
150	2900	-	6	76
200	3600	-	6.5	76
250	4100	-	7	76
300	4900	-	7.5	76
350	5500	-	8	76
400	6280	-	8.5	76
450	7310	-	9	76
500	8480	55	10	77
550	10100	150	10.5	84

TABLE XXIII (CONTD.)

Frequency (Hz.)	Secondary voltage (volts)	Concentration (ppm)	Secondary current (mA)	Temperature (deg. F)
570	11570	200	11	87
580	11760	220	11.25	90
600	12210	250	11.5	93
630	12480	265	11.5	96
640	12650	285	11.5	99
650	12600	265	11.5	98
700	12170	195	12	95
710	11730	150	11.75	90
720	11520	125	11.5	88
750	11110	100	11	84
800	9680	60	10.5	80
850	8720	25	9	79
900	6600	5	8	78
950	5490	-	7	78
1000	5000	-	6	77

TABLE XXIV

Experimental data for 3/16 inch air-gap thickness (varying surface area and annulus test)

RUN 8**System Conditions :****Gas :** Air**Inlet temperature :** 76 deg. F**Flow rate :** 3500 ml/min.**Material :** Acrylic (plexiglas)**Reactor dimensions :****Breakdown Characteristics :****Breakdown voltage :** 8450 volts**Breakdown frequency :** 490 Hz.**Breakdown strength :** 45 KV/inch

Inner tube		Outer tube		Air gap thickness
Outer diameter (inch)	Wall thickness (inch)	Outer diameter (inch)	Wall thickness (inch)	
3/8	1/16	1	1/8	3/16 inch.

Reactor length : 6 inches**Primary voltage :** 60 volts

Frequency (Hz.)	Secondary voltage (volts)	Concentration (ppm)	Secondary current (mA)	Temperature (deg. F)
60	800	-	6	76
100	2000	-	6	76
150	2900	-	6	76
200	3700	-	7	76
250	4000	-	7	76
300	4800	-	7.5	76
350	5400	-	8.5	76
400	6200	-	8.5	76
450	7200	-	9	76
500	8600	50	10	78
550	10400	150	10.75	84

TABLE XXIV (CONTD.)

Frequency (Hz.)	Secondary voltage (volts)	Concentration (ppm)	Secondary current (mA)	Temperature (deg. F)
570	11300	180	11	87
580	11820	200	11	89
600	12590	250	11.5	92
630	12650	270	11.75	94
640	12860	280	11.75	96
650	12800	295	11.75	99
700	12200	200	12	98
710	11930	170	12	98
720	11520	145	11.5	97
750	11300	120	11.5	96
800	10000	80	10.75	92
850	8400	55	9	88
900	6600	20	7.5	83
950	5600	5	7	81
1000	5000	-	6	78

TABLE XXV

Experimental data for 1/4 inch air-gap thickness (varying surface area and annulus test)

RUN 9**System Conditions :****Gas :** Air**Inlet temperature :** 76 deg. F**Flow rate :** 3500 ml/min.**Material :** Acrylic (plexiglas)**Reactor dimensions :****Breakdown Characteristics :****Breakdown voltage :** 9000 volts**Breakdown frequency :** 520 Hz.**Breakdown strength :** 36 KV/inch

Inner tube		Outer tube		Air gap thickness
Outer diameter (inch)	Wall thickness (inch)	Outer diameter (inch)	Wall thickness (inch)	1/4 inch.
3/8	1/16	1 1/8	1/8	

Reactor length : 6 inches**Primary voltage :** 60 volts

Frequency (Hz.)	Secondary voltage (volts)	Concentration (ppm)	Secondary current (mA)	Temperature (deg. F)
60	950	-	7	76
100	1580	-	7	76
150	2000	-	7	76
200	2500	-	7	76
250	3200	-	7.5	76
300	3650	-	8	76
350	4050	-	8.5	76
400	4650	-	9	76
450	5400	-	9.5	76
500	8400	-	10	76
550	10200	95	12	79

TABLE XXV (CONTD.)

Frequency (Hz.)	Secondary voltage (volts)	Concentration (ppm)	Secondary current (mA)	Temperature (deg. F)
570	10740	130	12	81
580	11330	150	12	83
600	11950	180	12	85
630	12280	200	12	86
640	12510	210	12.5	88
650	12700	235	12.5	90
700	12770	265	12.5	94
710	12540	245	12.5	93
720	12370	220	12.5	93
750	12250	200	12.5	93
800	11100	110	11.5	91
850	10000	75	10.5	90
900	8600	60	9.25	88
950	6600	35	8	82
1000	5000	-	7	81

TABLE XXVI

Experimental data for 5/16 inch air-gap thickness (varying surface area and annulus test)

RUN 10

System Conditions :

Gas : Air
Inlet temperature : 76 deg. F
Flow rate : 3500 ml/min.
Material : Acrylic (plexiglas)
Reactor dimensions :

Breakdown Characteristics :

Breakdown voltage : 9600 volts
Breakdown frequency : 540 Hz.
Breakdown strength : 30.7 KV/inch

Inner tube		Outer tube		Air gap thickness
Outer diameter (inch)	Wall thickness (inch)	Outer diameter (inch)	Wall thickness (inch)	
3/8	1/16	1 1/4	1/8	5/16 inch.

Reactor length : 6 inches
Primary voltage : 60 volts

Frequency (Hz.)	Secondary voltage (volts)	Concentration (ppm)	Secondary current (mA)	Temperature (deg. F)
60	920	-	7	76
100	1460	-	7	76
150	2000	-	7	76
200	2500	-	7	76
250	3160	-	7	76
300	3600	-	7	76
350	3960	-	8	76
400	4500	-	8.5	76
450	5300	-	9	76
500	8200	-	9.75	76
550	10000	70	11.5	79

TABLE XXVI (CONTD.)

Frequency (Hz.)	Secondary voltage (volts)	Concentration (ppm)	Secondary current (mA)	Temperature (deg. F)
570	10800	95	11.5	80
580	11210	130	11.5	81
600	11700	150	11.5	83
630	12420	200	11.5	85
640	12540	225	11.5	88
650	12800	260	11.5	90
700	12600	235	11.5	89
710	12320	215	11.5	88
720	12010	195	11.5	87
750	11900	185	11	87
800	10600	90	10	82
850	8800	30	9	79
900	7200	5	7.5	78
950	5000	-	7	78
1000	4600	-	7	77

TABLE XXVII

Experimental data for 7/16 inch air-gap thickness (varying surface area and annulus test)

RUN 11

System Conditions :

Gas : Air
Inlet temperature : 76 deg. F
Flow rate : 3500 ml/min.
Material : Acrylic (plexiglas)
Reactor dimensions :

Breakdown Characteristics :

Breakdown voltage : 11200 volts
Breakdown frequency : 550 Hz.
Breakdown strength : 25.6 KV/inch

Inner tube		Outer tube		Air gap thickness
Outer diameter (inch)	Wall thickness (inch)	Outer diameter (inch)	Wall thickness (inch)	7/16 inch.
3/8	1/16	1 1/2	1/8	

Reactor length : 6 inches
Primary voltage : 60 volts

Frequency (Hz.)	Secondary voltage (volts)	Concentration (ppm)	Secondary current (mA)	Temperature (deg. F)
60	1200	-	5	76
100	2000	-	5	76
150	2800	-	5	76
200	3600	-	5	76
250	4000	-	5	76
300	4800	-	5	76
350	5400	-	5	76
400	6200	-	5	76
450	7000	-	5	76
500	8200	-	5	76
550	11200	15	5	77

TABLE XXVII (CONTD.)

Frequency (Hz.)	Secondary voltage (volts)	Concentration (ppm)	Secondary current (mA)	Temperature (deg. F)
570	11440	30	5.5	78
580	11600	40	5.5	79
600	11800	50	5.5	79
630	12100	110	5.5	80
640	12440	130	5.5	81
650	12500	155	5.5	82
690	12730	200	5.5	85
700	12900	240	5.5	88
710	12900	255	5.5	89
720	12200	150	5.25	84
750	11600	90	5.25	80
800	10200	40	5	79
850	8400	20	5	78
900	7000	5	5	78
950	5200	-	5	79
1000	4400	-	5	77

TABLE XXVIII

Experimental data for 1/2 inch air-gap thickness (varying surface area and annulus test)

RUN 12**System Conditions :****Gas :** Air**Inlet temperature :** 76 deg. F**Flow rate :** 3500 ml/min.**Material :** Acrylic (plexiglas)**Reactor dimensions :****Breakdown Characteristics :****Breakdown voltage :** 11600 volts**Breakdown frequency :** 600 Hz.**Breakdown strength :** 23.2 KV/inch

Inner tube		Outer tube		Air gap thickness
Outer diameter (inch)	Wall thickness (inch)	Outer diameter (inch)	Wall thickness (inch)	1/2 inch
3/8	1/16	1 5/8	1/8	

Reactor length : 6 inches**Primary voltage :** 60 volts

Frequency (Hz.)	Secondary voltage (volts)	Concentration (ppm)	Secondary current (mA)	Temperature (deg. F)
60	1200	-	7	76
100	2000	-	7	76
150	2950	-	7	76
200	3700	-	7	76
250	4000	-	7	76
300	4600	-	7	76
350	5400	-	7.5	76
400	6000	-	8	76
450	7000	-	8	76
500	8000	-	9	76
550	9600	-	10.75	76

TABLE XXVIII (CONTD.)

Frequency (Hz.)	Secondary voltage (volts)	Concentration (ppm)	Secondary current (mA)	Temperature (deg. F)
570	10380	-	11.5	76
580	10970	-	12	76
600	11600	20	13	77
630	12130	45	13	78
640	12440	60	13.5	78
650	12980	70	13.5	81
690	13160	150	13.5	84
700	13200	170	12.5	86
710	12880	145	12.5	85
720	12540	130	12	85
750	12400	120	11.5	83
800	11200	90	11.5	80
850	9400	60	10.75	79
900	8000	20	9.5	78
950	7000	-	8	78
1000	4800	-	7	77

TABLE XXIX

Experimental data for 11/16 inch air-gap thickness (varying surface area and annulus test)

RUN 13

System Conditions :

Gas : Air
Inlet temperature : 76 deg. F
Flow rate : 3500 ml/min.
Material : Acrylic (plexiglas)
Reactor dimensions :

Breakdown Characteristics :

Breakdown voltage : 12980 volts
Breakdown frequency : 650 Hz.
Breakdown strength : 18.9 KV/inch

Inner tube		Outer tube		Air gap thickness
Outer diameter (inch)	Wall thickness (inch)	Outer diameter (inch)	Wall thickness (inch)	11/16 inch.
3/8	1/16	2	1/8	

Reactor length : 6 inches
Primary voltage : 60 volts

Frequency (Hz.)	Secondary voltage (volts)	Concentration (ppm)	Secondary current (mA)	Temperature (deg. F)
60	1200	-	7	76
100	2000	-	7	76
150	2950	-	7	76
200	3700	-	7	76
250	4000	-	7	76
300	4450	-	7	76
350	5320	-	7.5	76
400	5890	-	8	76
450	6680	-	8.5	76
500	7730	-	9	76
550	8780	-	10.75	76

TABLE XXIX (CONTD.)

Frequency (Hz.)	Secondary voltage (volts)	Concentration (ppm)	Secondary current (mA)	Temperature (deg. F)
570	9820	-	11.5	76
580	10210	-	12	76
600	11100	-	13.5	76
630	11940	-	13.5	76
640	12460	-	13.5	76
650	12980	25	13.5	77
700	13400	150	12.5	84
710	12980	135	12.5	84
720	12690	115	12	83
750	12400	110	12	82
800	11250	85	12	80
850	9380	60	10.75	78
900	8000	20	9.5	77
950	7000	-	8	77
1000	4850	-	7.5	77

Appendix D2

Varying wall thickness and annulus width tests

TABLE XXX

Experimental data for 1/32 inch wall thickness (varying wall thickness and annulus test)

RUN 14**System Conditions :****Gas :** Air**Inlet temperature :** 76 deg. F**Flow rate :** 3500 ml/min.**Material :** Acrylic (plexiglas)**Reactor dimensions :****Breakdown Characteristics :****Breakdown voltage :** 5600 volts**Breakdown frequency :** 450 Hz.**Breakdown strength :** 19.9 KV/inch

Inner tube		Outer tube		Air gap thickness
Outer diameter (inch)	Wall thickness (inch)	Outer diameter (inch)	Wall thickness (inch)	
3/8	1/16	1	1/32	9/16 inch.

Reactor length : 6 inches**Primary voltage :** 60 volts

Frequency (Hz.)	Secondary voltage (volts)	Concentration (ppm)	Secondary current (mA)	Temperature (deg. F)
60	1200	-	7	76
100	2000	-	7	76
150	2900	-	7.25	76
200	3200	-	7.25	76
250	3600	-	8	76
300	4000	-	8	76
350	4600	-	8.5	76
400	5000	-	9	76
450	5600	15	9.75	77
500	8400	40	10.5	78
550	10600	70	11.75	82

TABLE XXX (CONTD.)

Frequency (Hz.)	Secondary voltage (volts)	Concentration (ppm)	Secondary current (mA)	Temperature (deg. F)
570	11000	80	11.75	86
580	11480	95	11.75	92
600	12000	110	11.75	100
630	12000	130	11.75	102
640	12000	150	11.75	104
650	12000	170	11.75	106
700	11400	145	12	106
710	11200	125	12	104
720	11100	115	12	104
750	10600	100	11.5	99
800	9400	60	10.75	93
850	7800	35	9	89
900	6200	5	7.5	88
950	5200	-	6	84
1000	4600	-	5	80

TABLE XXXI

Experimental data for 1/16 inch wall thickness (varying wall thickness and annulus test)

RUN 15

System Conditions :

Gas : Air
Inlet temperature : 76 deg. F
Flow rate : 3500 ml/min.
Material : Acrylic (plexiglas)
Reactor dimensions :

Breakdown Characteristics :

Breakdown voltage : 7650 volts
Breakdown frequency : 480 Hz.
Breakdown strength : 30.6 KV/inch

Inner tube		Outer tube		Air gap thickness
Outer diameter (inch)	Wall thickness (inch)	Outer diameter (inch)	Wall thickness (inch)	
3/8	1/16	1	1/16	1/4 inch.

Reactor length : 6 inches
Primary voltage : 60 volts

Frequency (Hz.)	Secondary voltage (volts)	Concentration (ppm)	Secondary current (mA)	Temperature (deg. F)
60	1120	-	7	76
100	2000	-	7	76
150	2800	-	7	76
200	3600	-	7	76
250	4000	-	7	76
300	4600	-	7	76
350	5200	-	7.5	76
400	6000	-	8	76
450	6900	-	8.5	76
500	8200	40	10	78
550	10000	100	11.5	80

TABLE XXXI (CONTD.)

Frequency (Hz.)	Secondary voltage (volts)	Concentration (ppm)	Secondary current (mA)	Temperature (deg. F)
570	11000	140	11.5	84
580	11480	160	11.5	90
600	11800	180	11.75	93
630	11900	200	11.75	97
640	12000	225	11.75	100
650	12200	270	11.75	100
700	11800	150	11.5	99
710	11520	120	11.5	97
720	11290	95	11.5	94
750	11000	70	11.5	92
800	9800	60	10.5	89
850	8200	55	8.75	88
900	6600	20	7.5	83
950	5600	5	7	81
1000	5000	-	6	78

TABLE XXXII

Experimental data for 3/16 inch wall thickness (varying wall thickness and annulus test)
RUN 16

System Conditions :

Gas : Air
Inlet temperature : 76 deg. F
Flow rate : 3500 ml/min.
Material : Acrylic (plexiglas)
Reactor dimensions :

Breakdown Characteristics :

Breakdown voltage : 8800 volts
Breakdown frequency : 520 Hz.
Breakdown strength : 70.4 KV/inch

Inner tube		Outer tube		Air gap thickness
Outer diameter (inch)	Wall thickness (inch)	Outer diameter (inch)	Wall thickness (inch)	1/8 inch.
3/8	1/16	1	3/16	

Reactor length : 6 inches
Primary voltage : 60 volts

Frequency (Hz.)	Secondary voltage (volts)	Concentration (ppm)	Secondary current (mA)	Temperature (deg. F)
60	850	-	5	76
100	2000	-	5	76
150	2850	-	5	76
200	3700	-	5	76
250	4000	-	5	76
300	4600	-	6	76
350	5300	-	6	76
400	6100	-	7.5	76
450	7000	-	7.5	76
500	8100	-	8.5	76
550	10200	120	11	82

TABLE XXXII (CONTD.)

Frequency (Hz.)	Secondary voltage (volts)	Concentration (ppm)	Secondary current (mA)	Temperature (deg. F)
570	10900	145	11	84
580	11680	180	11	87
600	12300	220	11	89
630	12660	240	11	92
640	12930	265	11	95
650	13200	295	11	98
700	12650	220	11	96
710	11520	180	10.75	95
720	11290	155	10.75	94
750	11980	130	10.5	93
800	10650	100	10	90
850	8950	60	8.5	87
900	6800	20	7.5	82
950	5600	5	7	80
1000	5000	-	6	78

Appendix D3

Varying wall thickness and surface area tests

TABLE XXXIII
 Experimental data for 1/8 inch dielectric wall thickness
 (varying wall thickness and surface area test)
RUN 17

System Conditions :

Gas : Air
Inlet temperature : 76 deg. F
Flow rate : 3500 ml/min.
Material : Acrylic (plexiglas)
Reactor dimensions :

Breakdown Characteristics :

Breakdown voltage : 8450 volts
Breakdown frequency : 490 Hz.
Breakdown strength : 45.1 KV/inch

Inner tube		Outer tube		Air gap thickness
Outer diameter (inch)	Wall thickness (inch)	Outer diameter (inch)	Wall thickness (inch)	3/16 inch.
3/8	1/16	1	1/8	

Reactor length : 6 inches
Primary voltage : 60 volts

Frequency (Hz.)	Secondary voltage (volts)	Concentration (ppm)	Secondary current (mA)	Temperature (deg. F)
60	800	-	6	76
100	2000	-	6	76
150	2900	-	6	76
200	3700	-	7	76
250	4000	-	7	76
300	4800	-	7.5	76
350	5400	-	8.5	76
400	6200	-	8.5	76
450	7200	-	9	76
500	8600	50	10	78
550	10400	150	10.75	84

TABLE XXXIII (CONTD.)

Frequency (Hz.)	Secondary voltage (volts)	Concentration (ppm)	Secondary current (mA)	Temperature (deg. F)
570	11300	180	11	87
580	11820	210	11	89
600	12400	250	11.5	92
630	12600	270	11.75	94
640	12710	280	11.75	96
650	12800	295	11.75	99
700	12200	200	12	98
710	11930	170	12	98
720	11520	145	11.5	97
750	11300	120	11.5	96
800	10000	80	10.75	92
850	8400	55	9	88
900	6600	20	7.5	83
950	5600	5	7	81
1000	5000	-	6	78

TABLE XXXIV
 Experimental data for 1/16 inch dielectric wall thickness
 (varying wall thickness and surface area test)
RUN 18

System Conditions :

Gas : Air
Inlet temperature : 76 deg. F
Flow rate : 3500 ml/min.
Material : Acrylic (plexiglas)
Reactor dimensions :

Breakdown Characteristics :

Breakdown voltage : 7650 volts
Breakdown frequency : 480 Hz.
Breakdown strength : 30.6 KV/inch

Inner tube		Outer tube		Air gap thickness
Outer diameter (inch)	Wall thickness (inch)	Outer diameter (inch)	Wall thickness (inch)	
3/8	1/16	1	1/16	1/4 inch.

Reactor length : 6 inches
Primary voltage : 60 volts

Frequency (Hz.)	Secondary voltage (volts)	Concentration (ppm)	Secondary current (mA)	Temperature (deg. F)
60	1120	-	7	76
100	2000	-	7	76
150	2800	-	7	76
200	3600	-	7	76
250	4000	-	7	76
300	4600	-	7	76
350	5200	-	7.5	76
400	6000	-	8	76
450	6900	-	8.5	76
500	8200	40	10	78
550	10000	100	11.5	80

TABLE XXXIV (CONTD.)

Frequency (Hz.)	Secondary voltage (volts)	Concentration (ppm)	Secondary current (mA)	Temperature (deg. F)
570	11000	140	11.5	84
580	11480	160	11.5	90
600	11800	180	11.75	93
630	11900	200	11.75	97
640	12000	225	11.75	100
650	12200	270	11.75	100
700	11800	150	11.5	99
710	11520	120	11.5	97
720	11290	95	11.5	94
750	11000	70	11.5	92
800	9800	60	10.5	89
850	8200	55	8.75	88
900	6600	20	7.5	83
950	5600	5	7	81
1000	5000	-	6	78

TABLE XXXV
 Experimental data for 1/8 inch dielectric wall thickness
 (varying wall thickness and surface area test)
RUN 19

System Conditions :

Gas : Air
Inlet temperature : 76 deg. F
Flow rate : 3500 ml/min.
Material : Acrylic (plexiglas)
Reactor dimensions :

Breakdown Characteristics :

Breakdown voltage : 9000 volts
Breakdown frequency : 520 Hz.
Breakdown strength : 36 KV/inch

Inner tube		Outer tube		Air gap thickness
Outer diameter (inch)	Wall thickness (inch)	Outer diameter (inch)	Wall thickness (inch)	
3/8	1/16	1 1/8	1/8	1/4 inch.

Reactor length : 6 inches
Primary voltage : 60 volts

Frequency (Hz.)	Secondary voltage (volts)	Concentration (ppm)	Secondary current (mA)	Temperature (deg. F)
60	950	-	7	76
100	1580	-	7	76
150	2000	-	7	76
200	2500	-	7	76
250	3200	-	7.5	76
300	3650	-	8	76
350	4050	-	8.5	76
400	4650	-	9	76
450	5400	-	9.5	76
500	8400	-	10	76
550	10200	95	12	79

TABLE XXXV (CONTD.)

Frequency (Hz.)	Secondary voltage (volts)	Concentration (ppm)	Secondary current (mA)	Temperature (deg. F)
570	10740	130	12	81
580	11330	155	12	83
600	11950	180	12	85
630	12280	195	12	86
640	12510	210	12.5	88
650	12700	235	12.5	90
700	12700	265	12.5	94
710	12540	245	12.5	93
720	12370	220	12.5	93
750	12250	200	12.5	93
800	11100	110	11.5	91
850	10000	75	10.5	90
900	8600	60	9.25	88
950	6600	35	8	82
1000	5000		7	81

TABLE XXXVI
 Experimental data for 1/4 inch dielectric wall thickness
 (varying wall thickness and surface area test)

RUN 20

System Conditions :

Gas : Air
Inlet temperature : 76 deg. F
Flow rate : 3500 ml/min.
Material : Acrylic (plexiglas)
Reactor dimensions :

Breakdown Characteristics :

Breakdown voltage : 11100 volts
Breakdown frequency : 580 Hz.
Breakdown strength : 44.4 KV/inch

Inner tube		Outer tube		Air gap thickness
Outer diameter (inch)	Wall thickness (inch)	Outer diameter (inch)	Wall thickness (inch)	1/4 inch.
3/8	1/16	1 1/4	1/4	

Reactor length : 6 inches
Primary voltage : 60 volts

Frequency (Hz.)	Secondary voltage (volts)	Concentration (ppm)	Secondary current (mA)	Temperature (deg. F)
60	900	-	5	76
100	1580	-	5	76
150	2000	-	5	76
200	2550	-	5	76
250	3380	-	5	76
300	3790	-	5	76
350	4200	-	5	76
400	4900	-	5.5	76
450	5680	-	6	76
500	8720	-	6.5	76
550	10370	-	7	76

TABLE XXXVI (CONTD.)

Frequency (Hz.)	Secondary voltage (volts)	Concentration (ppm)	Secondary current (mA)	Temperature (deg. F)
570	10740	-	8	76
580	11330	-	8.5	76
600	11100	90	10.5	79
630	12280	120	11	81
640	12510	145	11	82
650	13200	170	11	84
700	13350	225	11	89
710	13350	230	11	89
720	13350	235	11	90
750	13350	240	11	90
800	13200	165	11	86
850	11690	95	10	83
900	9200	20	8.5	81
950	6800	-	7	79
1000	5300	-	6	77

Appendix D4

Heat generation tests

TABLE XXXVII

Variation of secondary voltage with frequency at constant primary voltage (heat generation test)
EXPERIMENTAL DATA CORRESPONDING TO FIGURE 25

RUN 21**System Conditions :****Gas :** Air**Inlet temperature :** 76 deg. F**Flow rate :** 3500 ml/min.**Reactor dimensions :** as presented in Table VIII**Reactor length :** 6 inches**Primary voltage :** 60 volts

Material											
	PVC, rigid	Poly carbonate	Quartz glass	PVC, nonrigid	Cellulose Acetate Butyrate	Acrylic (plexiglas)	Poly vinylidene fluoride	Phenolic (paper- filled)	Alumina	Pyrex glass	Phenolic (glass- filled)
Frequency (Hz.)	Secondary Voltage (volts)										
60	1020	860	820	800	930	890	1260	880	1200	1160	1200
100	2040	1460	1360	1380	1440	1460	2000	1260	2030	2020	2180
150	3200	2100	2150	2910	2130	3200	2800	2030	2900	2360	2880
200	3900	2680	2800	3680	2860	3860	3590	2600	3620	2670	3640
250	4180	3190	3300	4380	3400	4750	3890	3200	4020	3480	4360
300	4460	3620	3600	4940	3900	5400	4500	3780	4600	3670	4680
350	5500	4010	4500	5500	4300	5980	5500	4210	5210	4560	5460
400	6010	4760	8000	6590	4860	6910	6390	4730	6290	6160	6640
450	6650	5180	9200	7200	5760	7900	7200	5360	7160	7280	8000
500	7100	5560	9450	7750	6320	8560	8400	5840	8410	11800	9460

Table XXXVII (CONTD.)

Material											
	PVC, rigid	Poly carbonate	Quartz glass	PVC, nonrigi d	Cellulose Acetate Butyrate	Acrylic (plexiglas)	Poly vinylidene fluoride	Phenolic (paper- filled)	Alumina	Pyrex glass	Phenolic (glass- filled)
Frequency (Hz.)	Secondary Voltage (volts)										
550	8580	6640	9720	8290	7680	11110	10500	6720	10360	12120	10280
580	12100	8300	10760	10470	9720	14720	11790	8600	11500	11580	12400
600	12960	12100	11620	11200	10400	14910	12300	11680	11620	11200	12930
630	13610	13200	11850	12640	11660	15060	13960	12670	11780	10620	13180
650	14480	13850	11690	12990	12040	14830	14610	13460	11800	10110	13580
700	14820	14770	10430	13260	12380	12010	14990	14080	11840	8800	14460
710	15010	12880	9010	14800	11970	10970	13590	13620	11400	8620	14960
720	14780	11200	7950	15010	10590	9980	13300	11830	11360	8480	14890
750	13480	8220	6540	14610	9590	8640	13100	8730	11020	7890	12720
800	10920	6340	4120	10600	7410	6870	11220	6320	10760	7010	10320
850	8750	5920	3650	8490	6160	5920	9190	5820	8000	6030	8160
900	6800	4980	2910	6300	5110	5080	7180	4730	6600	4820	5180
950	5200	3500	2110	4980	4490	4850	5760	2940	5170	3990	2380
1000	2310	2100	1230	2300	1920	2470	2480	1900	2460	3600	1980

TABLE XXXVIII

Variation of secondary current with frequency at constant primary voltage (heat generation test)

EXPERIMENTAL DATA CORRESPONDING TO FIGURE 24

RUN 21**System Conditions :****Gas :** Air**Inlet temperature :** 76 deg. F**Flow rate :** 3500 ml/min.**Reactor dimensions :** as presented in Table VIII**Reactor length :** 6 inches**Primary voltage :** 60 volts

Frequency (Hz.)	Material										
	PVC, rigid	Poly carbonate	Quartz glass	PVC, nonrigid	Cellulose Acetate Butyrate	Acrylic (plexiglas)	Poly vinylidene fluoride	Phenolic (paper- filled)	Alumina	Phenolic (glass- filled)	Pyrex glass
	Secondary Current (mA)										
60	5	6.5	5	7	7	5	5	7	6.5	5	6
100	5	6.5	5	7	7	6.5	5	7.5	6.5	5	6.5
150	5	6.5	5	7	7	6.5	5	8	6.5	5	6.5
200	5	6.5	7	7	7.5	6.5	5	9	6.5	5	6.5
250	5	6.5	7	7	7.5	6.5	5	9.5	6.5	5	7
300	5	7	7	7	7.5	7	5	10.5	6.5	6	8
350	5	7	7.25	7.5	7.5	7	5	10.5	6.5	6	8.5
400	5	7.5	7.5	8	8	7	5	10.5	6.5	6	9.25
450	5	7.5	7.5	9	8	7	5	11	6.5	7	10.5
500	5	8	8	9	8	7	7	11	6.5	7	12
550	5	8.5	8.25	12	8	9	7	11.5	7	7	12.5

Table XXXVIII (CONTD.)

Frequency (Hz.)	Material										
	PVC, rigid	Poly carbonate	Quartz glass	PVC, nonrigid	Cellulose Acetate Butyrate	Acrylic (plexiglas)	Poly vinylidene fluoride	Phenolic (paper- filled)	Alumina	Phenolic (glass- filled)	Pyrex glass
	Secondary Current (mA)										
560	6.25	11	9	13	8.25	9	7	11.5	7	5.5	12.5
570	6.25	13	9.5	13.5	11	9	7	12	7	5.5	12.5
580	7	13	10.5	14	11.25	9	7	12.5	6.5	5.5	12.5
600	7	14	12	14	13.25	9.5	7.5	13.5	6.5	5.5	12.5
630	7	14.5	13	14.5	14	9.5	7.5	14	6.25	5.5	12.25
650	7.5	14.5	12	14.5	14	10	7	14.5	6	5.5	11.5
700	7.5	14.5	10	14.5	13	12	7	14.5	6	5	10.25
710	7.5	14.5	9.5	14.5	12.5	9.5	7	14	5	5	10.25
720	7.5	12.5	9	14	12	9.5	7	13.5	5	4	10
750	6.5	11	9	13	11	9.5	7	13.5	5	4	9.5
800	6	10	7.25	12	11	9	6.25	13	5	4	9
850	5.5	9.5	7	10	10	8.5	6	12.5	5	4	8
900	5.5	9	6.5	9	9.5	8	5.5	11.5	5	4	7
950	5	8.5	6.5	8.5	9.5	7	5	11.5	4	4	5
1000	5	8	6	8.5	9.5	6	5	11	4	4	4

TABLE XXXIX

Variation of exit gas temperature with frequency at constant primary voltage (heat generation test)
EXPERIMENTAL DATA CORRESPONDING TO FIGURE 23

RUN 21System Conditions :

Gas : Air

Inlet temperature : 76 deg. F

Flow rate : 3500 ml/min.

Reactor dimensions : as presented in Table VIII

Reactor length : 6 inches

Primary voltage : 60 volts

Material										
	PVC, rigid	Poly carbonate	Quartz glass	PVC, nonrigid	Cellulose Acetate Butyrate	Acrylic (plexiglas)	Poly vinylidene fluoride	Alumina	Pyrex glass	Phenolic (glass- filled)
Frequency (Hz.)	Temperature (deg. F)									
60	76	76	76	76	76	76	76	76	76	76
100	76	76	76	76	76	76	76	76	76	76
150	76	76	76	76	76	76	76	76	76	76
200	76	76	76	76	76	76	76	76	76	76
250	76	76	76	76	76	76	76	76	76	76
300	76	76	76	76	76	76	76	76	76	76
350	76	76	76	76	76	76	76	76	76	76
400	76	76	77	76	76	76	76	76	76	76

Table XXXIX (CONTD.)

Material										
	PVC, rigid	Poly carbonate	Quartz glass	PVC, nonrigid	Cellulose Acetate Butyrate	Acrylic (plexiglas)	Poly vinylidene fluoride	Alumina	Pyrex glass	Phenolic (glass- filled)
Frequency (Hz.)	Temperature (deg. F)									
450	76	76	81	76	76	76	76	76	78	76
500	76	76	94	76	76	76	76	76	79	77
550	76	76	105	76	76	78	78	78	91	78
580	82	76	115	78	76	90	80	86	93	85
600	85	80	122	79	79	93	81	90	91	88
630	88	86	126	84	86	98	89	94	89	89
650	91	92	118	88	89	94	94	95	87	91
700	96	95	117	92	92	93	90	96	85	95
710	99	90	110	99	90	92	88	93	83	97
720	97	89	108	97	87	91	87	91	82	93
750	96	86	102	95	85	90	85	89	81	89
800	94	86	99	93	84	88	82	88	80	85
850	88	81	96	87	81	84	80	82	79	81
900	82	82	94	80	78	81	79	81	78	78
950	79	78	86	78	77	79	78	80	78	77
1000	78	77	81	77	77	77	77	79	77	77

TABLE XXXX

Variation of ozone concentration with frequency at constant primary voltage (heat generation test)

EXPERIMENTAL DATA CORRESPONDING TO FIGURE 26

RUN 21**System Conditions :****Gas :** Air**Inlet temperature :** 76 deg. F**Flow rate :** 3500 ml/min.**Reactor dimensions :** as presented in Table VIII**Reactor length :** 6 inches**Primary voltage :** 60 volts

	Material										
	PVC, rigid	Poly carbonate	Quartz glass	PVC, nonrigid	Cellulose Acetate Butyrate	Acrylic (plexiglas)	Poly vinylidene fluoride	Phenolic (paper- filled)	Alumina	Phenolic (glass- filled)	Pyrex glass
Frequency (Hz.)	Concentration (ppm)										
60	-	-	-	-	-	-	-	-	-	-	-
100	-	-	-	-	-	-	-	-	-	-	-
150	-	-	-	-	-	-	-	-	-	-	-
200	-	-	-	-	-	-	-	-	-	-	-
250	-	-	-	-	-	-	-	-	-	-	-
300	-	-	-	-	-	-	-	-	-	-	-
350	-	-	-	-	-	-	-	-	-	-	-
400	-	-	35	-	-	-	-	-	-	-	-

Table XXXX (CONTD.)

Material											
	PVC, rigid	Poly carbonate	Quartz glass	PVC, nonrigid	Cellulose Acetate Butyrate	Acrylic (plexiglas)	Poly vinylidene fluoride	Phenolic (paper- filled)	Alumina	Phenolic (glass- filled)	Pyrex glass
Frequency (Hz.)	Concentration (ppm)										
450	-	-	70	-	-	-	-	15	-	-	30
500	-	-	90	-	-	-	-	40	-	20	75
550	-	-	105	-	-	80	50	80	60	55	180
570	65	-	150	-	-	150	95	90	135	120	235
580	115	-	255	55	60	175	110	115	170	150	265
600	145	95	310	80	70	225	170	185	220	180	230
630	175	150	270	140	140	260	225	220	240	200	175
640	200	190	210	165	220	275	240	245	250	220	155
650	230	220	180	215	195	250	255	255	265	240	125
700	255	290	135	250	250	210	270	275	255	255	70
710	270	260	95	270	220	185	245	260	260	270	55
720	260	230	50	280	185	140	230	205	230	260	40
750	250	200	35	270	110	120	205	120	205	220	20
800	210	175	15	220	75	105	180	60	175	120	-
850	140	80	-	135	60	65	145	45	95	75	-
900	85	30	-	75	45	20	65	10	55	40	-
950	55	-	-	30	15	-	35	-	10	-	-
1000	-	-	-	-	-	-	15	-	-	-	-

TABLE XXXXI

Variation of exit gas temperature with time at constant primary voltage (heat generation test)

EXPERIMENTAL DATA CORRESPONDING TO FIGURE 28

RUN 22

System Conditions :

Gas : Air

Inlet temperature : 76 deg. F

Flow rate : 3500 ml/min.

Reactor dimensions : as presented in Table VIII

Reactor length : 6 inches

Primary voltage : 60 volts

Material						
Frequency	PVC, rigid (720 Hz.)	Poly carbonate (700 Hz.)	PVC, nonrigid (710 Hz.)	Acrylic (plexiglas) (600 Hz.)	Poly vinylidene fluoride (650 Hz.)	Alumina (ceramic) (700 Hz.)
Time (hours)	Temperature (deg. F)					
0	97	95	96	93	93	95
1	98	95	96	94	94	96
2	99	95	96	95	95	97
3	100	95	96	95	96	98
4	100	95	97	97	97	98
5	101	96	98	97	98	98
6	101	96	98	98	99	99
7	102	97	98	99	99	100
8	102	97	98	100	99	102
9	102	97	98	101	100	103
10	103	97	96	101	103	104

TABLE XXXXI (CONTD.)

	Material					
Frequency	PVC, rigid (720 Hz.)	Poly carbonate (700 Hz.)	PVC, nonrigid (710 Hz.)	Acrylic (plexiglas) (600 Hz.)	Poly vinylidene fluoride (650 Hz.)	Alumina (ceramic) (700 Hz.)
Time (hours)	Temperature (deg. F)					
11	103	97	98	103	105	105
12	103	97	98	104	105	105
13	103	97	98	106	106	106
14	103	98	100	108	107	107
15	103	98	101	110	108	109
16	104	98	102	113	110	110
17	104	99	104	115	112	110
18	104	99	105	118	114	111

TABLE XXXXII
 Variation of ozone concentration with time at constant primary voltage
 (heat generation test)
 EXPERIMENTAL DATA CORRESPONDING TO FIGURE 29
RUN 22

System Conditions :

Gas : Air

Inlet temperature : 76 deg. F

Flow rate : 3500 ml/min.

Reactor dimensions : as presented in Table VIII

Reactor length : 6 inches

Primary voltage : 60 volts

Frequency	Material					
	PVC, rigid (720 Hz.)	Poly carbonate (640 Hz.)	PVC, nonrigid (700 Hz.)	Acrylic (plexiglas) (600 Hz.)	Polyvinylidene fluoride (640 Hz.)	Alumina (ceramic) (600 Hz.)
Time (hours)	Concentration (ppm)					
0	270	290	280	275	270	265
1	275	290	280	280	270	265
2	280	290	285	280	270	270
3	280	290	285	285	255	275
4	280	290	295	290	240	280
5	285	290	295	295	220	280
6	295	270	290	295	210	280
7	295	270	285	295	170	295
8	290	270	275	295	160	280
9	290	270	265	290	160	270
10	290	270	265	240	130	270
11	290	270	265	220	130	270
12	275	270	265	175	120	250
13	275	250	265	160	105	245
14	275	250	265	125	100	240
15	275	250	255	115	100	235
16	275	250	255	100	95	230
17	270	250	255	90	90	230
18	270	250	255	80	75	230

TABLE XXXXIII

Variation of secondary voltage with time at constant primary voltage (heat generation test)

EXPERIMENTAL DATA CORRESPONDING TO FIGURE 30

RUN 22

System Conditions :

Gas : Air

Inlet temperature : 76 deg. F

Flow rate : 3500 ml/min.

Reactor dimensions : as presented in Table VIII

Reactor length : 6 inches

Primary voltage : 60 volts

Material						
Frequency	PVC, rigid (720 Hz.)	Poly carbonate (700 Hz.)	PVC, nonrigid (710 Hz.)	Acrylic (plexiglas) (600 Hz.)	Poly vinylidene fluoride (650 Hz.)	Alumina (ceramic) (700 Hz.)
Time (hours)	Secondary voltage (volts)					
0	14780	14770	14800	14900	14990	11840
1	14850	14770	14800	14950	14990	11840
2	14910	14770	14840	14960	14990	11910
3	14930	14770	14840	14960	14910	11960
4	14930	14770	14880	14960	14800	12050
5	14960	14770	14880	14990	14720	12090
6	14990	14730	14830	14990	14420	12160
7	14990	14730	14830	14920	14330	12220
8	14960	14700	14800	14920	14270	12160
9	14960	14700	14800	14920	14270	12140
10	14960	14700	14800	14760	14180	12120

Table XXXXIII (CONTD.)

Material						
Frequency	PVC, rigid (720 Hz.)	Poly carbonate (700 Hz.)	PVC, nonrigid (710 Hz.)	Acrylic (plexiglas) (600 Hz.)	Poly vinylidene fluoride (650 Hz.)	Alumina (ceramic) (700 Hz.)
Time (hours)	Secondary voltage (volts)					
11	14940	14700	14800	14760	14180	11890
12	14900	14700	14800	14690	14100	11890
13	14900	14650	14800	14420	14030	11850
14	14900	14650	14800	14270	13950	11850
15	14900	14650	14030	14030	13950	11850
16	14900	14650	13890	13890	13920	11820
17	14880	14650	13820	13820	13870	11780
18	14880	14650	13640	13640	13690	11780

TABLE XXXIV

Variation of secondary current with time at constant primary voltage (heat generation test)

EXPERIMENTAL DATA CORRESPONDING TO FIGURE 31

RUN 22

System Conditions :

Gas : Air

Inlet temperature : 76 deg. F

Flow rate : 3500 ml/min.

Reactor dimensions : as presented in Table VIII

Reactor length : 6 inches

Primary voltage : 60 volts

Material						
	PVC, nonrigid	Poly carbonate	PVC, rigid	Acrylic (plexiglas)	Polyvinylidene fluoride	Alumina (ceramic)
Frequency	(700 Hz.)	(700 Hz.)	(720 Hz.)	(600 Hz.)	(650 Hz.)	(650 Hz.)
Time (hours)	Secondary current (mA)					
0	14.5	14.5	7.5	9.5	7	6
1	14.5	14.5	7.5	9.5	7	6
2	14.5	14.5	7.5	10	7.5	6
3	14.5	14.5	7.5	11	8	6.5
4	15	14.5	8	12	8.5	7
5	15	14.5	8.5	13.5	10	7
6	15	15	9	15	11	7
7	15.5	15	9	16	11.5	7
8	16	15	9.5	16.5	12	7
9	16	15	9.5	16.5	12.5	7
10	16	15	10	16.5	13	7
11	16	15	10	16.5	13.5	7
12	16.5	15	10.5	17	14	7.5
13	17	15	10.5	17	15	8
14	17.5	15	10.5	17	16	8
15	18	15	10.5	17	16	8
16	18	15	10.5	17	16.5	8
17	18	15	10.5	17.5	17	8.5
18	18	15	10.5	17.5	17.5	9

Appendix E

Reproducibility tests

Table XXXXV
 Reproducibility data for open-circuit tests

Primary voltage (volts)	Frequency (Hz.)	Secondary voltage (volts)				% error for secondary voltage	Primary current (mA)				% error for primary current
		RUN 1	RUN 23	RUN 27	RUN 28		RUN 1	RUN 23	RUN 27	RUN 28	
60	100	1925	1950	1970	2060	7.0	0.31	0.31	0.31	0.31	-
	350	4580	4670	4590	4740	3.5	0.13	0.13	0.13	0.13	-
	500	5680	5620	5630	5790	3.0	0.14	0.14	0.15	0.15	7.1
	750	8480	8580	8530	8650	2.0	0.3	0.32	0.32	0.3	6.7
	950	13800	13760	13630	13920	2.1	0.77	0.8	0.79	0.79	3.9

Table XXXXVI
 Reproducibility data for variation of secondary voltage with frequency

Frequency (Hz.)	PVC (nonrigid)						Alumina					
	RUN 2	RUN 21	RUN 24	RUN 29	RUN 30	% Error	RUN 2	RUN 21	RUN 24	RUN 29	RUN 30	% Error
100	1380	1380	1470	1460	1580	14.5	1980	2030	2110	2220	2200	12.1
200	3800	3680	3810	3890	3970	7.9	3600	3620	3680	3750	3740	4.2
400	6000	6590	6330	6580	6470	9.8	6200	6290	6170	6200	6230	1.9
500	7030	7750	7440	7650	7380	10.2	8600	8410	8330	8840	8580	6.1
600	12900	11200	11970	12200	11870	15.2	11600	11620	11710	11810	11430	3.3
700	14810	13260	13980	13990	13880	11.7	11800	11840	11940	11730	11910	1.8
800	10990	10600	10770	10800	11110	4.8	10800	10760	10960	10970	10640	3.1
900	6850	6300	6680	6900	7210	14.4	6400	6600	6980	7010	6610	9.5
1000	2370	2300	2420	2280	2410	6.1	2410	2460	2580	2660	2630	10.4

Table XXXXVI
 Reproducibility data for variation of secondary current with frequency

Frequency (Hz.)	PVC (nonrigid)						Alumina					
	RUN 2	RUN 21	RUN 24	RUN 29	RUN 30	% Error	RUN 2	RUN 21	RUN 24	RUN 29	RUN 30	% Error
100	7	7	7	7	7	-	6.5	6.5	6.5	6.5	6.5	-
200	7	7	7	7	7	-	6.5	6.5	6.5	6.5	6.5	-
400	8	8	8	8	8	-	6.5	6.5	6.5	6.5	6.5	-
500	10	9	9.5	9.5	10	11.1	7	6.5	6.5	7	7	7.7
600	14	14	14	14.5	15	7.1	7.5	6.5	6.5	7	7	15.4
700	14.5	14.5	14.5	15	15	3.4	6.5	6	5.5	6	6.5	8.3
800	11.5	12	11.5	11.5	11.5	4.3	6.25	5	6	6	6	13.6
900	9.25	9	9	9.5	9.5	5.6	5	5	5	5	5	--
1000	8	8.5	8	9	9	12.5	5	4	5	4.5	5	11.1

Table XXXXVI
 Reproducibility data for variation of temperature with frequency

Frequency (Hz.)	PVC (nonrigid)						Alumina					
	RUN 2	RUN 21	RUN 24	RUN 29	RUN 30	% Error	RUN 2	RUN 21	RUN 24	RUN 29	RUN 30	% Error
100	76	76	76	76	76	-	76	76	76	76	76	-
200	76	76	76	76	76	-	76	76	76	76	76	-
400	76	76	76	76	76	-	76	76	76	76	76	-
500	76	76	76	76	76	-	76	76	76	76	76	-
600	79	79	78	80	80	2.6	90	89	91	90	91	2.2
700	92	92	91	94	94	3.3	96	94	95	95	96	2.1
800	93	93	96	96	96	3.2	88	88	88	89	90	2.3
900	80	80	83	85	84	6.3	81	81	81	83	82	2.5
1000	77	77	79	78	80	3.9	79	79	79	80	80	1.3

Table XXXXVI
 Reproducibility data for variation of ozone concentration with frequency

Frequency (Hz.)	PVC (nonrigid)						Alumina					
	RUN 2	RUN 21	RUN 24	RUN 29	RUN 30		RUN 2	RUN 21	RUN 24	RUN 29	RUN 30	
100	-	-	-	-	-	-	-	-	-	-	-	-
200	-	-	-	-	-	-	-	-	-	-	-	-
400	-	-	-	-	-	-	-	-	-	-	-	-
500	-	-	-	-	-	-	-	-	-	-	-	-
600	80	75	75	85	80	13.3	200	220	220	230	210	15
700	250	240	250	260	260	8.3	265	270	275	285	255	11.8
800	220	215	230	235	240	11.6	175	155	160	180	160	12.5
900	75	70	80	80	75	14.3	55	55	60	60	60	9.1
1000	-	-	-	-	-	-	-	-	-	-	-	-

Table XXXXVII
 Reproducibility data for variation of secondary voltage/current,
 temperature and concentration with time

Time (hours)	Material - PVC (nonrigid)															
	Concentration (ppm)															
	RUN 22	RUN 26	RUN 31	% Error	RUN 22	RUN 26	RUN 31	% Error	RUN 22	RUN 26	RUN 31	% Error	RUN 22	RUN 26	RUN 31	% Error
0	280	270	280	3.7	14840	14760	14890	0.9	14.5	14.5	14.5	-	96	96	96	-
2	290	290	295	1.7	14830	14740	14940	1.4	15	16	16	6.7	98	98	99	1.0
6	265	280	285	7.5	14800	14740	14920	1.2	16	16.5	16.5	3.1	98	98	99	1.0
10	265	280	280	5.7	14800	14740	14890	1.0	16.5	16.5	16.5	-	98	100	102	4.1
12	265	280	275	5.7	14800	14690	14740	0.7	17.5	18	18	2.9	100	102	104	4.0
14	255	280	280	9.8	14540	14690	14650	1.0	18.5	18	18.5	2.8	105	106	107	1.9
18																

VITA

Arun Krishnamoorthy

Candidate for the Degree of

Master of Science

Thesis: EVALUATION OF DIELECTRIC MATERIALS FOR OZONE GENERATION
IN PLASMA REACTORS

Major Field: Chemical Engineering

Biographical:

Personal Data: Born in Madras, INDIA, on February 27, 1971, the son of Anandhi and Krishnamoorthy.

Education: Graduated from Bharathi Vidya Bhavan, Erode, INDIA in May 1989; received Bachelor of Engineering with Honors in Chemical Engineering from Birla Institute of Technology & Science, Pilani, INDIA in May 1993. Completed the requirements for the Master of Science degree with a major in Chemical Engineering at Oklahoma State University in December 1996.

Experience: Completed a six-month intern at Grasim Industries, Nagda, INDIA; GRASIM Industries, Viscose Division, January to June, 1993. Employed by Imperial Chemical Industries (ICI), Agrochemicals & Pharmaceuticals Division, Madras, India as a Management Trainee; ICI, Agrochemicals & Pharmaceuticals Division, June 1993 to August 1994. Employed by Oklahoma State University, School of Chemical Engineering as a graduate teaching assistant; Oklahoma State University, School of Chemical Engineering, January 1995 to April 1996.

Professional Memberships: AIChE, Omega Chi Epsilon